Sustainable removal of micropollutant from wastewater via sonochemical degradation with techno-economic analysis and life cycle assessment

Zhiyuan Zong

St. Anne's College

Department of Engineering Science

University of Oxford

A thesis submitted for the degree of

Doctor of Philosophy

Abstract

Conventional wastewater treatment often fails to remove persistent antibiotic micropollutants like tetracycline, which spread antimicrobial resistance. This thesis comprehensively develops, optimizes, and benchmarks advanced oxidation processes (AOPs) for the eco-friendly degradation of these contaminants.

The work begins with the design and experimental validation of a novel sono-reactor system that utilizes TiO_2 fractured nanoshells to enhance acoustic cavitation and radical generation. Through a detailed parametric investigation—including reaction time, acoustic pressure, pH, catalyst loading, and hybrid conditions—rapid tetracycline degradation was achieved (100% degradation from 5 mg/L in 5 minutes).

In the second phase, a process-level environmental evaluation was conducted using life cycle assessment to compare different experimental scenarios. It was found that while sono-based systems excelled in operational performance, they incurred high electricity-related emissions under current UK grid conditions. However, under projected 2050 green electricity scenarios, the environmental burden shifted toward catalyst synthesis. An improved continuous-flow system employing metal foam instead of synthesized nanoparticles was proposed, resulting in a significant reduction in CO_2 emissions.

The third research phase expanded the analysis to a comparative LCA and techno-economic assessment (TEA) of five representative AOP technologies: sono-, photo-, sonophoto-, Fenton-, and electrochemical processes. The results showed that electricity

usage (up to 83%) and catalyst synthesis (up to 98%) were dominant contributors to environmental impact. The sono-based method offered superior operational performance but high emission due to massive electricity consumption, while conventional Fenton processes exhibited low emission under present conditions (1.2 vs 0.478 kg-CO_2/L).

By integrating experimental innovation with environmental and economic evaluation, this thesis provides a novel framework for guiding the development of AOP technologies for their effectiveness in pollutant degradation and life cycle sustainability. The outcomes emphasize a crucial shift in research perspective—from prioritizing performance alone to making environmentally-informed decisions in the design and implementation of future water treatment systems.

Acknowledgements

Pursuing a PhD at the University of Oxford has been a transformative journey—intellectually demanding, personally enriching, and made possible through the support of many individuals to whom I owe deep gratitude.

First and foremost, I would like to thank my supervisor, Professor Nicholas Hankins. His mentorship and guidance were invaluable throughout my doctoral research. I am also grateful to Professor James Kwan for his valuable advice and useful help throughout the project. Their insights, encouragement, and steady support shaped both the direction and quality of my work.

I am also grateful to my collaborators and group members—Professor Chester Upham, Professor Qianhong She, Dr. Christian Peters, Dr. Jason Raymond, Yihao Huang, Cherie Wong, Peng Yang, Omar Daoud, and Gayatri Sundar Rajan—whose expertise and contributions greatly enriched my research experience.

Equally important was the emotional support from my family and friends. Their constant encouragement helped sustain me through the inevitable challenges and doubts that came with this path. I would also like to acknowledge St. Anne's College for awarding me the Graduate Research Grant, which provided additional resources crucial to the development of my project.

Lastly, I want to take a moment to acknowledge myself—for choosing this path, for enduring the long nights and uncertain outcomes, and for embracing the many challenges that came with doctoral research. Choosing to pursue a DPhil and

committing to its demands has opened a new chapter in my life, one filled with knowledge, growth, and possibility.

Table of Contents

List of Figures

List of Tables

Nomenclature

Abbreviation	Description
AOPs	Advanced Oxidation Processes
ARB	Antibiotic-resistant bacteria
ARGs	Antibiotic-resistant genes
C0	Concentration of tetracycline initially
Ct	Concentration of tetracycline after the reaction
Cads	Concentration of tetracycline after the adsorption
CAPEX	Capital expenditures
CED	Cumulative Energy Demand
CEPCI	Chemical Engineering Plant Cost Index
EDTA	Ethylenediaminetetraacetic acid
EoL	End-of-life
GWP	Global warming potential
GHG	Greenhouse gas
HPLC	High-Performance Liquid Chromatography
IEA	International Energy Agency
IRR	Internal Rate of Return
LCA	Life Cycle Assessment
LCI	Life Cycle Inventory
LCIA	Life Cycle Impact Assessment
LCSA	Life cycle social analysis
NGCC	Natural gas combined cycle
NPV	Net Present Value
OPEX	Operating expenditures
PPM	Parts per million
pHpzc	Point of zero charge
PS	Polystyrene
ROS	Reactive oxygen species
RPM	Revolutions per minute
TEA	Techno-Economic Analysis
TFNs	TiO2 fractured nanoshells
WWTPs	Wastewater treatment plants

Chapter 1: Introduction

1.1 Background

The growing global demand for clean water, driven by population growth, industrialization, and climate change, has placed unprecedented pressure on freshwater resources. Compounding this issue is the increasing contamination of aquatic environments with micropollutants—trace-level compounds such as pharmaceuticals, personal care products, and pesticides. Among these, antibiotics represent a particularly concerning class of pollutants due to their widespread use, environmental persistence, and role in promoting antimicrobial resistance [1–3].

Conventional wastewater treatment plants (WWTPs) are not designed to remove many emerging contaminants, including antibiotics such as tetracycline and ciprofloxacin, which are commonly detected in effluents. These compounds resist biodegradation and often pass through treatment systems largely unchanged, entering natural water bodies and contributing to ecological disruption and the proliferation of antibiotic-resistant bacteria (ARB) and genes (ARGs) [4].

To address these challenges, Advanced Oxidation Processes (AOPs) have emerged as a promising class of technologies capable of degrading persistent organic pollutants through the generation of highly reactive oxygen species [5,6]. AOPs such as photolysis, ozonation, Fenton reactions, and sonolysis have demonstrated potential in degrading pharmaceuticals in water. However, despite their proven effectiveness in lab-scale studies, many AOPs remain limited by high energy demands, the use of hazardous

chemicals, scalability issues, and uncertain long-term sustainability [7–9].

In particular, sono-based AOPs, which rely on acoustic cavitation to generate oxidative radicals, offer several advantages—such as operation under ambient conditions, minimal chemical input, and potential compatibility with complex wastewater matrices [10,11]. However, sonochemical processes are still under development and require further research to optimize performance and assess environmental and economic feasibility on scale.

However, in the context of sustainable water treatment, pollutant degradation performance alone is no longer an adequate metric [12,13]. A technology that efficiently removes contaminants but consumes excessive energy or relies on unsustainable chemicals may ultimately cause more harm than good. Therefore, beyond evaluating removal efficacy, there is a growing need to assess the broader environmental and economic impacts of AOPs from a life cycle perspective. This is particularly important as research advances from lab-scale innovation to real-world deployment, where energy use, chemical inputs, and material sustainability play increasingly pivotal roles. These considerations form the foundation for the subsequent investigations presented in this thesis.

1.2 Motivation and Objectives

Sono-based AOPs, though promising, remain underexplored in both reactor design and process optimization. Existing studies often rely on generic ultrasonic systems with

limited adaptation for practical wastewater treatment. There is a clear need to develop tailored sono-chemical degradation processes in both experimental performance and environmental impact—especially when dealing with persistent contaminants like tetracycline [14]. Current ultrasonic systems face significant challenges, including inefficient reactor design, low energy efficiency, and high energy consumption. These limitations hinder scalability and make the technology unsuitable for commercialization [15]. Due to the challenges of commercialization, the economic feasibility of sonochemical-based AOPs is rarely discussed, and life cycle assessments are seldom conducted [16].

In parallel, while many AOPs demonstrate high degradation efficiency under controlled conditions, there is a growing recognition that operational performance alone is not enough. Technologies must also be evaluated based on their environmental and economic sustainability. Yet, most comparative studies focus only on pollutant removal and rarely account for key factors such as:

- Energy consumption during operation,
- Emissions and resource use is associated with chemical and catalyst production,
- True financial costs, including monetized environmental impacts.

This DPhil research addresses these gaps through a multi-stage investigation. The overarching motivation of this research is to bridge the gap between high-efficiency degradation of micropollutants and the broader sustainability implications of such treatment processes. This study therefore aims to integrate experimental investigation

with system-level sustainability assessment to inform practical, scalable solutions for antibiotic removal in wastewater. The research pursues the following specific objectives:

1. To experimentally develop and optimize a sono-based AOP for tetracycline degradation, focusing on reaction performance, and to explore the effects of key reaction parameters.
2. To assess the environmental performance of the proposed system using Life Cycle Assessment (LCA) and to propose improvements for reducing its environmental footprint.
3. To conduct a comparative Techno-Economic Analysis (TEA) and LCA benchmarking study of several representative AOP technologies under harmonized conditions to identify the most sustainable method for tetracycline degradation.

By integrating experimental work with sustainability assessment and cross-technology comparison, this research contributes to the broader goal of advancing water treatment technologies that are not only effective—but also viable and responsible in the long term.

1.3 Thesis structure

This thesis is presented in the conventional format and overall consists of six chapters. Chapters 3 to 5 form the core of the research. The chapters are outlined as

follows:

Chapter 1 – Introduction: presents the background, research motivation, objectives, and thesis structure.

Chapter 2 – Literature Review: reviews the occurrence and impact of antibiotic micropollutants in wastewater, current AOPs for micropollutants including sono-based processes, and the use of LCA and TEA for sustainability evaluation.

Chapter 3 – Experimental Development of a Sono-Based AOP System: Describes the design and operation of a novel sono-reactor, the use of cavitation agents, and a detailed investigation of reaction parameters affecting tetracycline degradation performance.

Chapter 4 – Environmental optimization of the Proposed System: Applies LCA to quantify the environmental footprint of the developed process and identify key environmental hotspots and propose optimization strategies

Chapter 5 – Comparative TEA/LCA Benchmarking of AOP Technologies: Conducts a standardized comparison of multiple AOP technologies using a unified LCA framework, identifying the measurement of sustainability for tetracycline removal.

Chapter 6 – Conclusions and perspectives: Summarizes key findings, discusses the limitations of this work, outlines future research directions and broader implications.

1.4 Research output

To date, I have published one peer-reviewed paper (Chapter 3) and presented work in two conferences, which is directly related to the results of my DPhil research, as

detailed below. In addition, Chapters 4 and 5 contain the content of the manuscripts to be submitted for publication.

Peer-Reviewed Publications:

Zong, Zhiyuan, Emma Gilbert, Cherie CY Wong, Lillian Usadi, Yi Qin, Yihao Huang, Jason Raymond, Nick Hankins, and James Kwan. "Efficient sonochemical catalytic degradation of tetracycline using TiO_2 fractured nanoshells." *Ultrasonics Sonochemistry* 101 (2023): 106669. [17]

Conference Presentations:

Zong, Zhiyuan and Nick Hankins, “Sonochemical catalytic removal of antibiotics using converging ultrasounds and cavitation agent with life cycle assessment”. VI Iberoamerican Conference on Advanced oxidation Technologies (6^{th} CIPOA), Florianopolis, Brazil, October 7^{th} -11^{th} , 2024

Zong, Zhiyuan, Economic and environmental evaluation: toward net zero emission and circular economy in 2050/2060. The second Yongjiang Laboratory Global Young Elite Forum on Science and Technology. Ningbo, China, Jul 13-16, 2024

In addition, I have contributed to several other peer-reviewed papers and a book chapter in fields related to water treatment, which have helped me to improve life cycle assessment and process modelling skills, and gain knowledge in sustainable water

engineering. Some modelling and analytical methods were taken from the following publications.

Zong, Zhiyuan, Nick Hankins, and Fozia Parveen. "The Application of Nanofiltration for Water Reuse in the Hybrid Nanofiltration-Forward Osmosis Process." In *Nanofiltration for Sustainability*, pp. 153-170. CRC Press, 2023. [18]

Zong, Zhiyuan, Omar Daoud, Nicholas P. Hankins, Qianhong She, and Christian D. Peters. "Valorising Desalination Brine for Green Cement Production: Toward Mitigating Global CO_2 Emissions." *Water Research* (2025): 123930. [19]

Rantissi, Tony, Vitaly Gitis, **Zhiyuan Zong *(corresponding author)**, and Nick Hankins. "Transforming the water-energy nexus in Gaza: A systems approach." *Global Challenges* 8, no. 5 (2024): 2300304. [20]

Chapter 2: Literature review

Chapter 2 reviewed the growing issue of antibiotic micropollutants in wastewater, focusing on tetracycline and the limitations of conventional treatment methods. AOPs, particularly sono-based systems, were explored for their potential to degrade persistent contaminants. The chapter highlighted the advantages of sonochemical oxidation and the importance of optimizing reactor parameters and cavitation conditions.

It also emphasized the need to go beyond performance-based evaluations by integrating LCA and TEA to assess environmental and economic sustainability. Current life cycle assessments (LCA) of AOPs for wastewater treatment often lack a complete inventory list [21], ignore the impacts of material synthesis (e.g., membranes and catalysts) [22,23], and report inconsistent outputs [24]. Moreover, LCAs specifically for sonochemical-based AOPs are rarely conducted. This lack of standardisation represents a critical research need and highlights the importance of developing a framework for future consistent analysis.

2.1 Micropollutants and Antibiotics in Wastewater

With the development of the economy and global population, the lack of freshwater becomes a severe problem where freshwater only consists of 2.5% of the global water resources [25]. Today, more than 40% of the world's population cannot achieve sufficient water [26]. Compounding this issue is the increasing contamination of water bodies by micropollutants—trace-level contaminants that are resistant to conventional

wastewater treatment.

Micropollutants include a broad spectrum of synthetic and natural compounds such as pharmaceuticals, personal care products, pesticides, and industrial chemicals. Though typically present at low concentrations (ng/L to lower ug/L range [27]), many of these compounds are persistent, bioactive, and capable of accumulating in ecosystems and human bodies [28–30]. Their small molecular size and chemical stability make them particularly difficult to remove using standard treatment methods. Micropollutants have three primary transfer pathways from the sources to the human body. The first transfer pathway is intake directly, for example, from untreated water and food packages and containers that contain micropollutants [28–30]. The second transfer pathway is mostly from agriculture and industry use, constituting over 80% of water withdrawals. During agriculture and chemical processing activities, numerous persistent organic pollutants, such as pesticides, are used. Those micropollutants can be carried by the product and transported easily over thousands of miles from their sources [31,32]. Even though some of the micropollutants are less severe and harmful, the continuous long-distance transfer would significantly raise the accumulation risk [33,34].

Among the various micropollutants, antibiotics have emerged as a critical area of concern [35–39]. Widely used in human medicine, veterinary applications, and agriculture, antibiotics are frequently detected in wastewater due to incomplete metabolism in the body and improper disposal. WWTPs, which are not specifically designed to eliminate these bioactive compounds, often discharge residual antibiotics

into aquatic environments [40].

This results in the continuous release of residual antibiotics into surface waters, contributing to the development and spread of antibiotic-resistant bacteria and resistance genes. The presence of antibiotics in treated effluent can have serious ecological and public health consequences. Continuous low-level exposure in the environment contributes to the development of ARB and the spread of ARGs, a major global health threat recognized by the World Health Organization [41]. These contaminants can enter food chains via aquatic organisms and irrigation practices, creating long-term risks that extend beyond the immediate vicinity of the pollution source.

Tetracycline and ciprofloxacin are among the most frequently detected antibiotics in wastewater:

- Tetracycline, a broad-spectrum antibiotic used extensively in both human medicine and livestock production, is frequently found in municipal and agricultural wastewater (3-500 ng/L [42]). It exhibits a strong affinity for organic matter and sediments, making it prone to accumulation in sludge and aquatic ecosystems. Tetracycline is relatively persistent and has a low biodegradability index, making it difficult to remove through biological treatment processes [43–46].
- Ciprofloxacin, a widely used fluoroquinolone antibiotic, is particularly concerning due to its high antibacterial potency, environmental persistence, and strong tendency to form complexes with metal ions. Ciprofloxacin resists

biodegradation and can remain active in the environment for extended periods, posing toxicity risks to aquatic organisms and fostering the selection of resistant strains [47–49].

While WWTPs typically involve a multi-stage process—including physical separation, biological degradation, and sometimes advanced tertiary treatments—antibiotic compounds are often only partially removed [50]. In this context, AOPs are gaining attention for their potential to degrade antibiotics effectively at trace concentrations.

2.2. Advanced oxidation process treatment

The presence of persistent contaminants such as antibiotics in wastewater has highlighted the limitations of conventional treatment technologies. While typical WWTPs involve a multi-stage process—consisting of primary (physical), secondary (biological), and tertiary (chemical or advanced) treatments—these systems are often inadequate for removing low-concentration, biologically active compounds like tetracycline and ciprofloxacin. As a result, AOPs have gained increasing attention for their ability to degrade such micropollutants through non-selective oxidation [51–53].

AOPs are based on the generation of highly reactive oxygen species (ROS), primarily hydroxyl radicals (·OH), which possess a high oxidation potential (~2.8 eV). These radicals can attack a wide range of organic pollutants, leading to the cleavage of chemical bonds and eventual mineralization into harmless end-products, such as carbon dioxide and water [54].

Several conventional AOPs have been widely investigated for wastewater treatment, including:

- Hydrogen peroxide (H_2O_2)-based processes, where ·OH radicals are generated through the decomposition of H_2O_2 [55].
- Fenton and photo-Fenton reactions, which use a combination of ferrous ions (Fe^{2+}) and hydrogen peroxide to produce ·OH radicals [56,57]. The classical Fenton reaction involves multiple steps, with the key reactions initiating radical formation. This reaction system is effective but operates best under acidic conditions (pH 2–4), which can limit practical applications [58,59].
- Ozonation and UV-based advanced oxidation processes (AOPs) directly initiate radical production via ozone or ultraviolet light. They further enhance the breakdown of organic precursors by employing additives (e.g., hydrogen peroxide) or photocatalysts (e.g., TiO_2) [60,61]. For instance, UV/O_3 systems promote the in-situ formation of H_2O_2, followed by photolysis to yield hydroxyl radical.

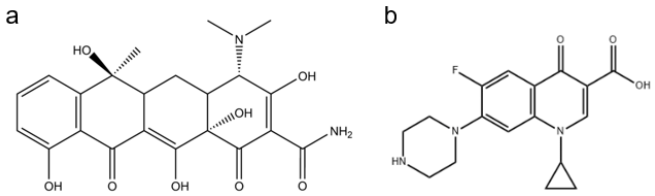

Figure 2.1: Structure and formulae of (a) tetracycline and (b) ciprofloxacin

These methods have demonstrated effectiveness in degrading various pharmaceuticals, including tetracyclines, although they may face limitations related to

cost, pH sensitivity, or incomplete mineralization.

Table 2.1. Summary of AOPs for tetracycline degradation. Sono: 1-[62] 2-[63] 3-[64] 4-[65]; Photo: 1-[66] 2-[67] 3-[68] 4-[69] 5-[70]; Sonophoto: 1-[71] 2-[72] 3-[73]; Photofenton: 1-[74] 2-[75]; Sonofenton: 1-[76].

		PPM	Volumn ml	g	Conversion	g removed	Time minutes	Dosage mg/ml	Catalyst type	Catalyst amount (g)	Power W
Sono	1	45	20	0.0009	0.7	0.00063	120	0.5	Ag3PO4/CoWO4	0.01	500
	2	10	150	0.0015	0.8647	0.00129705	300	1	SrTiO3/Ag2S/CoWO4	0.15	300
	3	20	10	0.0002	0.911	0.0001822	90	2	BiOBr/MgFe2O4	0.02	500
	4	50	50	0.0025	0.876	0.00219	45	0.5	ZnO/cellulose	0.025	256
Photo	1	10	50	0.0005	0.9164	0.0004582	60	0.3	rGO/Ag2CO3	0.015	500
	2	10	100	0.001	0.87	0.00087	60	0.5	CoO octahedrons	0.05	300
	3	10	50	0.0005	0.75	0.000375	180	0.5	RGO-Cu2O/Bi2O3	0.025	250
	4	15	100	0.0015	0.95	0.001425	60	0.5	CdS/ZnS	0.05	300
	5	20	200	0.004	0.8041	0.0032164	60	1	Bi2Sn2O7-C3N4	0.2	400
Sono-photo	1	15	40	0.0006	0.736	0.0004416	60	0.25	TiO2 (Au/B-TiO2/rGO)	0.01	900
	2	60	300	0.018	1	0.018	240	0.7	WO3/CNT	0.21	440
	3	10	150	0.0015	0.998	0.001497	180	1	Ca-doped ZnO	0.15	101.6
Photo-fenton	1	20	100	0.002	0.903	0.001806	80	0.5	Fe/SCN	0.05	300
	2	20	40	0.0008	0.95	0.00076	80	0.625	FeWO4/BiOCl	0.025	300
Sono-fenton	1	10	50	0.0005	0.99	0.000495	30	0.25	SmFeO3/Ti3C2Tx	0.0125	300

Despite the progress in AOP development, challenges remain, including the formation of toxic transformation products, low energy efficiency, and variable performance depending on wastewater matrix composition [77,78]. These limitations have motivated the exploration of alternative and complementary AOP methods, among which sonochemical oxidation has shown considerable promise. This technique offers notable advantages, such as operating under ambient conditions without chemical additives and producing highly reactive radicals through cavitation, which may reduce toxic byproduct formation and improve energy efficiency.

Sonochemistry, which involves the application of ultrasonic waves to induce radical formation via acoustic cavitation, offers several advantages such as operation under ambient conditions, improved mass transfer, and potential for use in complex wastewater matrices.

The next section will delve deeper into sono-based AOPs, their mechanisms, and their specific application for antibiotic degradation in wastewater.

2.3. Sonolytic oxidation process

Sonochemical AOPs utilize ultrasonic irradiation to generate highly reactive species through a mechanism known as acoustic cavitation. This approach has shown great promise for degrading recalcitrant micropollutants, particularly antibiotics, due to its ability to operate under ambient conditions and its minimal dependence on chemical additives, such as hydrogen peroxide [79,80].

When high-intensity ultrasound is applied to an aqueous medium, microscopic gas bubbles form, grow, and violently collapse [81]. This cavitation collapse generates localized hot spots with transient temperatures exceeding 5000 K and pressures over 1000 atm. These extreme conditions lead to the homolytic cleavage of water molecules, producing highly reactive radicals such as hydroxyl (·OH) and hydrogen (·H) radicals, which can effectively degrade a wide range of organic pollutants [82–84].

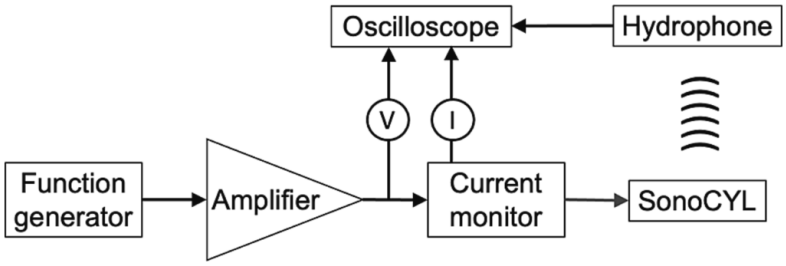

Figure 2.2: Schematic of a typical sonochemical process configuration (adapted from [85])

The efficiency of the sonochemical process is closely linked to cavitation dynamics. Two primary forms of cavitation are observed:

- Stable cavitation, where bubbles oscillate steadily with the applied ultrasound frequency and persist over many cycles around an equilibrium size [86].
- Inertial cavitation, where bubbles grow rapidly under high-intensity ultrasound and collapse violently, generating intense physical and chemical effects [87].

Key parameters influencing cavitation include ultrasound frequency and amplitude. Higher amplitude increases cavitation intensity, while frequency governs bubble size and growth time. Lower frequencies (e.g., ~20 kHz) allow larger bubbles to form and collapse more forcefully, enhancing radical production. In contrast, higher frequencies

(e.g., >1 MHz) generate smaller bubbles and favour stable cavitation with less extreme conditions [88].

In some cases, dual-frequency excitation can be used to enhance cavitation by lowering the energy threshold needed to initiate bubble collapse. A larger difference between the two frequencies has been shown to further reduce this threshold, improving overall radical yield [89].

To further improve radical generation and degradation efficiency, nanostructured catalysts can be introduced as the cavitation nuclei in order to initiate the inertial cavitation. These materials serve as nucleation sites for cavitation bubbles and often exhibit high surface roughness and hydrophobicity—key factors that reduce the energy barrier for cavitation initiation [16,84,90].

Although sonochemical degradation can be performed without light, many of these catalysts also function as semiconductors, making them responsive to photonic excitation [91,92]. Under certain conditions, especially during high-intensity cavitation, a phenomenon known as sonoluminescence occurs—where the collapse of cavitation bubbles emits light in the 200–700 nm range [93].

This internally generated light can activate the semiconductor catalyst if its energy exceeds the material's bandgap, initiating photocatalytic reactions even without an external light source [94]. The most popular and well-studied photocatalyst is TiO_2. Other than that, the photocatalysts include but are not limited to bismuth oxide [95,96], tungsten oxide [97] and cerium oxide [98]. It is worth noting that both TiO_2 and ZnO-based photocatalysts are affordable, show high stability, and are easy to modify by

metal doping. As a result, both TiO_2 and ZnO-based catalysts should be the main research objects in the current context [99].

For instance, TiO_2 nanostructures, including hollow spheres or fractured nano-cup morphologies, have shown enhanced degradation efficiency due to their favourable surface properties and ability to harness sonoluminescence. These catalysts facilitate dual activation: mechanical cavitation effects and light-induced charge separation, both contributing to radical generation [100].

The combination of acoustic cavitation and catalytic enhancement creates a highly reactive environment capable of breaking down complex antibiotic molecules such as tetracycline and ciprofloxacin. These compounds are often resistant to biodegradation but are susceptible to oxidative pathways triggered by ·OH and superoxide radicals [42,50]. Sonochemical systems offer the potential to degrade antibiotics without the need for harsh chemical additives, and can be adapted to various water chemistries. In summary, sono-based AOPs provide a powerful, energy-efficient, and scalable approach to degrade antibiotics in wastewater. Their ability to operate without external reagents or light sources makes them particularly attractive for sustainable water treatment [85,101,102], especially degradation antibiotics such as tetracycline [17,43,62–65,72,103–105].

2.4. Life cycle assessment and techno-economic analysis in AOP-Based Wastewater Treatment

AOPs encompass a broad spectrum of techniques, such as sonolysis, photolysis,

Fenton and Fenton-like reactions, hybrid approaches like sono-photo-Fenton, and thermally assisted oxidative processes. Each of these technologies operates under different mechanisms and conditions, employs different energy sources and chemical reagents, and varies in terms of material inputs, particularly with regard to catalysts and reactor components. Consequently, they exhibit diverse performance characteristics, including degradation rates, energy demands, chemical consumption, and by-product formation [106].

Literature abounds with studies exploring these processes. For instance, numerous researchers have investigated the efficiency of UV-based photolysis and UV/H_2O_2 systems for antibiotic degradation, highlighting the importance of light intensity, irradiation time, and the presence of oxidants [69,82,95,98,107]. Similarly, Fenton and Fenton-like processes have been widely studied for their ability to generate hydroxyl radicals under acidic conditions, with ongoing advancements focusing on catalyst regeneration, heterogeneous catalysts, and the use of iron-bearing waste materials to enhance sustainability [108]. Sonolysis, relying on acoustic cavitation to produce reactive species, has also received attention, particularly for its synergy when combined with other AOPs. Sono-photo and sono-Fenton systems have demonstrated enhanced degradation efficiencies due to combined physical and chemical effects, although these benefits often come with increased energy consumption [109,110]. Thermal AOPs, involving elevated temperatures (30 – 80 °C) to enhance oxidation reactions, have been less explored due to their high energy demands, but certain studies indicate that moderate thermal assistance can significantly improve reaction rates and mineralization

efficiencies [104,111,112]. Across these studies, the role of catalyst design has been central. Researchers have developed a variety of catalysts, including doped metal oxides, carbon-based materials, perovskites, and nanocomposites, each offering unique advantages in terms of reactivity, stability, and reusability. However, many of these catalysts involve synthesis routes that require hazardous chemicals, high temperatures, or rare elements, raising concerns about their environmental viability.

While AOPs have received widespread attention for their high efficacy in removing persistent micropollutants—including antibiotics—from wastewater, the broader environmental and economic implications of these technologies in terms of resource use, environmental emissions, and economic viability remain underexplored [24,113–115]. All the existing studies entioned in Section 2.3 emphasize performance metrics only, such as characterization of catalysts, removal efficiency and degradation rate. However, these indicators alone are insufficient for evaluating the true sustainability and feasibility of AOP systems, particularly when considering real-world implementation. As environmental challenges grow more complex and interdependent, evaluating water treatment technologies requires a shift from purely technical or performance-based assessments to a holistic sustainability perspective.

To fill this gap, researchers and decision-makers are increasingly turning to LCA and TEA—two complementary tools that quantify the broader environmental and financial impacts of treatment technologies across their life cycles. LCA quantifies environmental impacts across the full life cycle of technology—from raw material extraction and chemical production to operational energy use and emissions. TEA, on

the other hand, evaluates economic viability by assessing both capital and operational expenditures, and increasingly, the monetization of environmental impact. When applied together, these frameworks offer a comprehensive picture of a technology's long-term performance, which is applicable beyond immediate treatment outcomes.

LCA is a systematic methodology standardized by ISO 14040/14044 [116] that evaluates the environmental impacts associated with a product, process, or system from a life cycle perspective. In the context of wastewater treatment, LCA enables the assessment of not just the treatment stage itself, but also the upstream emissions and resource inputs related to energy use, chemical production, and material synthesis (e.g., catalysts or membranes), as well as downstream impacts when data are available [116].

A typical LCA follows four key phases [117,118]:

1. Goal and Scope Definition – Establishing the purpose, functional unit (e.g., per m^3 of treated wastewater), and system boundaries (e.g., cradle-to-gate or cradle-to-grave).
2. Life Cycle Inventory (LCI) – Compiling data on material and energy inputs, emissions, and waste streams for all life cycle stages.
3. Life Cycle Impact Assessment (LCIA) – Translating inventory data into environmental impact categories.
4. Interpretation – Analysing results to identify trade-offs, data gaps, and recommendations for improvement.

In AOP systems, LCA reveals that those upstream activities—such as catalyst manufacturing, reagent production, and energy generation—often contribute significantly to the total environmental burden. For example, even chemical-free systems like sonolysis can have high carbon footprints due to electricity consumption if powered by fossil-based energy. Another critical consideration is the environmental impact of catalyst and membrane synthesis, which is often overlooked. The production of nanostructured materials may involve [119–121]:

- High-temperature processes (e.g., calcination, thermal drying),
- Hazardous chemicals (e.g., solvents, metal salts, surfactants),
- Non-renewable or rare elements, which raise concerns about resource depletion and supply chain risks.

These factors can contribute significantly to the overall carbon footprint and toxicity potential of an AOP system [122]. Therefore, sustainable process development should aim for not only high performance but also low-impact material design.

TEA assesses the economic feasibility of a technology by estimating both capital expenditures (CAPEX) and operating expenditures (OPEX), often linked to a defined functional unit (e.g., cost per m^3 or L of treated wastewater) [123–125]. Modern TEA practices increasingly include external cost accounting, where environmental impacts are monetized using established values. This allows for a more complete picture of technology's true cost, extending beyond immediate financial expenditure to encompass long-term societal and environmental costs [126].

Ultimately, integrating LCA and TEA into the development and comparison of AOP technologies is essential for identifying truly scalable, environmentally responsible, and cost-effective solutions. These tools help shift the focus from short-term treatment efficacy to long-term viability, aligning with global goals for climate resilience, circular economy, and sustainable development.

As the development of AOP technologies advances, it becomes increasingly important to assess not only "what works," but also what works sustainably. To make informed decisions, researchers and policymakers require integrated evaluation frameworks that [127,128]:

- Standardize comparison criteria across technologies.
- Include both technical performance and life cycle metrics.
- Account for both direct costs (OPEX), monetized cost from the environmental impact and the politically related cost from carbon tax.
- Enable "true cost" assessment over the full life cycle.

These frameworks are particularly important for sono-based AOPs, which may offer operational advantages such as chemical-free treatment but must also be assessed for their energy intensity and catalyst fabrication impacts. Furthermore, hybrid systems require careful analysis to ensure that performance gains do not come at disproportionate environmental or economic costs.

2.5 Rationale for the Scope of This PhD Study

The preceding sections have reviewed the growing problem of micropollutants in wastewater, particularly antibiotics such as tetracycline and ciprofloxacin. Due to their low biodegradability, environmental persistence, and potential to foster antimicrobial resistance, these compounds are now recognized as priority contaminants in both environmental and public health contexts. Conventional WWTPs are insufficient to remove antibiotics effectively, leading to the increasing adoption of AOPs as a promising remediation approach.

A wide range of AOPs—such as photolysis, Fenton-based oxidation, sonolysis, thermally assisted AOPs, and various hybrid processes—have been investigated for their capacity to degrade antibiotics at trace levels. Despite considerable research, most studies remain focused on degradation efficiency, kinetic behaviour, and catalytic activity, with less attention given to how these technologies perform in terms of long-term sustainability, environmental trade-offs, and economic feasibility.

In particular, sonochemical processes have shown significant promise due to their ability to generate highly reactive radicals without the need for chemical oxidants, their compatibility with complex wastewater matrices, and their potential for hybridization with other AOPs [129]. However, the scalability and sustainability of sono-based AOPs are not yet well understood, especially regarding energy demand, material selection for cavitation agents, and reactor design. Furthermore, the literature lacks consensus on the comparative advantages of sono-based AOPs over other techniques, particularly when

environmental and economic factors are considered alongside degradation performance. Currently, no comprehensive life cycle assessment (LCA) study provides a standardized comparison of different advanced oxidation processes (AOPs). This research gap is particularly evident for sonochemical-based AOPs, the environmental impacts of which are consistently overlooked.

In response to these gaps, this DPhil study is structured around a multi-phase investigation that integrates experimental research with life cycle and economic assessment. The overarching objective is to develop and evaluate a sustainable AOP system for tetracycline degradation, with a specific focus on sono-based technologies.

This study is guided by the following key research questions:

1. How can sonochemical AOP systems be optimized through reactor design and sonocatalyst utilization to enhance the degradation of tetracycline in wastewater?
2. What are the environmental trade-offs and improvement opportunities among different configurations of sono-based AOP systems, as revealed through scenario-based LCA?
3. What is the environmental performance associated with sono-based AOPs compared to other AOP technologies? From a sustainability perspective, which AOP technology offers the most favourable balance between degradation performance, environmental impact, and economic feasibility?

The research milestone and goals are as follows:

1. **Milestone 1:** Experimental development and performance evaluation of a novel sonochemical AOP system — Develop and test a sono-based AOP system for tetracycline degradation, focusing on optimized reactor design, cavitation-enhancing agents, and the influence of key operating parameters on operational performance and efficiency. (Chapter 3)

2. **Milestone 2:** Environmental assessment of the sono-based system through case-study-based LCA — Evaluate the environmental performance of the developed sono-based AOP system using life cycle assessment, identify key environmental hotspots, and propose improvements to reduce impacts while maintaining treatment effectiveness. (Chapter 4)

3. **Milestone 3**: Cross-technology benchmarking of AOPs using integrated LCA and TEA - Conduct a comparative life cycle and techno-economic assessment of multiple AOP technologies (sonolysis, photolysis, Fenton-like, sono-photo, and thermal oxidation) under standardized conditions for tetracycline removal, to identify the most sustainable treatment option from both environmental and economic perspectives. (Chapter 5)

Together, these milestone and research questions aim to bridge the gap between experimental development, system-level sustainability analysis and cross-technology comparison—providing a foundation for future decision-making in the design, selection, and implementation of AOPs for the treatment of antibiotic-contaminated wastewater.

Chapter 3: Efficient sonochemical catalytic degradation of tetracycline using TiO_2 fractured nanoshells

Published as: **Zong, Zhiyuan**, Emma Gilbert, Cherie CY Wong, Lillian Usadi, Yi Qin, Yihao Huang, Jason Raymond, Nick Hankins, and James Kwan. "Efficient sonochemical catalytic degradation of tetracycline using TiO_2 fractured nanoshells." *Ultrasonics Sonochemistry* 101 (2023): 106669. [17]

All the work that reported in this chapter have been done by Zhiyuan Zong

Abstract

The widespread presence of antibiotics like tetracycline in wastewater poses significant environmental and public health risks, as conventional treatment methods often fail to remove such persistent compounds. This study investigates the degradation of tetracycline using a combination of TiO_2 fractured nanoshells (TFNs) and a bespoke sonoreactor designed to generate focused and pulsed ultrasound. A comprehensive parametric study was conducted to evaluate the effects of various factors, including TFN adsorption behaviour, reaction time, initial pollutant concentration, solution pH, acoustic pressure amplitude, number of acoustic cycles, catalyst dosage, TFN reusability, and the influence of co-treatments such as visible light and hydrogen peroxide. While TFNs alone exhibited notable adsorption capacity, complete degradation of tetracycline was achieved within six minutes under optimized

sonocatalytic conditions. The process demonstrated significantly reduced power input and CO_2 emissions because of the use of converging and pulsed ultrasonic wave compared to typical values reported in similar sonocatalytic studies. These findings highlight the potential of optimized low-power sonocatalysis for efficient and sustainable micropollutant removal.

3.1 Introduction

The presence of antibiotics such as tetracycline in wastewater remains a critical environmental concern due to their persistence, resistance to biodegradation, and potential to foster antibiotic-resistant bacteria. Although various AOPs have been developed for micropollutant removal, many rely on chemical reagents or hybrid systems that pose challenges in terms of operational complexity, secondary pollution, or high energy consumption [130–132].

Sonochemical AOPs have emerged as a promising alternative, offering reagent-free degradation driven by acoustic cavitation—a process in which collapsing microbubbles produce localized hot spots with extreme temperatures and pressures. These conditions generate highly reactive species, such as hydroxyl radicals, capable of breaking down complex organic contaminants. Compared to other AOPs, sonochemistry offers potential advantages in simplicity, selectivity, and adaptability to complex water matrices [103]. However, its practical application remains limited by suboptimal energy efficiency, incomplete degradation pathways, and lack of reactor

standardization [85].

Researchers have typically focused on either reactor or catalyst design, with little attention being given to the simultaneous use of an advanced acoustic system and a cavitation agent. In addition, hybridization of different technologies [133] has often led to excessive energy consumption and CO_2 emissions, rather than utilizing a stand-alone system with optimal acoustic and sonochemical parameters.

This chapter presents a systematic experimental investigation into the sonocatalytic degradation of tetracycline using a bespoke ultrasonic reactor and TFNs [100]. The reactor is designed to generate a cylindrically focused acoustic field to enhance cavitation intensity, while the TFNs serve as cavitation nuclei and catalysts, promoting localized radical formation and mass transfer. This combination aims to overcome current limitations by maximizing degradation efficiency without the need for chemical oxidants. The experimental work includes a detailed parametric study, evaluating how different factors influence degradation efficiency and energy consumption.

By identifying optimal operational conditions, this study aims to demonstrate a more effective and potentially scalable sono-based AOP system. The results also provide a data foundation for the environmental and economic assessments that follow in Chapters 4 and 5.

3.2 Method

3.2.1 TiO_2 fractured nanoshell synthesis

Synthesis of the catalyst was carried out using sol-gel templates in two primary steps involving the synthesis of polystyrene (PS) beads and TFNs, which have been reported before [100,134,135]. TFNs are hollow, spherical nanoparticles that are proven to act as cavitation nuclei. A mixture of 5 mL styrene (Sigma) and 40 mL deionised water was stirred at 200 RPM and degassed with Argon. A stock solution of potassium persulfate (KPS, Sigma) was prepared at 160 mM, and 5 mL was added to the degassed styrene/water mixture. The resulting solution was heated under reflux at 75℃ for 5 hours, cooled to room temperature, and stored at 4℃. The concentration of polymerised solids was approximately 10 wt.%, and the resulting particles were approximately 300 nm in size, given the use of 5 mL styrene in 45 mL H_2O.

The PS particles were dispersed in absolute anhydrous ethanol (1:11 v/v) and sonicated for 10 minutes. Titanium butoxide (Reagent grade, 97%, Sigma, 0.2:2 in ethanol v/v) was added, dropwise, to the solution under stirring at 400 Revolutions per minute (RPM). The resulting mixture was stirred for 2 hours at room temperature, followed by three times washing with ethanol through centrifugation at 5000 RPM for 10 minutes. The particles were dried overnight at 60℃, and calcined at 500℃ for 3 hours with a temperature ramp of 5℃/min. After cooling to ambient temperature, the particles were collected and stored in a dry cabinet before use.

3.2.2 Acoustic reaction system

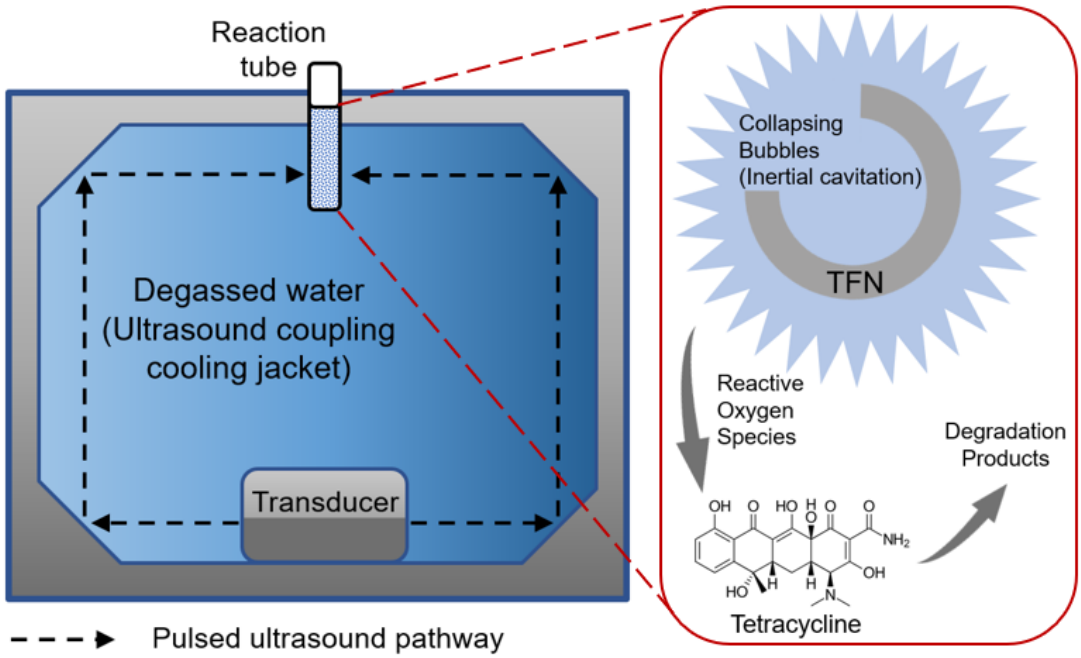

Figure 3.1. Schematic diagram of the cylindrical sonoreactor utilizing converging ultrasound for sonocatalytic degradation of tetracycline

The sonoreactor was built from 316 stainless steel with two 45° bevel conical reflectors to centralize the ultrasound to the top centre of the cylindrical reactor. Figure 3.1 shows a schematic cross-sectional representation of the bespoke sonoreactor to facilitate the proposed sonocatalytic activity for tetracycline degradation [85,102]. Photos of the transducer and sonoreactor are shown in Figure A.2

A reaction tube (5mL polyethylene test tube) was positioned at the top centre of the cylindrical sonoreactor to receive the ultrasound generated by the transducer located at the bottom, after folding the acoustic wave 180 degrees. Hydrophone measurements and subsequent experiments were conducted at 1.083 MHz. Ultrasound emitted by the piezoelectric ceramic transducer (PZT, APC International, Ltd) was reflected by the smooth conical reflector surfaces and directed to the reaction tube, which was

surrounded by cooling liquid. The transducer was supplied with the desired electrical signal using a function generator (Keysight Waveform Generator 33400A) and an amplifier (Electronics & Innovation 1040L RF Amplifier). The acoustic field in the reaction vessel was measured using a 0.2 mm diameter needle hydrophone (Precision Acoustics, SN 3222), controlled by a 3D positioning system (3-Stepping Motor Controller, Velmex VXM). The relationship between acoustic pressure and drive voltage was measured at the focal point of the acoustic field within the reaction tube. The pressure amplitudes reported were peak-to-peak amplitudes. The input voltage (a sine wave signal), current, phase angle, and maximum/minimum/peak-to-peak amplitudes were measured with an oscilloscope (LeCroy LT264). Power input, duty cycle, and energy consumption of the transducer were then calculated using the following equations (Eq 1,2,3). I and V denote the current and voltage of the ultrasonic reactor. The burst period is the length of time for which the transducer is actively sending out a burst of sound waves, and the number of cycles is the count of waves within each of those short bursts. The duty cycle (in %) compares the burst period to the entire period of one on/off pulse.

$$P = I_{rms,A}\, V_{rms,V} \cos(\theta) \qquad \text{Eq 3.1}$$

$$Duty\ cycle(\%) = \frac{Number\ of\ cycles\ /\ Frequency\ (Hz)}{Burst\ period\ (s)} \times 100\% \qquad \text{Eq 3.2}$$

$$Energy(Wh) = Power(W) * time(h) * Duty\ cycle(\%) \qquad \text{Eq 3.3}$$

Pulsed-wave ultrasound bursts were employed to enhance the cavitation probability and reduce the energy consumption, rather than employ conventional continuous wave excitations. The amplitude, frequency, number of cycles, and burst

period of the ultrasound exposure were controlled by the waveform generator. Static capacitance and impedance were measured using an LCR meter (BK precision 879B) and an impedance analyser (Digilent Analog discovery 2), respectively. Table 3.1 lists the base case experimental parameters.

3.2.3 Sonocatalytic degradation of tetracycline

To prevent cavitation outside the reaction tube and to protect the transducer crystal from overheating, degassed water was used as the coupling and cooling medium. A degassing system, consisting of a circulating positive-displacement diaphragm pump feeding the lumenside of a membrane contactor (3M Liqui-Cel™ G541) with shellside vacuum (<100 mbar), continuously degassed the cooling water for approximately 20 minutes until the oxygen concentration in the water reached 20% (Duo pH/Ion/DO meter SG98, Mettler Toledo). The degassed water was then introduced into the cooling jacket at a low flow rate to avoid gas bubble formation.

To prepare the tetracycline solution, tetracycline powder (Fisher Scientific) and type 1 water (Millipore Direct Q5-UV) were mixed. In base case experiments, the concentration of the tetracycline was set to 40 mg/L. Even though the concentration of tetracycline found in the wastewater is often much lower, this concentration was chosen to ensure precise measurement with our HPLC equipment. It also allows for a direct comparison with the methods and results of previous studies, which is necessary for the life cycle and economic comparisons discussed in Chapters 4 and 5. To measure the maximum catalyst adsorption, TFNs and the tetracycline solutions were mixed and

stirred in a dark place over time and up to 180 minutes. The absorption portion at different time and concentration will be subtracted from the degradation results. For the sono-catalytic experiment, 1.5 mg of TFNs were added to a reaction tube followed by 3 mL of the tetracycline solution before sealing. Prior to the reaction, air was charged into the tetracycline solution by shaking the reaction tube. If experiments proceeded for longer durations, the solution was recharged with gas by shaking every two minutes. After the reaction, the sample was collected, and nanoparticles were removed by centrifugation at 12,200 rpm for ten minutes.

The supernatant was gathered and subjected to analysis through High-Performance Liquid Chromatography (HPLC) using a Shimadzu LC-2030C 3D plus instrument. The concentration of tetracycline was determined utilizing a well-established analytical method from Sigma Aldrich [136], where tetracycline concentration was computed based on the peak area observed at a retention time of 5.4 minutes. The catalytic removal efficiency was calculated using equation 4 below. Both the adsorbed portion by TFNs and the unreacted amount were subtracted from the initial concentration to show the net removal efficiency by catalytic reactions. The % conversion in Eq 3.4 and the following figures represents the removal of the parent rather than the mineralization of tetracycline.

$$Catalytic\ \%\ conversion\ = \frac{C_0 - C_t - C_{ads}}{C_0} \qquad \text{Eq 3.4}$$

Furthermore, the degradation values are based on subtracting dark adsorption measurements. The adsorption equilibrium under ultrasonic irradiation may differ from static conditions, as ultrasound irradiation may alter the adsorption kinetics and capacity.

This means the reported efficiencies are operational estimates of the sonocatalytic contribution, which may still include a marginal uncertainty due to this dynamic.

All experiments were conducted in triplicate, and the error bars presented in the graphs indicate the standard deviation of the replicates' results. The used catalyst is centrifuged at 10,000 RPM, and the supernatant is removed after centrifuge. The separated catalyst was dried using a vacuum oven overnight to remove any liquid residue and used for the reusability test. The intention of this aspect of the study was to determine whether TFNs could maintain stable performance under optimum acoustic parameters when collected, dried, and subsequently re-employed in degradation reactions and whether the adsorbed tetracycline could poison the catalyst. Factors that potentially affect tetracycline degradation were investigated, including initial concentration, pH, catalyst dosage, and acoustic parameters. The pH was adjusted using 0.1M HCl or NaOH.

The effect of hybridized AOPs with the sono-catalytic process was also explored. The impact of the external light source, provided by the most readily accessible and affordable visible light, on photocatalysis was assessed by directly applying LED light (EasyLED Microscopy Illumination, Schott) to the top of the reaction tube. To test the existence of ROS and the effect of hydroxyl radicals, ethanol (pure, anhydrous, Sigma) and H_2O_2 (35% w/w in water, Sigma) were employed as the hydroxyl radical booster and scavenger, respectively.

Table 3.1. Base case experimental parameters of tetracycline degradation

Tetracycline concentration (mg/L)	40
Volume (mL)	3
Number of cycles	100
Burst period (ms)	1
Frequency (MHz)	1.083
Duty cycle (%)	9.23
Static capacitance (nF)	17.1
Impedance (Ohm)	9.6
Acoustic pressure (MPa $_{PKPK}$)	12.9
Peak power (Watt)	225
Reaction time (minutes)	6
Temperature profile	[85]
Catalyst dosage (mg/mL)	0.5

3.2.4 Preliminary energy and emission assessment

An environmental analysis was conducted to quantify the CO_2 footprints of various sono/photo-based AOP technologies used to degrade low-concentration, i.e., <50 Parts per million (mg/L) tetracycline. The conversion of tetracycline in the selected studies should be at least 70% to ensure sufficient degradation. The optimal operation

conditions were selected for each study, such as catalyst dosage and power input. Embodied CO_2 and relative greenhouse gas (CH_4, SO_x, NO_2) emissions from both electricity generation and chemical production were also considered. The power input included any equipment used, such as an ultrasound sonicator or a UV/Xenon lamp. The carbon footprint for electricity generation was assumed to be Europe's average of 0.279 kg/kWh [137]. Based on the GREET@ model, the overall CO_2eq produced in a 100-year global warming potential is 1.2 kg CO_2eq per 1 kg of hydrogen peroxide produced [138]. The specific CO_2eq emission was calculated using the following equation (Eq.5):

$$Specific\ CO_2\ emission\ = \frac{CO2_{ultrasound} + CO2_{light} + CO2_{chemical}\ (kg)}{Trtracycline\ degraded\ (g)} \quad \text{Eq 3.5}$$

3.3 Results

3.3.1 Sonocatalytic degradation of tetracycline

The TEM image in Figure A.1 confirmed the shape of the TFNs, with an average particle size of approximately 260 nm. The ratio of PS to Titanium Butoxide during catalyst synthesis affected the shell thickness. The optimal 5:1 ratio for the conversion was shown in Figure A.3.

Figure 3.2(a) shows the adsorption potential of tetracycline by the TFNs. Surprisingly, TFNs continuously adsorbed tetracycline for two hours, instead of reaching adsorption-desorption equilibrium in 30 minutes, as previously reported for other catalysts [62,63,139,140]. Q_E and Q_t were the amount of tetracycline absorbed

(in % at the given concentration) at equilibrium and at a given time, respectively [141]. In the first six minutes, TFNs adsorbed around 8% of tetracycline (40 mg/L) and the equilibrium adsorption was approximately 50%. The adsorption trend followed the pseudo-first-order adsorption film model [25]. To show the net degradation, fresh catalysts were used in experiments, and the adsorption portion was subtracted.

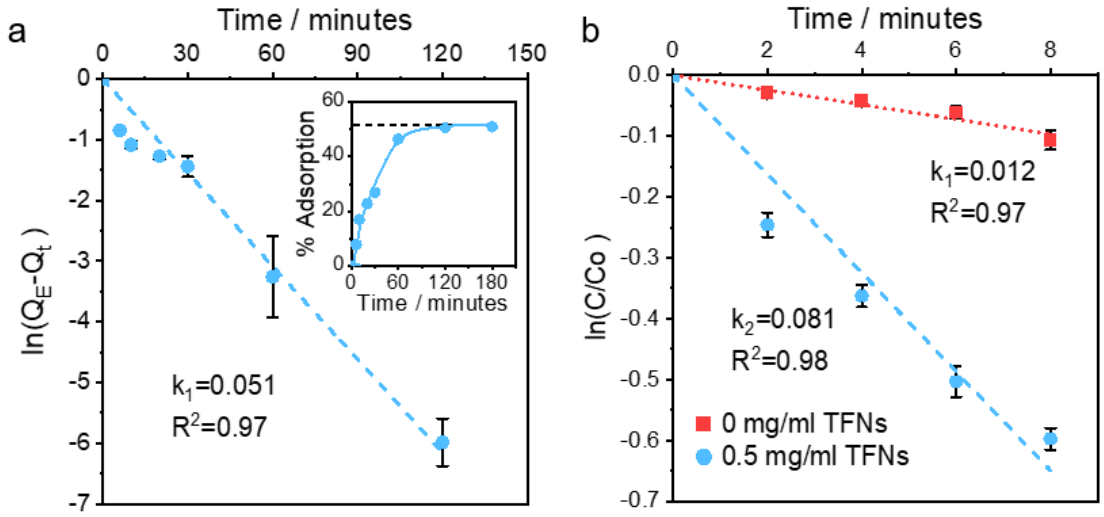

Figure 3.2. Tetracycline adsorption and degradation over time with base case acoustic parameters (experimental conditions given in Table 3.1)

(a) Linearized plot for Pseudo-first order adsorption in first two hours (Insert: long-term adsorption (three hours) in a dark place until the adsorption-desorption equilibrium was reached). (b) First-order degradation with and without catalyst for the initial eight minutes (units of rate kinetics: min^{-1}).

The effect of employing the catalyst was compared to non-catalytic degradation, and Figure 3.2(b) displays the results for both reaction scenarios over eight minutes. Both exhibited linear first-order degradation. After 8 minutes, the non-catalytic reaction degraded 10.1% of tetracycline, showing noticeable degradation without any catalyst

or chemicals present. However, applying 0.5 mg/mL TiO_2 as a catalyst significantly enhanced the final conversion to 40%, including 8% adsorption and 32% degradation, which showed the promise in stimulating cavitation to increase the number of free radicals and enhance the reaction rate.

The adsorbed tetracycline is not permanently retained. It can be subsequently degraded on the catalyst surface by reactive oxygen species or desorbed back into the bulk solution due to ultrasonic mixing and cavitational shear forces, where it is further degraded. Thus, adsorption is a key intermediate step in the overall remediation process.

Micropollutants in wastewater are typically present at low concentrations, which makes them difficult to remove. The sonocatalytic activity was found to be suitable for various initial concentrations (5-40 mg/L) of tetracycline. Figure 3.3(a) shows that, at a fixed reaction time, the percentage level of both adsorption and degradation gradually decreased as the initial concentration increased. Tetracycline was no longer detectable in the aqueous phase (i.e., 100% removal) at a low initial concentration of 5 mg/L within a time of six minutes. The conversions were over 90% and 80% for initial concentrations of 10 and 15 mg/L, respectively. The presented sonocatalytic activity showed remarkable efficacy in the rapid treatment of low-concentration tetracycline.

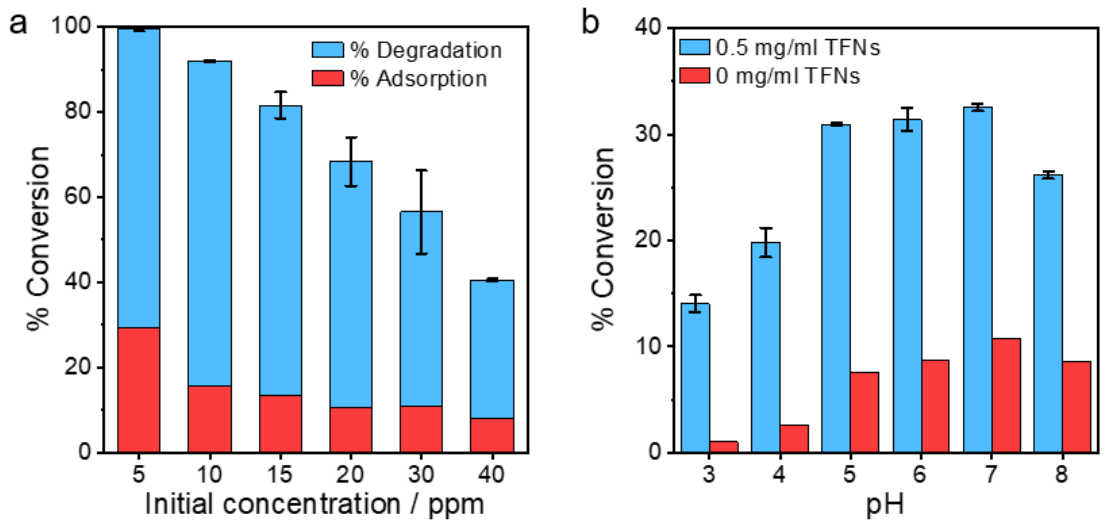

Figure 3.3. Tetracycline degradation under different conditions with base case acoustic parameters (experimental conditions given in Table 3.1). (a) varying initial concentrations (5-40 mg/L) (b) varying pH (3-8)

In Figure 3.3(b), the most significant difference in net conversion between catalytic and non-catalytic degradation was 23% at pH 6 and 7. TFNs, across all pH levels, substantially enhance the degradation rate. Compared to tetracycline degradation relying solely on the stochastic homogeneous-phase inception of cavitation, TFNs are cavitation nuclei. Specifically, the gas trapped on the TFNs facilitates the nucleation of cavitation bubbles at sub-resonant frequencies, leading to the subsequent inertial collapse of bubbles and the production of hydroxyl radicals. Therefore, TFNs ultimately reduce the energy required for cavitation and ensure that cavitation occurs near TFNs. The proximity of cavitation also activates the catalytic effects of the titanium dioxide to further amplify the production of reactive oxygen species (ROS) [100,142]. These heterogenous nuclei significantly enhance cavitation events and the generation of ROS, thus greatly benefiting the degradation of tetracycline. This pH range between 5 and 6

proved optimal for the TFNs to contribute the most to tetracycline conversion. Tetracycline is characterized by three pKa values: 3.3, 7.7, and 9.7, attributable to the presence of three distinct acidic functional groups [143]. The sonocatalytic activity was found to be more effective when operating at the point of zero charge (pH_{pzc}) of the catalyst. Due to its functional groups, tetracycline can accept or donate protons. When the pH was far below pH_{pzc}, electrostatic repulsion was created between the cationic tetracycline molecules and the positively charged catalyst surface, while a high pH environment created the opposite case- electrostatic repulsion between anionic tetracycline molecules and the negatively charged catalyst surface, thereby hindering the degradation rate [70,82]. The previous XRD scan showed that the crystallographic structure of TFNs was anatase [100]. The average pH_{pzc} of anatase TiO_2 was 5.8, which was in accordance with our observation above [144].

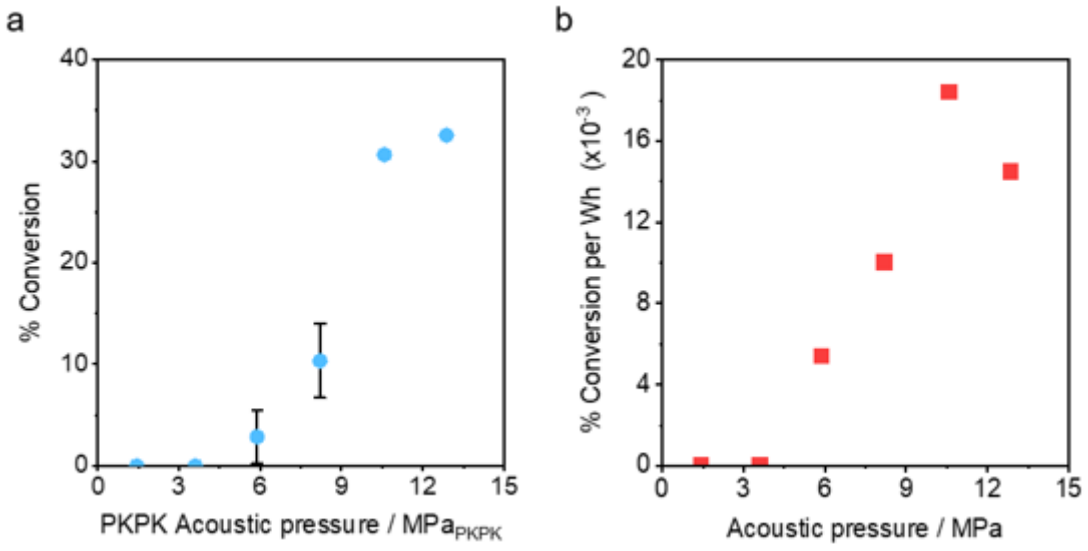

Figure 3.4. Tetracycline degradation under different acoustic pressures in six minutes. (experimental conditions given in Table 3.2)

Table 3.2. Acoustic parameters of tetracycline degradation under different power inputs

and acoustic pressures

Parameters	Sonoreactor				
RMS voltage / Vrms	17.6	28.8	40.2	51.8	63
RMS Current / Arms	1.17	1.84	2.58	3.22	3.92
Phase angle / degree	10	32	100	320	1000
Peak Power / W	20.6	53	103.7	166.8	225
Acoustic Pressure / Mpa $_{PKPK}$	3.7	6	8.3	10.6	12.9

Duty cycle measurements
Frequency / MHz: 1.083
Number of cycles: 100
Burst period / ms: 1
Duty cycle / %: 9.23

Table 3.3. Acoustic parameters of tetracycline degradation under different numbers of cycles and burst periods at a fixed duty cycle.

Parameters	Sonoreactor				
Time / min	6	6	6	6	6
Frequency / MHz	1.083	1.083	1.083	1.083	1.083
Number of cycles	10	32	100	320	1000
Burst period / ms	0.1	0.32	1	3.2	10
Duty cycle / %	9.23	9.23	9.23	9.23	9.23

Power measurements
RMS voltage / Vrms: 63
RMS Current / Arms: 3.9

Phase angle / degree: 23.73
Peak Power / W: 225

The current study also investigated the impact of acoustic pressure and the number of cycles in the acoustic wave burst on the sonocatalytic degradation process. Operational parameters are presented in Table 3.2 and Table 3.3.

Under a particular band and frequency, the higher acoustic pressure can produce higher accumulated broadband noise amplitude, namely the inertial cavitation dose [145]. Figure 3.4 illustrates the relationship between acoustic pressure and degradation rate, indicating that higher acoustic pressure resulted in an increased degradation. The minimum acoustic pressure required for detectable degradation was 6 MPa and the curve is characterized by a moderate increase in conversion from 3.7 to 8.3 MPa, whereas the degradation rate exhibited a significant increase from 8.3 MPa to 10.6 MPa. After 10.6 MPa, the conversion increased more slowly again. One possible explanation for these observations is as follows. The increase in acoustic pressure from 3.3 to 6 MPa initiated cavitation. The degradation rate then significantly increased from 6 MPa to 10.6 MPa, potentially due to the rapid increase in the amount and intensity of cavitation in this regime. After reaching 10.6 MPa acoustic pressure, the rate of increase slowed down, potentially due to the saturation of the inertial cavitation dose [145,146]. To enhance economic competitiveness, it is crucial to exploit the regime of potential rapid increase in degradation caused by cavitation, which lies below the saturation regime. At 10.6 MPa, the sonocatalytic activity achieved the highest conversion per unit of energy consumed (Wh), making it ideal for energy-efficiency purposes. Operating the

reaction at the optimal acoustic pressure below the inertial cavitation dose saturation regime resulted in the highest energy efficiency (18.5%/Wh 10^{-3}).

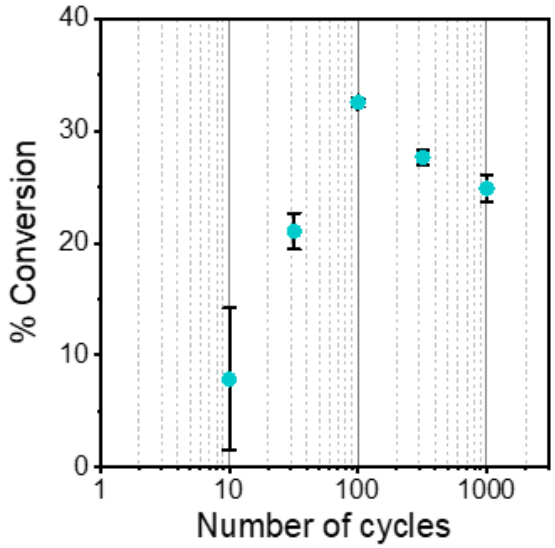

Figure 3.5. Tetracycline degradation under different numbers of cycles (experimental conditions given in Table 3.3)

The number of cycles in the acoustic wave burst was found to affect cavitation performance, as shown in Figure 3.5. Testing was conducted using different numbers of cycles ranging from 10 to 1000, and burst periods were adjusted to maintain a constant duty cycle of 9.3% and a constant power input. The optimal duty cycle was found to be 100 cycles, yielding the highest conversion. The degradation rate decreased significantly at low cycle numbers, most likely due to insufficient acoustic pressure to initiate inertial cavitation consistently and repeatedly within the sample volume. Exceeding 100 cycles resulted in a lower conversion and had less pronounced effect than was seen for bursts of less than 100 cycles. During longer cycle periods, it is possible that cavitation only occurs in the early period of the burst and bubbles later dissolve in the liquid, resulting in a decrease in the number of cavitation sites and a

generally reduced cavitation efficiency [147]. Overall, the trend of degradation performance at different cycle numbers was consistent with previously reported research [85,148].

3.3.2 Influencing factors of the tetracycline degradation process

The investigation and discussion regarding TFNs' reusability and lifetime are crucial for demonstrating their applicability in industrial wastewater treatment. This information will further facilitate subsequent process-level optimization and economic competitiveness analysis. Figure 3.6(a) exhibits the reusability of the TFNs, showing that its catalytic performance remained stable, with less than a 1% change in the first four runs of use, and it had an insignificant drop following the fifth run. In general, the TFNs were found to be suitable for continuous work, although intensive short-time decontamination was preferred due to the reduced efficiency associated with longer bursts. It is a good sign that we do not need to remove the adsorbed tetracycline between runs and have it still functioning. It suggests that the adsorbed tetracycline does not appear to poison the catalyst.

The relationship between catalyst loading and degradation rate was studied. The reaction rate was not linearly proportional to the catalyst dosage. Finding the optimum catalyst loading rate was necessary to improve economic viability by avoiding catalyst overdose. In Figure 3.6(b), the catalytic degradation rate at different catalyst dosages was compared to non-catalytic degradation. The net degradation was calculated by

subtracting the adsorption portion at different catalyst dosages. The results showed that the catalytic degradation rate was significantly higher than the non-catalytic degradation, even with only 0.3 mg/mL of catalyst added. The catalyst promoted inertial cavitation by providing nuclei. However, an excessive catalyst dosage had a negative effect, and the degradation percentage (conversion) gradually decreased when the catalyst dosage was increased over 0.5 mg/mL. This suggested that the catalyst dosage affected the relative degradation rate. The underlying reason for this could be that insufficient micro gas bubbles in the solution were present and provided limited cavitation potential. Also, excessive catalyst dosage made the sample turbid and viscous, hampering both ultrasound transmission and the probability of cavitation. Agglomeration can also occur, reducing degradation if the catalyst is overdosed [82,139]. The optimal catalyst dosage is a trade-off between a satisfactory degradation rate and a high economic viability.

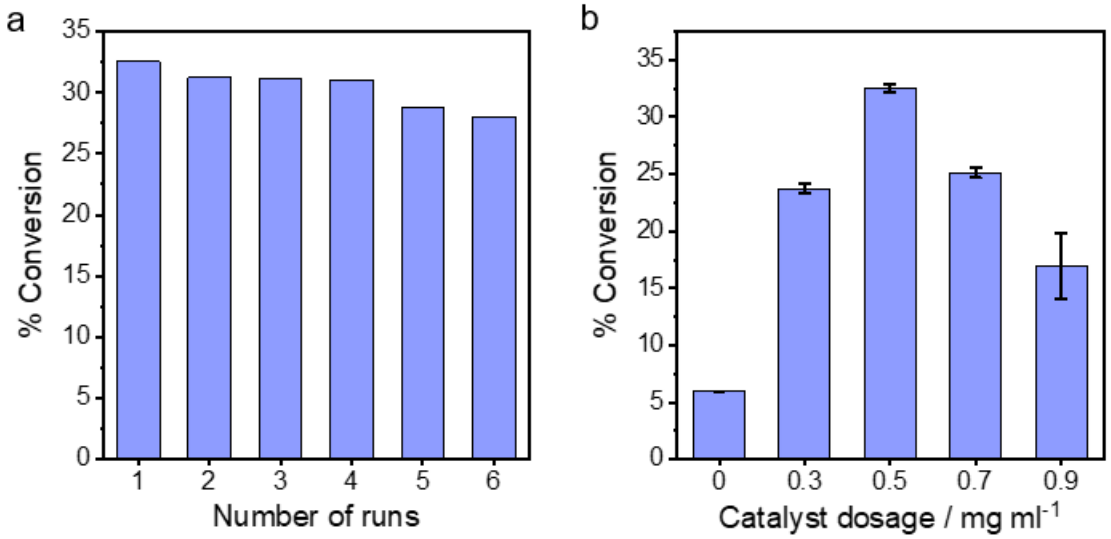

Figure 3.6. Catalyst performance of tetracycline degradation (a) The reusability of TFNs. (b) Effect of different catalyst dosages (experimental conditions given in Table

3.1)

The TiO_2 particles also responded photo-catalytically, particularly the anatase TFNs which were the most active polymorph for photocatalytic performance [149]. A photocatalyst is also a light-sensitive semiconductor with a band gap lying between the valence and conduction bands, which varies with the material composition [91,92]. Under light irradiation, electrons in the valence band jump to the conduction band, leaving behind holes (h+) that are highly reactive. The holes react with water and generate hydroxyl radicals and hydrogen ions through a chain reaction [92]. In this study, sono-photocatalytic degradation was observed to occur when external light sources such as visible light were directly applied. In Figure 3.7, the conversion increased by 2% when the external LED light and TNFs were used in combination, as compared to the sonocatalytic degradation by the standalone TFNs.

As an emerging technology, sonocatalysis can be combined with conventional AOP water treatment methods. Hydrogen peroxide (H_2O_2) is a well-known oxidative chemical used in wastewater treatment, and is considered the basic chemical AOP because it decomposes to release hydroxyl radicals. Compared to the non-catalytic benchmark test (0 mg/mL TFNs, six minutes), the addition of one μmol of H_2O_2 increased the degradation rate from 6% to 22% in six minutes. When H_2O_2 and TFNs were used simultaneously, the degradation percentage further increased to 36%. With the combined use of all boosters in terms of TFN, H_2O_2, and light, the degradation reaches 45%.

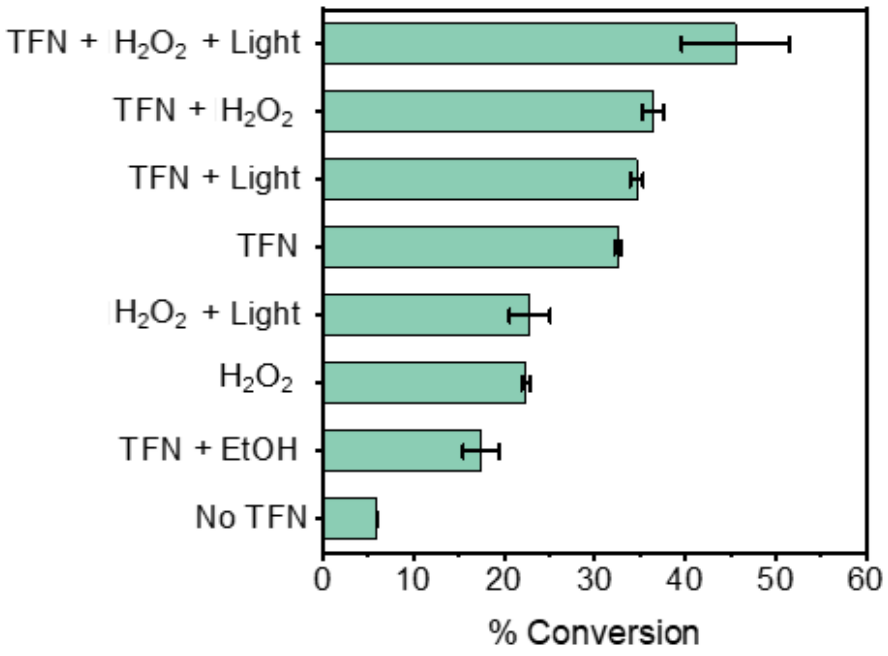

Figure 3.7. Tetracycline degradation with different catalytic boosters and hole scavengers (experimental conditions given in Table 3.1).

To confirm the existence of ROS, one μmol of ethanol was utilized as a hydroxyl radical scavenger. When ethanol was introduced into the reaction, it was observed that the sonocatalytic conversion decreased significantly to 17%, in contrast to the value of the conversion seen without adding the scavenger (32%), suggesting that the hydroxyl radical was scavenged by ethanol thus limiting the ROS potential. An enhanced conversion rate was observed upon the application of H_2O_2 (36%), underscoring the pivotal role played by hydroxyl radicals in the degradation of tetracycline. Another potential explanation for the conversion decrease was that ethanol also acted as a hole scavenger [150]. In comparison to the use of an external light source only, highly intensive cavitation also generates light by itself, which is referred to as sonoluminescence. Light emissions from sonoluminescence are known to have a high intensity and a wide range of wavelengths, ranging from 200 to 700 nm [93]. When the

energy of this light exceeds the band gap of the semiconductor catalyst, similar photocatalytic phenomena are known to occur [91,92,94]. By incorporating TFNs, the cavitation occurring in proximity to these nuclei may amplify the production of ROS. Inertial cavitation in the designed system becomes less stochastically distributed throughout the water but rather becomes concentrated around heterogeneous nuclei. This localized and intensified cavitation may induce sonoluminescence and efficiently activate the light-sensitive catalyst surface for further in-situ ROS generation [151]. This nanostructured catalyst has been shown effective in degrading methylene blue dye with substantially reduced energy consumption, which was attributed to the synergistic effects of both sonochemical and photochemical processes [100]. Ethanol can block the hole, hinder the potentially existing sonoluminescence, and hamper ROS generation from photocatalytic reactions.

We hypothesize that enhancing the sonoluminescent activation phenomena can effectively improve the overall catalytic performance. Modification methods, such as metal doping, can shift the band gap and affect catalytic performance, as shown in Figure A.4, where the TiO_2 shell doped with iron enhanced the conversion by 6%. Compared to the direct application of external light sources, maximizing the efficiency of sonoluminescence can help develop highly efficient and economically viable technologies to address micropollutant persistence in wastewater, thereby enhancing environmental protection [152].

Through the combination of multiple AOP technologies, free radicals were generated from various sources, including the decomposition of the H_2O_2 reagent, water

pyrolysis, cavitation collapse, and photocatalytic action. The combined effects of sonocatalytic activity, external light stimulation, and H_2O_2 oxidation resulted in a significant enhancement of overall conversion to 45.5% in Figure 3.7. These findings indicate that combining these multiple AOP technologies simultaneously increases the overall removal efficiency.

3.3.3 Preliminary energy and environmental assessment

Figure 3.8 presents a summary of the recently published studies on the sonocatalytic degradation of tetracycline, comparing their energy efficiencies. The efficiency denotes the amount of electrical energy required to degrade one gram of tetracycline in a low-concentration (<50 mg/L) aqueous environment. The combined use of converging ultrasound and TFNs required nearly one order of magnitude less electricity than previous studies (Figure 3.8), regardless of whether external light was applied or not. Furthermore, ultrasound frequency appears to correlate with specific energy consumption per unit. Lower frequencies allow bubbles to grow for longer, whereas higher frequencies generate more inertial cavitation bubbles with shorter growth time. The efficiency of sonochemistry can be improved by designing advanced sonoreactors that utilize high-frequency ultrasound.

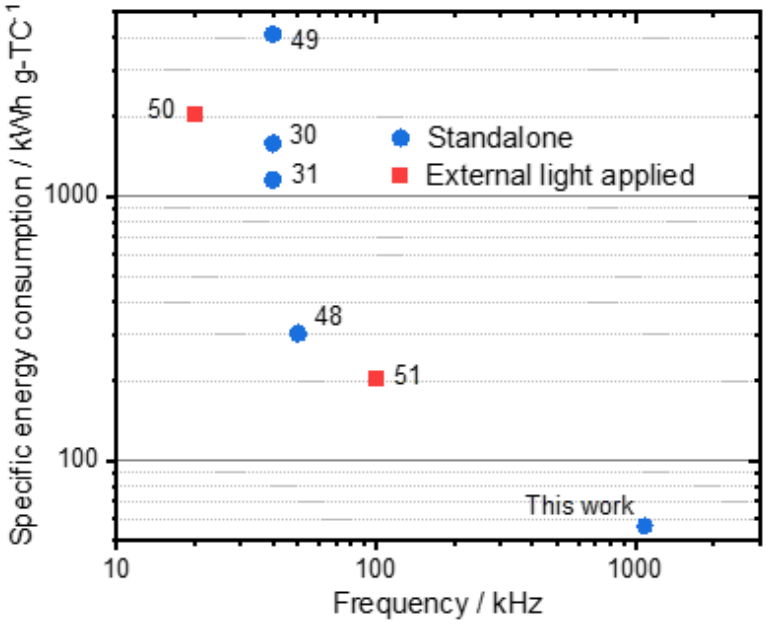

Figure 3.8. Comparative plot of specific energy consumption (kWh/g-TC) for sonocatalytic degradation of tetracycline at low concentrations (<50 mg/L). Standalone: [62–64,105]; External light applied:[71,73].

Studies suggest that the degradation efficiency can be significantly enhanced by combining physically based AOPs with additional chemicals, such as the Fenton process. The Fenton reaction, considered one of the most reliable AOP technologies, was proposed over 100 years ago [55]. The Fenton process relies on hydrogen peroxide solution as an oxidant, and ferrous iron as the catalyst [56,57]. Despite the advantages, the environmental impact of hydrogen peroxide production remains a concern, encouraging research to find more sustainable production methods.

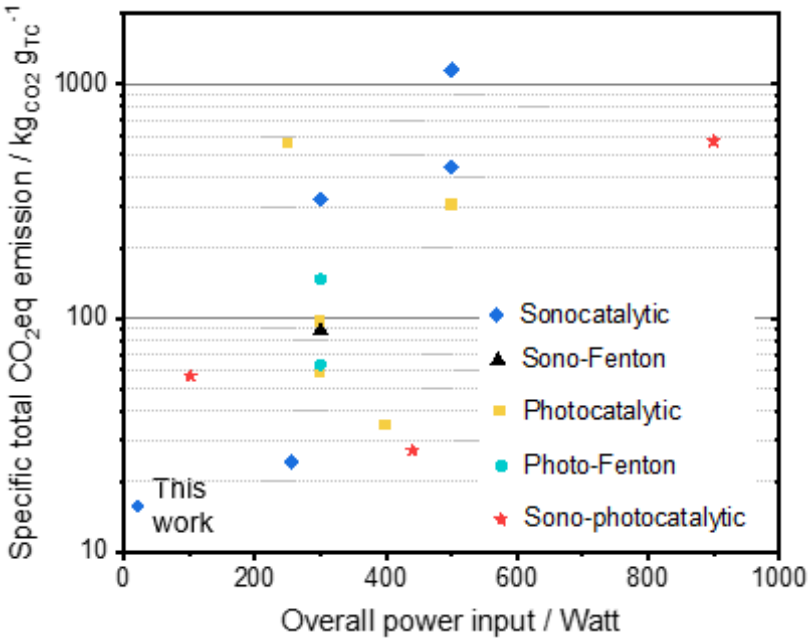

Figure 3.9. Total CO_2eq emission of different AOP methods to degrade tetracycline.

Sonocatalytic [62–65,105]. Sono-Fenton: [76]. Photocatalytic: [66–70]. Photo-Fenton: [74,75]. Sono-photocatalytic: [71–73]. Plotted against power input. Note: Power input is used here instead of energy consumption due to the unique nature of the sonoreactor employed, which operates with a pulsed waveform and extremely low duty cycle (9.23%) and power input (~21 W), unlike conventional continuous-wave systems such as sono-tips/baths or UV/visible light sources.

Figure 3.9 indicates that while hybrid processes might improve degradation performance, the CO_2 emission per unit pollutant degradation was sometimes higher than the standalone physically based AOPs. Moreover, it was found that low specific energy consumption was not achieved with high overall power input. For instance, although the combination of a conventional lamp and ultrasound bath demands significant power, it yields suboptimal results [71]. This finding applied to our proposed process and other sono/photo-based AOPs, suggesting that constantly improving

desired technologies was more effective than overloading different technologies simultaneously. Operating the reaction with low power (21 W) in a suitable regime was recommended. As shown in Figure 3.9, our proposed simple method, which used a specially designed sonoreactor and sonocatalyst, received the highest environmental credit based on CO_2 emissions compared to all other sono- and photo-based processes. The utilization of free radicals in order to minimize the adverse effects of micropollutants in the aquatic environment necessitates further investigation.

3.4 Discussion and outlook

While this chapter demonstrates the promising performance of a bespoke sono-reactor and TFNs for tetracycline degradation, several limitations and constraints should be acknowledged to frame the scope of the findings and guide further analysis.

First, the energy consumption and CO_2 emission estimates provided here are based only on the operational phase of the reaction—specifically, the energy required to power the ultrasound system and the use of chemical reagents such as hydrogen peroxide. Although this offers a useful preliminary comparison with other AOP systems, it does not include upstream or embodied emissions, such as those associated with catalyst synthesis, material processing, or infrastructure. Furthermore, the CO_2 emissions were calculated using simplified equations and fixed emission factors, rather than through a comprehensive and standardized LCA framework.

Second, differences in experimental setups—including reactor design, ultrasound

frequency, transducer power, and scale—pose challenges for comparing energy efficiency across studies. Equipment specifications are often not standardized, and discrepancies in acoustic field control, batch volumes, or power calibration introduce uncertainties when attempting to benchmark performance against other sono/photo-based systems in the literature.

Third, the comparative energy and emission assessments conducted here were based on studies that varied significantly in their tetracycline concentrations, reaction durations, and operational performance. As a result, while the current analysis provides valuable insight into the relative energy performance of the proposed system, the comparisons should be interpreted cautiously, as they may not fully reflect standardized or “apple-to-apple” conditions.

In the next chapter (Chapter 4), these limitations will be systematically addressed by applying a cradle-to-gate LCA This will allow for a more comprehensive evaluation of the environmental and economic performance of the proposed system. The analysis will include upstream emissions from catalyst production, embodied energy inputs, and system-wide operational impacts. Optimization scenarios will also be explored to identify design and operational strategies that reduce the environmental footprint while maintaining or improving treatment efficiency.

Together, these subsequent assessments will complement the experimental findings presented here and offer a broader view of the sustainability and practical viability of sonocatalytic AOPs in wastewater treatment.

3.5 Conclusion

This study demonstrated effective tetracycline degradation using a bespoke sonoreactor coupled with TFNs. The optimized system achieved rapid removal of low-concentration tetracycline (3 ml, 5 mg/L) within six minutes under a low power input of 21 W. TFNs exhibited high adsorption capacity, strong catalytic performance, and good reusability. The optimal degradation occurred near the pHpzc of anatase TiO_2, and the role of hydroxyl radicals was confirmed through scavenger and booster experiments.

Energy efficiency was maximized by operating just below the saturated inertial cavitation regime (~10.6 MPa), emphasizing that optimizing reactor and catalyst design is more effective than hybridizing multiple AOP methods. Compared to similar studies, the proposed system achieved the lowest reported power input and CO_2 emissions for tetracycline degradation.

However, this chapter focused only on operational-phase energy use and emissions. Embodied emissions from catalyst synthesis, such as upstream emissions of metal used, chemical consumption during the synthesis, electricity and heat demand, were not considered. The degradation performance under different scenarios was studied with a focus on degradation performance-oriented metrics, but an environment-oriented comparison was not conducted. These aspects will be addressed in the next chapter through an LCA-based optimization, providing a more comprehensive evaluation and pathway for system-level improvement.

Chapter 4: Process-level environmental-oriented case study of sonochemical degradation of tetracycline

Part of the following results were presented at the conference.

Zong, Zhiyuan, and Nicholas P. Hankins, “Sonochemical catalytic removal of antibiotics using converging ultrasounds and cavitation agent with life cycle assessment”. VI Iberoamerican Conference on Advanced oxidation Technologies (6th CIPOA), Florianopolis, Brazil, October 7th -11th , 2024

All the work that reported in this chapter have been done by Zhiyuan Zong

The conceptual framework of modelling and analytical methods is supported by a published paper in *Water Research*.

Zong, Zhiyuan, Omar Daoud, Nicholas P. Hankins, Qianhong She, and Christian D. Peters. "Valorising Desalination Brine for Green Cement Production: Toward Mitigating Global CO2 Emissions." *Water Research* (2025): 123930. [19]

Abstract

This chapter presents a process-level environmental evaluation of sonochemical AOPs for the degradation of tetracycline in wastewater. Building on experimental

results from Chapter 3, multiple operational scenarios—including blank cavitation, TFN-based sonocatalysis, and H_2O_2-assisted systems—were analyzed using standardized life cycle inventory benchmarking and LCA tools and methods (SimaPro, Ecoinvent, IPCC 2021, CED 1.1). The results showed that although TFNs enabled faster degradation with lower energy input, the embodied emissions from catalyst synthesis became dominant under low-carbon electricity conditions. Sensitivity analysis revealed that TFNs offer better environmental performance in most current national electricity grids, but H_2O_2 may become preferable with wider access to ultra-low-carbon electricity. To mitigate catalyst-related emissions, a continuous-flow system using metal foams as cavitation agents was proposed and evaluated. Despite the slower rate, this system achieved a 29% reduction in CO_2 emissions due to minimal material processing needs. These findings emphasize the importance of environmental-informed design in wastewater treatment and highlight the trade-offs between performance, materials, and system configuration.

4.1 Introduction

As demonstrated in Chapter 3, the sonocatalytic degradation of tetracycline using a bespoke ultrasonic reactor and TFNs offers promising potential for antibiotic removal from wastewater. However, while degradation efficiency and operational performance are often the primary focus of experimental studies [62,72,103,105,153], these performance metrics alone do not capture the full environmental implications of the treatment process. In real-world applications, the goal is not only to eliminate pollutants but to do so in a way that minimizes the overall environmental burden. A process that achieves rapid degradation but requires large energy inputs, rare materials, or intensive chemical usage may ultimately compromise the environmental benefits it aims to deliver.

To address this critical gap, this chapter presents a process-level, environment-oriented case study that reinterprets the experimental scenarios from Chapter 3 through the lens of environmental sustainability. Rather than focusing solely on removal rates or reaction mechanisms, this analysis quantifies and compares the climate change impacts—specifically, greenhouse gas emissions measured in terms of global warming potential (GWP)—associated with different tetracycline degradation scenarios. GWP was selected as the primary metric because climate change is one of the most universally recognized and policy-relevant environmental challenges. Additionally, greenhouse gas (GHG) emissions data are more consistently available across the assessed processes, enabling a more robust and comparable analysis. While other impact categories—such as toxicity, eutrophication, or resource depletion—are also

important, they often require more detailed chemical fate modelling or data that are not readily available for early-stage experimental systems. These additional metrics are recommended for future, more comprehensive assessments. The goal is to identify configurations that strike an optimal balance between degradation performance and environmental footprint.

This study responds to a broader challenge in the field: the lack of integration between laboratory-scale experimental research and life cycle-based environmental assessment. While many existing studies evaluate treatment technologies based on either performance or sustainability [21–23,27], few have attempted to combine these perspectives within a unified decision-making framework. This chapter aims to fill that gap by using LCA principles to contextualize experimental results, thereby enabling a more holistic understanding of process efficiency.

In addition to scenario-level comparisons, a sensitivity analysis is performed to examine how key operational factors—such as energy source, catalyst reuse, and system configuration—influence the overall carbon footprint. The outcomes are intended to inform both researchers and practitioners on how to select or modify sonochemical treatment processes under different real-world constraints.

Finally, the chapter presents a system-level improvement strategy in which the original batch system is modified into a continuous-flow design. Alongside this, a simplified metal-based cavitation agent is substituted for the synthesized TFNs to reduce emissions associated with material preparation. The environmental performance

of this improved setup is benchmarked against the original design to explore trade-offs between process complexity, material intensity, and sustainability.

The outcomes of this chapter contribute to a broader understanding of how sonochemical AOPs can be optimized not only for performance but for environmental sustainability. While this study focuses on process-level comparisons within a single technology, further cross-technology benchmarking will be addressed in the next stage of the research.

4.2 Method

4.2.1 Benchmarking the life cycle inventory assessment

In order to conduct a meaningful and comparable LCA across different technologies and operational scenarios, it is essential to establish a standardized approach to constructing the LCI [118,154]. One of the core challenges in environmental impact assessment—particularly in experimental and lab-scale studies—is the lack of consistency in reporting energy and material usage [155]. The heterogeneity in experimental setups, catalyst synthesis protocols, and laboratory-scale equipment usage makes direct comparison of environmental performance between studies inherently unreliable.

For example, common equipment used during catalyst synthesis and experimental preparation—such as furnaces, drying ovens, vacuum dryers, ultrasonic baths, magnetic stirrers, centrifuges, and filtration units—can vary widely in capacity,

efficiency, and operation time. Simply comparing the rated power or process duration across studies is insufficient. One laboratory may use a 10,000 W furnace to produce 1 g of catalyst, while another may use a 100 W unit for the same mass. However, the energy consumed per gram of catalyst cannot be directly inferred from these figures alone, as equipment utilization, loading capacity, and thermal transfer efficiency differ significantly between systems.

To address this, a benchmarking framework was developed to normalize energy and resource consumption associated with common equipment and synthesis steps. All equipment and processes are evaluated based on standardized energy consumption metrics (Table B.1), such as:

- kWh/kg of solid material treated (e.g., drying and grinding),
- kWh/L of liquid chemical processed (e.g., centrifuge and filtration),
- or W per unit volume of equipment capacity multiplied by the operating time. The operating time for each relevant step can be found in the respective literature, and this depends on the type of operation (e.g., furnace, stirrer, and ultrasonic bath).

Practical assumptions regarding equipment utilization were also introduced to reflect realistic laboratory practices. For heat-transfer-based processes (e.g., calcination in furnaces, drying in ovens), an effective capacity utilization of 10% was assumed. This refers to the proportion of a device's nominal capacity that can be realistically used under operational constraints. In thermal processes, materials (e.g., solids or powders) require sufficient space for uniform heat distribution and effective energy transfer—

meaning, for example, that a 1 L furnace cannot process 1 L of material efficiently. For all other operations, such as stirring, sonication, or centrifugation, a more conservative 30% utilization was applied to reflect typical laboratory-scale limitations and prevent overloading. These values were selected to represent typical experimental conditions and to avoid overstating the throughput capacity of lab-scale equipment.

In addition, routine operations such as washing and filtration were standardized. A single-use baseline was adopted for catalysts due to the absence of consistent reusability data in the literature. The influence of catalyst lifetime was further evaluated through a sensitivity analysis to quantify its effect on environmental impacts.

A three-step wash cycle (e.g., using ethanol or deionized water) was assumed for all catalyst washing procedures. For particle-based catalysts, three filtration cycles were included to account for solid-liquid separation stages commonly performed after synthesis or reaction.

Average consumption values for each type of equipment and process were compiled from a combination of peer-reviewed literature, equipment technical datasheets, and vendor specifications. These data are summarized in Appendix Table B.1 and form the basis of the life cycle inventory for each scenario evaluated in this chapter. It is important to note that the objective of this benchmarking framework is not to provide exact measurements for each individual study or lab configuration, but to establish a transparent, reproducible, and reasonably accurate set of assumptions that allow for comparative analysis. While some of the energy consumption values were derived from laboratory-scale data, others were sourced from pilot- or industrial-scale systems. These

values were normalized per functional unit and selected to represent typical operational conditions for each process. Although industrial-scale systems may offer greater efficiencies, particularly through improved heat integration or higher capacity utilization, the current assumptions provide a reasonable and transparent basis for comparative analysis—especially at this early stage of technology assessment. This analysis focuses on the environmental impact of the operating stage, which is more readily scalable to larger systems. Operating energy consumption can be proportionally adjusted based on system capacity, allowing for straightforward extrapolation to pilot- or industrial-scale scenarios.

By applying these standardized inventory metrics across all cases, this framework enables an "apple-to-apple" comparison of environmental impacts between different AOP systems and process configurations—thus supporting more robust conclusions about their relative sustainability.

4.2.2 Environmental impact comparison

The LCA process, as delineated by ISO 14044/40 guidelines, comprises four fundamental stages: goal and scope definition, inventory analysis, impact assessment, and results interpretation [116]. The objective is to evaluate and compare the environmental impacts associated with three operational scenarios for tetracycline degradation using sono-based AOPs:

1. Blank cavitation (no chemical additives or catalyst),
2. H_2O_2-assisted cavitation, and

3. TFNs-assisted cavitation using fractured TiO_2 nanoshells as cavitation-enhancing catalysts.

The goal is to determine the environmental performance of each scenario in degrading tetracycline under realistic operating conditions. The functional unit is defined as the treatment of 1 L of tetracycline-contaminated wastewater (40 mg/L) to achieve 90% degradation efficiency. The overall concentration of the solution is 40 mg/L to make consistent with the previous sections. The concentration for each antibiotic is 20 mg/L. This common endpoint allows for an apple-to-apple comparison across the three scenarios, regardless of differences in operational performance or process inputs. To enable fair comparison, degradation kinetics from Chapter 3 are used to estimate the reaction time required for each scenario to achieve the 90% degradation target. These values are then combined with measured power input and duty cycle settings to calculate total energy consumption per scenario. The catalyst-related emissions include both the material and process energy required for TFNs synthesis as benchmarked in Section 4.2.1 and detailed in Appendix Tables B.3 to B.5. TFNs dosage is set at 0.5 mg/mL, as determined from the experimental optimization in Chapter 3, and is assumed to be sufficient to reach the target degradation without re-dosing. A sensitivity analysis on TFNs reusability is conducted later in this chapter to evaluate how catalyst lifespan affects the overall environmental impact. The system boundary is cradle-to-gate (Figure B.1), covering all upstream processes associated with material and energy inputs, including:

- Electricity used during sonochemical operation,

- Emissions from chemical production and usage (when applicable),
- Emissions from TFNs catalyst synthesis (e.g., Ti-precursor, DI water, ethanol wash, calcination, drying etc),
- Indirect emissions associated with preparation steps (e.g., stirring, washing, filtration, etc.).

The production of raw materials and the energy expenditure associated with sonochemical degradation will be considered. In cases where nanoparticles are reused, it is assumed that filtration is performed three times, and the associated energy consumption is included in Table B.1. A cradle-to-gate boundary is used, excluding end-of-life stages such as waste disposal, equipment retirement, and recycling. These are acknowledged as important for future work. All raw material data were sourced from the Ecoinvent 3.9 database via SimaPro v9.5 software. Two characterization methods are employed:

- IPCC 2021 GWP 100 to assess greenhouse gas emissions in terms of CO_2-equivalents [156,157], and
- Cumulative Energy Demand (CED) v1.11 to quantify the total primary energy input (renewable and non-renewable) associated with each scenario [158].

The emission factors from chemicals used in this study are based on UK/EU datasets to ensure consistency across international case studies and to minimize regional bias in electricity grid emissions or chemical production pathways. The electricity consumption was predicted based on both UK-based grid and projected 2050 electricity supply as proposed by International Energy Agency (IEA) [159].

4.2.3 Alternative Reactor Configuration for Impact-Oriented Optimization

To complement the environmental analysis of previously tested sonochemical degradation scenarios, a modified reactor configuration was developed with the aim of exploring potential process-level optimizations. While the earlier experiments (Chapter 3) utilized a batch sonoreactor coupled with nanoscale TFNs as cavitation agents, this section introduces a continuous-flow sonoreactor system employing structured metallic foams as an alternative cavitation medium.

Although the two reactor systems differ in their operation mode—batch versus continuous-flow—their core design and acoustic mechanism remain fundamentally the same. Both rely on the generation of converging ultrasound fields to induce cavitation, with the primary distinction being how the liquid is introduced and how the cavitation-supporting medium is retained within the reactor. The acoustic and reaction parameters are listed in Appendix Table B.2. The continuous-flow setup enables the reactant (tetracycline solution) to pass through the reactor chamber, making the use of suspended nanoparticles impractical due to flushing and recovery challenges. As such, fixed-position porous metal foams (Cu, $Fe_{0.5}Ni_{0.5}$, Ti, Ni, ZnO) were employed as a passive, reusable cavitation agent, placed in the reactor's acoustic focal region. The metal foams were purchased from a commercial supplier (Yiminglong Co., Ltd, CN). Their general porous and three-dimensional structure is as provided by the supplier and is standard for such materials. The metal foam has a nominal pore density around 100 pores per inch (100 PPI). The size of the metal foam used in the reaction is listed in

Table B.2.

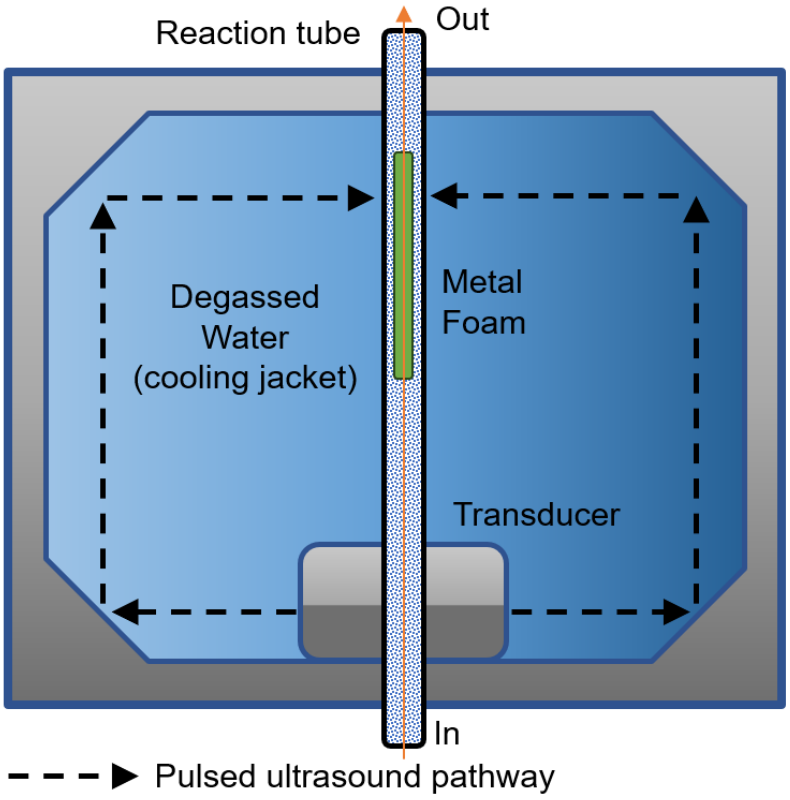

Figure 4.1. Schematic diagram of the continuous sonoreactor utilizing converging ultrasound and metal foam as the cavitation agent

The rationale behind this configuration shift is to evaluate an alternative that minimizes material inputs and avoids synthesis-related emissions, while still facilitating effective cavitation for pollutant degradation. Although this change inherently alters the operating dynamics—particularly in terms of catalyst type—it remains conceptually aligned with the sonochemical principles explored in earlier experiments. The same life cycle inventory framework and environmental impact assessment methodology (outlined in Sections 4.2.1 and 4.2.2) are applied here to ensure consistency and comparability of results.

In addition, preliminary experiments were conducted using this continuous-flow system to evaluate its capacity for the simultaneous degradation of multiple antibiotics, namely tetracycline and ciprofloxacin. While this multi-contaminant scenario extends slightly beyond the primary scope of this chapter, it is included here to illustrate the broader applicability and potential versatility of the optimized reactor configuration. The environmental implications and performance outcomes of these extended tests are discussed later in the chapter to maintain clarity and coherence in the methodological presentation.

This section thus serves to introduce the rationale, configuration, and methodological consistency of the alternative setup, without presenting results or conclusions prematurely. By maintaining alignment with the environmental benchmarking framework, the chapter continues its focus on impact-oriented process design and sets the stage for a more holistic evaluation of sustainability trade-offs in the following sections.

4.3 Results

4.3.1 CO_2 emissions and cumulative energy demand

To evaluate the environmental performance of the three sono-based degradation scenarios—blank cavitation, TFNs-assisted cavitation, and H_2O_2-assisted cavitation—we quantified both the CO_2-equivalent emissions, and the CED associated with achieving 90% tetracycline degradation in 1 Litre of wastewater. The degradation times

were estimated from kinetic data obtained in Chapter 3, with corresponding treatment durations of 191 minutes for blank cavitation, 28 minutes for TFNs, and 47 minutes for H_2O_2.

Figure 4.2 presents the cumulative energy demand per Litre of treated wastewater under two electricity grid conditions: Current UK electricity mix, and 2050 projected electricity mix, as outlined by the IEA Net Zero Scenario, which includes a substantially higher share of renewable energy sources. Under the current UK electricity scenario, blank cavitation exhibits the highest energy consumption, exceeding 200 MJ/L. This is primarily due to its prolonged treatment time and the lack of catalytic enhancement. In contrast, the TFNs-assisted process demonstrates the lowest energy requirement, attributed to its accelerated degradation kinetics and efficient radical generation. The H_2O_2-assisted process performs moderately, with energy demand between the other two scenarios.

When switching to the 2050 low-carbon electricity mix, all scenarios benefit from a marked reduction in cumulative energy demand. All scenarios show a reduction in Cumulative Energy Demand (CED) under a low-carbon electricity mix because the life-cycle energy cost of producing electricity from renewable sources (e.g., solar, wind) is significantly lower than that of fossil fuels. Although the operational energy consumed remains unchanged, the upstream energy required for fuel procurement, processing, and plant operation is drastically reduced, thereby lowering the total embedded energy footprint. CED values drop by approximately 50%, but the relative ranking remains unchanged: blank cavitation remains the most energy-intensive, while TFN-based

treatment remains the most efficient. This result reinforces the importance of operational performance in determining environmental performance, even in a decarbonized energy future.

While electricity consumption quantifies the electrical input required for a process, it does not directly equate to the total energy input, which may include thermal or other forms of energy. Moreover, the source of electricity plays a critical role in determining environmental impact. Electricity generated from fossil fuels typically involves lower conversion efficiencies and higher upstream energy losses, resulting in greater overall energy consumption and significantly higher carbon emissions. In contrast, renewable electricity is not only more efficient in terms of generation but also substantially greener per unit of energy delivered. In contrast, renewable electricity systems demonstrate superior life-cycle energy efficiency, as they avoid the continuous energy expenditure required for fossil fuel extraction, transportation, and processing, which leads to greener energy per unit delivered. Therefore, assessing carbon emissions requires a nuanced understanding of both the quantity of electricity consumed and the carbon intensity of its source.

In both electricity scenarios, non-renewable fossil energy constitutes the largest share of total energy demand, especially in the current grid. The projected 2050 mix substantially reduces the contribution from fossil sources, replacing them with renewables such as wind, solar, and hydro, as shown in the three right bars of Figure 4.2. However, even with a cleaner energy mix, the synthesis steps and operational duration continue to influence overall impact. The future electricity scenarios may also

benefit from improved generation efficiency, meaning that less primary energy is required to produce the same amount of usable electricity. This dual improvement—cleaner sources and higher efficiency—can significantly reduce the cumulative energy demand associated with the operation.

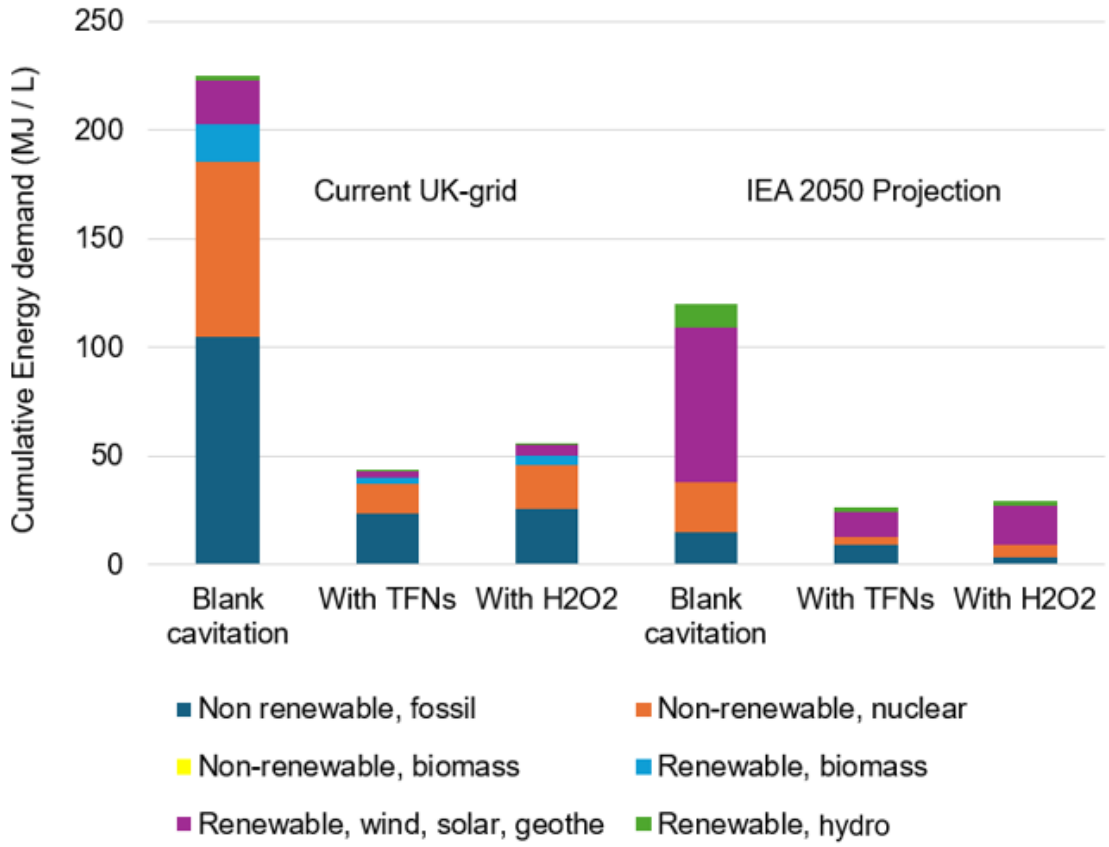

Figure 4.2. Cumulative Energy Demand (MJ/L) of Sonochemical Scenarios for tetracycline Degradation under current UK electricity (left group) and projected IEA 2050 low-carbon electricity (right group). The detailed breakdown of catalyst synthesis and operation regarding CO_2 emissions are listed in Figure 4.3 below.

A deeper breakdown of CO_2 emissions for the TFNs-assisted scenario is presented in Figure 4.3. The upper pie chart represents emissions under the current UK electricity mix (>300 g/kWh), while the low pie chart reflects the projected 2050 low-carbon grid

(~50 g/kWh). Although the electricity consumption remains constant between the two cases, the emission contribution shifts significantly due to the difference in electricity source. In the current scenario, the reactor's electricity use—calculated using region-specific emission factors (kg CO_2-eq/kWh)—accounts for 77% of total emissions, making it the dominant contributor to the overall footprint. This highlights how the carbon intensity of the electricity grid, rather than the quantity of energy consumed, drives the variation in emissions.

However, with a decarbonized energy supply, its share drops to 44.1%, and the catalyst-related emissions—including contributions from ethanol, styrene, titanium precursor, heating, and washing—emerge as the predominant contributors, collectively over 50%. This transition highlights the increasing importance of upstream emissions from material synthesis in low-carbon futures, where direct electricity-related impacts are significantly diminished. These results show a critical insight: while future energy decarbonization will significantly reduce total energy-related emissions, optimizing process design—especially minimizing reaction time and chemical inputs—remains crucial for long-term sustainability. The results also justify the exploration of alternative cavitation agents or reactor configurations, as discussed in Section 4.2.3, to further reduce upstream material burdens.

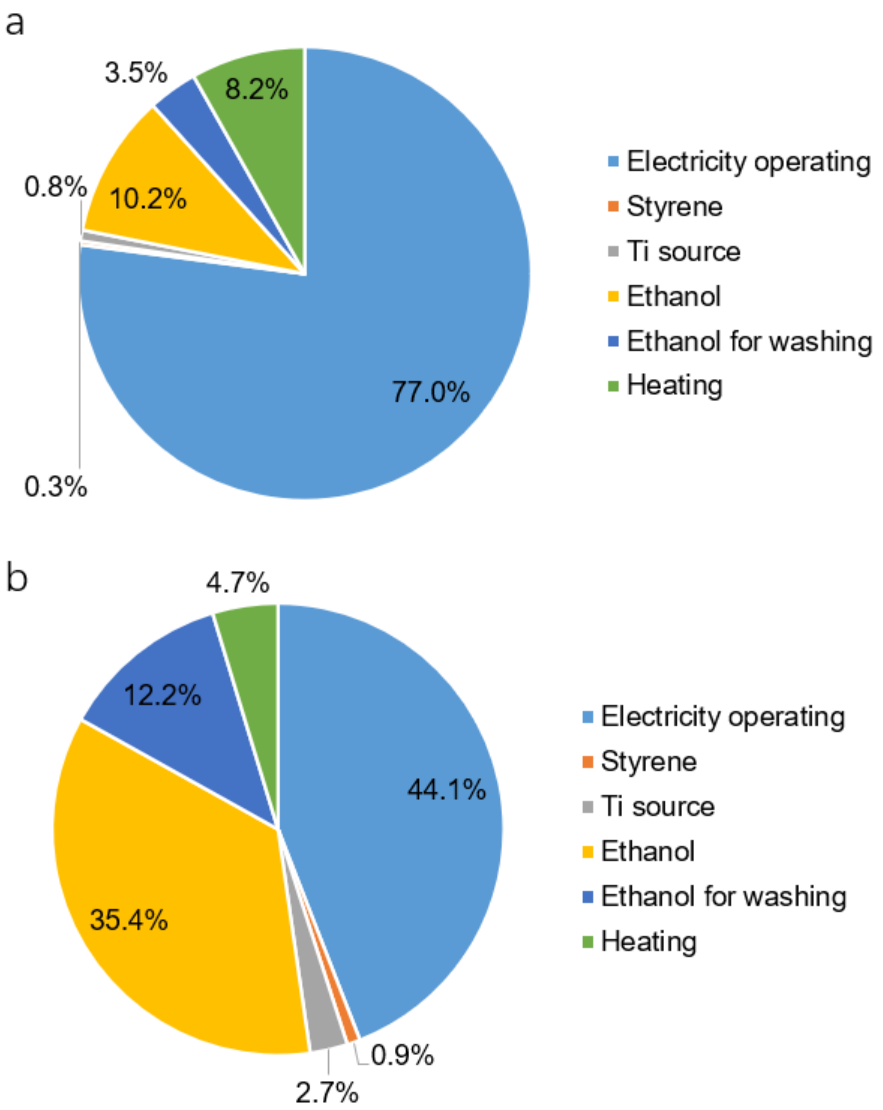

Figure 4.3. Breakdown of CO_2 Emissions by Source for TFN-Based tetracycline Degradation. (a) current UK grid-mixed electricity and (b) projected 2050 low-carbon electricity scenario. (the CO_2 emissions from other chemicals are very minor, i.e., < 0.1% and not listed in this figure)

These findings reinforce the need to evaluate not only operational energy but also the embodied emissions of catalyst production. To explore this further, a sensitivity analysis is presented in Section 4.3.2 to investigate how variations in key parameters influence the environmental profile of the sonocatalytic process.

4.3.2 Sensitivity analysis of CO_2 emissions

To explore how electricity sourcing affects the overall environmental performance of each treatment scenario, a sensitivity analysis was performed to evaluate the influence of the carbon intensity of electricity on the total carbon footprint of the process. To assess the impact of grid decarbonization, this parameter was varied across a plausible range from 50 (2050 NZE) to 300 (current UK grid) g CO_2-eq/kWh, encompassing potential future scenarios from a highly renewable grid to a fossil-fuel-intensive one. The model was run iteratively at each value within this range, and the corresponding total carbon footprint was calculated and compared. The total electricity consumption required to achieve 90% tetracycline degradation was estimated at 22.3 kWh for blank cavitation, 5.5 kWh for the H_2O_2-assisted process, and 3.3 kWh for the TFNs-assisted scenario. As expected, blank cavitation consistently resulted in the highest CO_2 emissions across all grid intensities due to its prolonged operating time and high energy demand.

At typical carbon intensities above 100 g CO_2eq/kWh, the TFN-based process demonstrated the lowest total GWP (see Figure 4.4), owing to its significantly lower energy input. Since carbon intensity is directly influenced by the electricity generation mix—such as fossil fuels versus renewables—this highlights the advantage of low-energy processes under carbon-intensive grids. In low-carbon energy systems such as wind and solar-based electricity (e.g., <100 g CO_2eq/kWh), the H_2O_2-assisted scenario

outperformed TFNs in terms of total emissions. It is worth noting that the carbon intensity of electricity for all kinds of renewable sources is below 100 g CO_2eq/kWh. The detailed carbon intensity of UK-based electricity from different sources is calculated by the IPCC 2021 method, and these values are exhibited in Appendix Figure B.2. This crossover occurs because emissions from catalyst synthesis in the TFNs scenario become dominant and are less affected by grid decarbonization. In the case of ultra-clean electricity grids (e.g., <11 g CO_2eq/kWh, specifically nuclear and hydro-based electricity, see Figure 4.4), the TFNs process actually becomes the least favourable option among the three, as its material-related emissions are largely fixed and no longer offset by lower operational energy. These results suggest that the optimal strategy for antibiotic degradation depends not only on operational performance but also on the carbon profile of the local electricity grid and the chemical/metal used for catalyst synthesis.

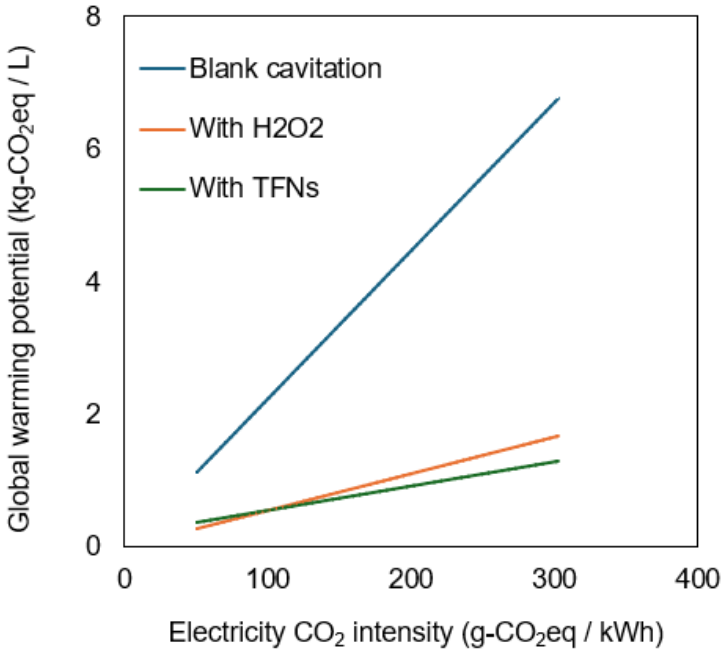

Figure 4.4. Sensitivity analysis of GWP_{100} to carbon intensity of electricity across

different degradation scenarios

To contextualize the influence of electricity CO_2 intensity globally, Figure 4.4 maps the preferred degradation pathway—either TFNs-assisted or H_2O_2-assisted—across countries based on their current national grid carbon intensities. As previously discussed, 100 g CO_2eq/kWh is identified as a key threshold: above this level, the TFN-based process exhibits lower emissions; below it, H_2O_2 becomes the more environmentally favourable option, due to its minimal synthesis-related footprint. The decarbonization of the electrical grid would also indirectly reduce the carbon footprint of non-electricity inputs, such as the embodied emissions in chemicals and equipment manufacturing, which are often produced using electricity.

According to current real-world electricity data, TFNs are preferred in the majority of countries (shown in green), while H_2O_2 is favoured in 19 countries (marked in orange), primarily those with low-carbon electricity grids such as Norway, Iceland, and several EU member states [137]. None of the countries in Asia, North America, or Oceania achieved a low electricity CO_2 intensity below the threshold of 100 g CO_2eq/kWh. This geographic distribution underscores the importance of location-specific considerations when evaluating the environmental impact of AOP technologies. While the TFNs system currently offers a broader advantage under the current grid with moderate carbon intensity, the number of countries favouring H_2O_2 is expected to gradually increase as grid decarbonization advances to meet global net-zero targets. These findings emphasize that focusing solely on operational performance or removal efficiency is insufficient; environmental context must also guide technology selection

and optimization.

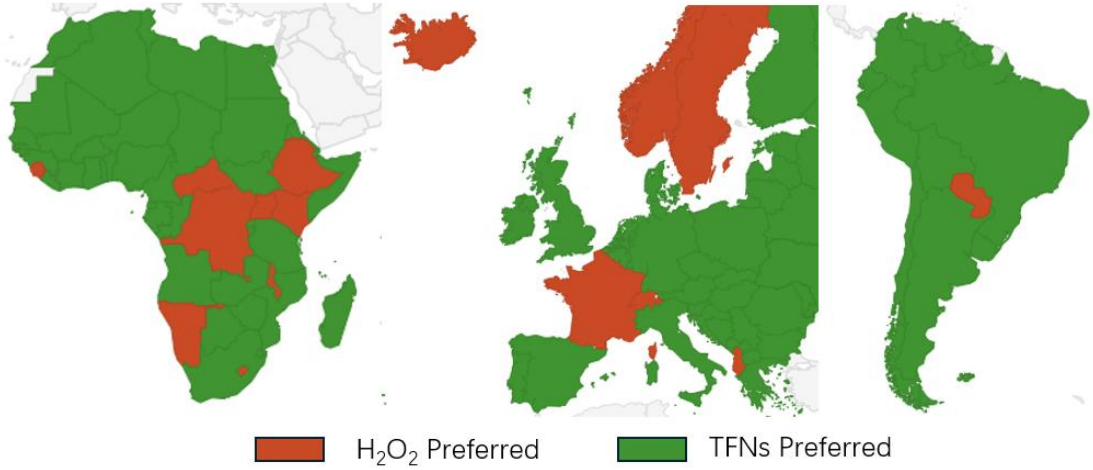

Figure 4.5. Geographical preference of tetracycline degradation scenarios based on the up-to-date and localized CO_2 intensity of electricity (TFNs are currently preferred except for those countries with a high nuclear or renewable energy input.)

Figure 4.6 presents the sensitivity analysis of global warming potential as a function of TFNs reusability under projected 2050 low-carbon electricity conditions. With an assumed CO_2 intensity, the carbon footprint of the TFNs-assisted process is 0.372 kg-CO_2eq, which is higher than the H_2O_2 scenario (0.276 kg-CO_2eq), but the embodied emissions from catalyst synthesis are still considerable. However, as TFNs are reused across more treatment cycles, the levelized CO_2 emissions (i.e., amortized over a greater treated volume) decline significantly, and the critical point here is 1.9 L in order to surpass the H_2O_2 case in terms of CO_2 emissions. If TFNs are reused to treat 100 Liters or more, their CO_2 emissions fall to approximately 0.166 kg-CO_2eq/L, representing a 40% reduction compared to the H_2O_2 scenario. This analysis highlights the pivotal role of material reusability in improving the environmental profile of catalyst-based AOP systems, especially under low-carbon energy conditions.

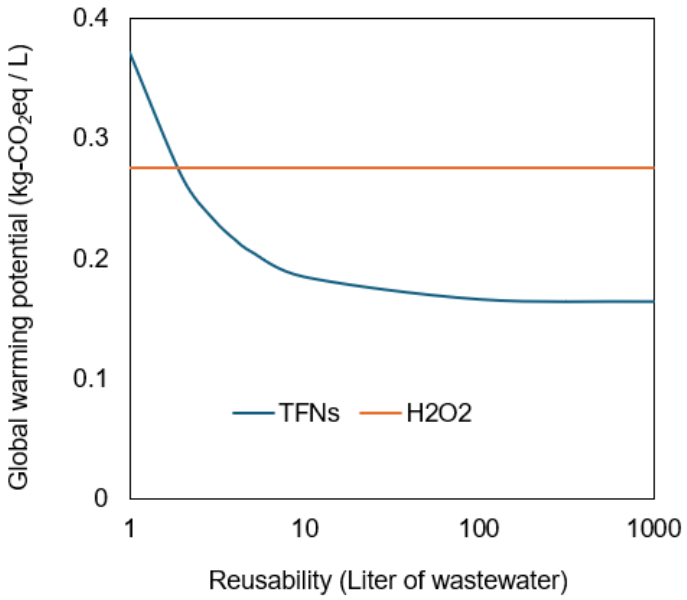

Figure 4.6. Sensitivity analysis of catalyst reusability on CO_2 emissions for TFN-based degradation

Figure 4.7 illustrates the wide variation in GWP associated with the production of different catalytic metals, highlighting the importance of material selection in AOP system design. While common metals such as aluminium, copper, and TiO_2 exhibit relatively low CO_2 emissions per kilogram of metal produced (typically under 10 kg-CO_2eq/kg), precious and rare metals like palladium (Pd) and platinum (Pt) can emit up to 10,000–100,000 kg-CO_2eq per kilogram—several orders of magnitude higher [160–162]. This stark contrast underscores a critical trade-off between performance and sustainability. Even if catalysts based on high-GWP metals offer enhanced degradation rates, their upstream environmental burdens can significantly offset operational gains. Therefore, the selection of metal-based materials must consider not only catalytic activity but also life cycle emissions, especially under future low-carbon electricity scenarios where upstream material impacts become more dominant.

Regarding the reactor itself, its material impact was not included in detail, as is common in early-stage LCAs where operational emissions dominate. Most reactors are assumed to be constructed from conventional materials such as stainless steel, which have significantly lower life cycle emissions compared to high-GWP metals used in catalysts (e.g., Pt or Pd). Moreover, when amortized over a typical 20-year lifespan, the construction-related emissions are relatively minor compared to ongoing inputs like energy and chemical use. Nonetheless, these impacts can be considered in future studies focused on full system infrastructure.

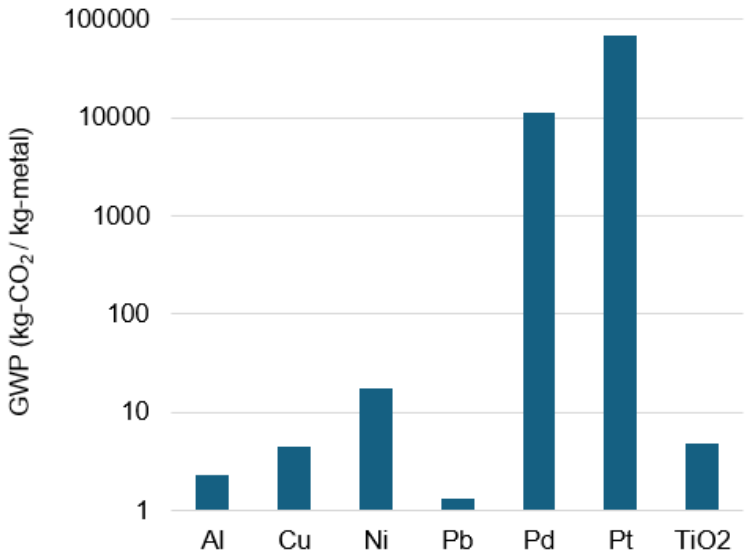

Figure 4.7. Comparison of cradle-to-gate global warming potential (GWP_{100}) for various metals commonly used in catalytic applications [163]

4.3.3 Environmental-oriented system improvement

Building on the findings of the sensitivity analysis, it is clear that system-level design choices, including catalyst selection and reactor configuration, play a pivotal

role in determining overall environmental performance. While previous scenarios relied on nanoparticle-based catalysts in batch systems, these approaches may face practical limitations such as catalyst recovery challenges and synthesis-related emissions. To address this, the next section explores an alternative continuous-flow sonoreactor design using non-synthesized metal structures as cavitation agents. This setup aims to reduce upstream emissions while maintaining satisfactory operational performance, particularly for recalcitrant antibiotics like tetracycline and ciprofloxacin.

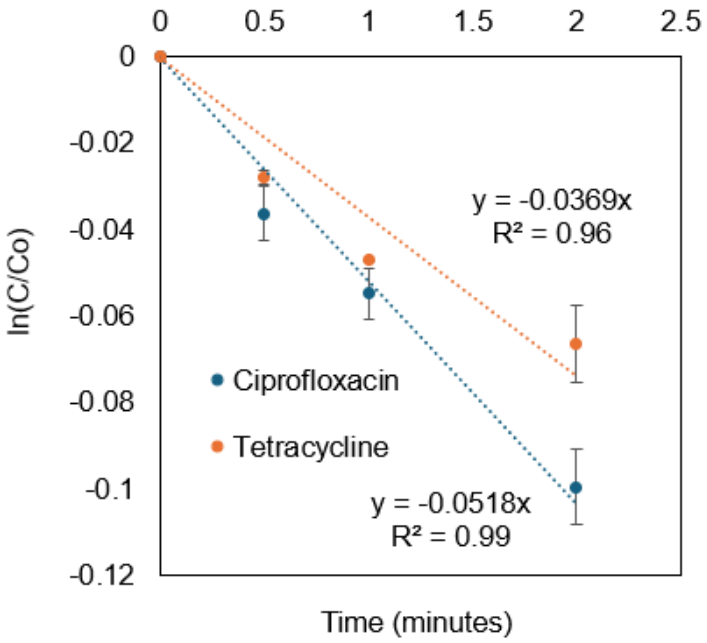

Figure 4.8. Degradation kinetics of ciprofloxacin and tetracycline under non-catalytic conditions (blank cavitation) using a continuous-flow sonoreactor

The kinetic plot (Figure 4.8) illustrates the degradation behaviour of ciprofloxacin and tetracycline over a short time period without the use of any metal catalyst, serving as a baseline for comparison. The linearity of both trends on a $\ln(C/C_0)$ versus time plot confirms that the degradation follows pseudo-first-order kinetics under these conditions. Ciprofloxacin degrades faster than tetracycline, with a rate constant (k) of 0.0518 min^{-1}

compared to 0.0369 min^{-1} for tetracycline. The high R^2 values (0.99 for ciprofloxacin and 0.96 for tetracycline) indicate strong model fits, suggesting that the kinetics are well described by a first-order model and likely governed by unimolecular, single-step and simple reaction mechanisms such as hydrolysis or photolysis in this setup.

The difference in degradation rates may be due to the inherent chemical structures and stability of the two antibiotics. Ciprofloxacin, a fluoroquinolone, contains functional groups such as a piperazine ring and a carboxylic acid moiety, which are theoretically prone to oxidative or hydrolytic cleavage [164]. In contrast, tetracycline features a more complex and stable polycyclic structure with multiple hydroxyl and amide groups, and is harder to complex with metal ions under acidic conditions [165]. Consistent with this structural analysis, numerous studies have reported tetracycline to be more readily degraded by conventional advanced oxidation processes (AOPs) than ciprofloxacin [166–168].

However, in this specific sonocatalytic system, we observed the opposite trend: ciprofloxacin degraded significantly faster than tetracycline (see Fig. 4.8 and 4.9). This suggests that the degradation pathway catalyzed by the metal foam/ultrasound combination uniquely targets the vulnerable sites in ciprofloxacin's structure more effectively than those in tetracycline. This reversal of the expected reactivity order underscores the novel and selective mechanism of our approach, which differs fundamentally from traditional AOPs.

Figure 4.9 presents the degradation efficiency of two mixed antibiotics—

ciprofloxacin and tetracycline—when exposed to different metal sheets over a one-minute interval. The metals tested include copper (Cu), iron-nickel alloy (FeNi), titanium (Ti), nickel (Ni), and zinc oxide (ZnO), with an "empty" control included for comparison. The results clearly show that ciprofloxacin underwent significantly more degradation than tetracycline across all tested materials. Among them, ZnO exhibited the highest degradation efficiency, especially for ciprofloxacin, which reached around 50% degradation within just one minute, while tetracycline showed a lower but still notable degradation of about 15%. Titanium also performed well, degrading approximately 40% of ciprofloxacin, though its impact on tetracycline remained below 10%.

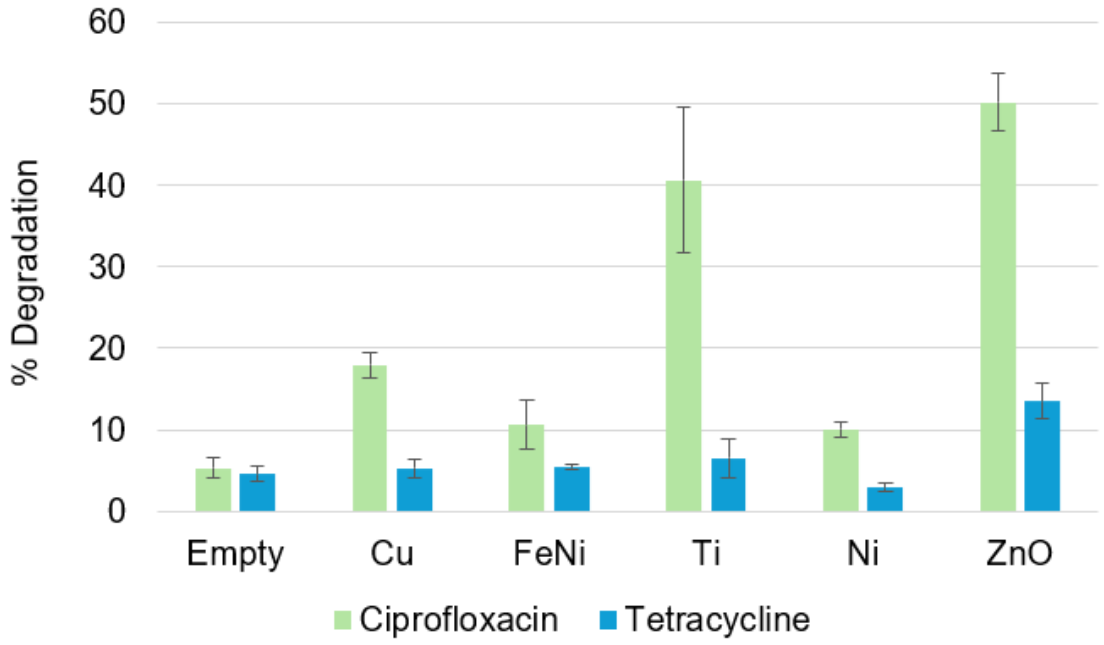

Figure 4.9. Degradation performance of ciprofloxacin and tetracycline using various catalytic metal-based cavitation agents in a continuous-flow sonoreactor (Total concentration 40 mg/L, $C_{0,TC}$=$C_{0,CP}$, Residence time=1 minute)

The superior performance of ZnO and Ti may be attributed to their photocatalytic or redox-active properties [169,170]. ZnO, in particular, is known for its strong photocatalytic behaviour under light exposure, generating ROS such as hydroxyl radicals that can rapidly degrade organic compounds, including antibiotics. Even if light was not used intentionally in this experiment, ambient light or surface catalytic effects could have contributed. Titanium, often used in the form of TiO_2 in photocatalysis, may exhibit similar properties, facilitating oxidative degradation through electron transfer reactions. In contrast, metals like Ni and the FeNi alloy show much lower activity, possibly due to their limited ability to generate ROS or participate in effective redox reactions over short exposure times.

Ciprofloxacin's higher degradation compared to tetracycline may also be influenced by the differences in their molecular structures, as discussed above. Ciprofloxacin is more susceptible to oxidative cleavage under catalytic conditions [171]. However, tetracycline is more complex and possibly more stable molecule under mild conditions [172].

The results suggest that materials like ZnO and Ti could be promising candidates for rapid removal of certain antibiotics from contaminated water, which is particularly relevant in the context of antibiotic pollution and the rise of antimicrobial resistance. Further studies involving different light conditions, pH levels, and extended time frames could provide deeper insights into the mechanisms and scalability of these degradation processes. Overall, this data provides a foundational understanding of the antibiotics' natural decay profiles, serving as a reference point for evaluating the

enhanced degradation observed in the presence of metal sheets—especially ZnO and Ti. This comparison also helps identify materials that perform well under different environmental conditions such as treating different antibiotics, making them more suitable for real-world applications.

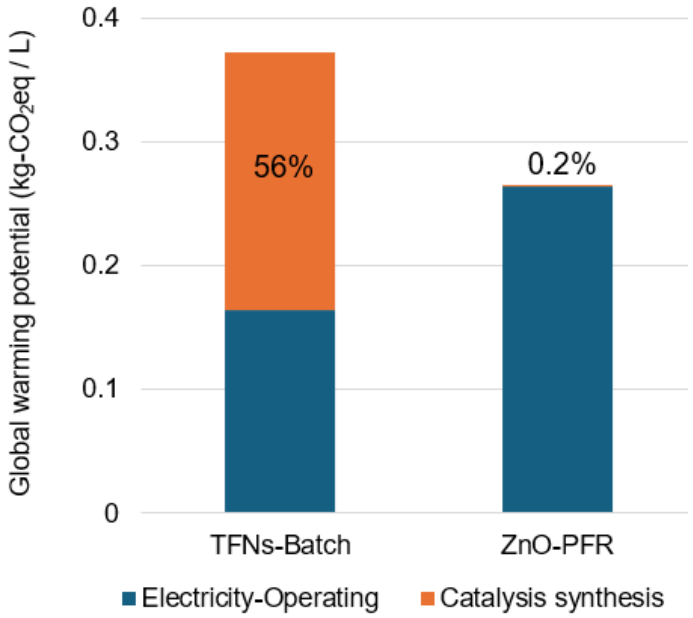

Figure 4.10. Global warming potential (GWP_{100}) of tetracycline degradation using TFNs in a batch reactor versus ZnO-based metal foam in a continuous-flow reactor

Figure 4.10 compares the GWP of the batch reactor using TFNs with the continuous-flow system utilizing ZnO metal foam. Based on the previously shown reactor configuration and degradation performance, ZnO is capable of degrading 90% of 0.314 mL of tetracycline within 2.3 minutes, resulting in total energy consumption of 5.25 kWh per Litre of wastewater treated. Although the TFN-based system achieved faster kinetics and consumed 38% less electricity, its catalyst synthesis contributed significantly to the total CO_2 emissions—accounting for 39% of the total impact. In

contrast, the ZnO-based continuous reactor, while slightly less energy-efficient, exhibited an almost negligible catalyst-related footprint, with synthesis emissions contributing only 0.2% of the total. As a result, the overall GWP was reduced by approximately 29% in the ZnO with continuous reactor scenario. The much lower emissions from the ZnO metal foam are primarily due to its simple composition and minimal processing requirements. Unlike TFNs, which involve complex nanostructuring, multiple chemical precursors, and energy-intensive synthesis steps, ZnO foams are fabricated through straightforward metallurgical processes with far fewer inputs. Additionally, while this comparison assumes single use for both materials, metal foams are far easier to recycle in practice. Being a single solid piece, they can often be reused or recovered without additional separation steps, unlike nanoparticles, which typically require filtration, chemical treatment, or loss-intensive recovery methods. These practical and environmental advantages contribute to the significantly lower life cycle footprint of ZnO foams. Further studies should focus on metals with low embodied emissions, durable and reliable structures, and high catalytic activity to further reduce the overall emissions of the process.

Beyond environmental metrics, this comparison also underscores a practical engineering consideration: highly decorative or complex nanostructured catalysts like TFNs, while offering superior performance, are often more susceptible to damage, deactivation, and reduced reusability in real-world applications [173,174]. In contrast, simple and robust materials such as metal foams not only have lower embodied emissions but also offer greater mechanical stability and operational reliability. This

reinforces the broader takeaway that degradation efficiency alone should not dictate process selection. Environmentally informed design—balancing performance, durability, and life cycle trade-offs—is essential for developing truly sustainable and scalable treatment solutions.

4.3.4 Social Considerations in Scenario Optimization

Although the primary focus of this chapter has been on reducing the environmental impact of a sono-based AOP system through scenario optimization, it is important to recognize that sustainability in water treatment also encompasses social dimensions. Incorporating such a broader lens can help to guide system-level decisions beyond environmental performance alone.

For instance, the use of TFN nanomaterials in cavitation enhancement, while effective in improving degradation rates, involves complex synthesis procedures that may be less accessible in low-resource settings. The use of engineered nanomaterials raises concerns about occupational exposure and long-term health effects, especially through inhalation or dermal contact during synthesis, handling, or disposal stages. These risks are amplified in poorly regulated or resource-limited environments, where protective infrastructure may be lacking. In contrast, scenarios utilizing conventional metal foam (e.g., ZnO) may offer lower material costs, reduced reliance on rare chemicals, and more straightforward preparation protocols, aligning better with equity and localization goals. These differences have implications for technological

accessibility, especially in regions where local production capacity and skilled labour are limited.

Additionally, the continuous-flow reactor configuration, while demonstrating environmental advantages over batch processing in some scenarios, may require more advanced infrastructure and higher operator skill levels. In contrast, batch systems—though less optimized—could be more suitable for decentralized applications, where ease of use and minimal training are critical for social acceptance and practical deployment. Meanwhile, it is well established that large-scale chemical processes are best carried out using continuous operation. While batch processing remains common in specialized sectors such as pharmaceuticals, the production of bulk chemicals—such as polymers, ammonia, and similar commodities—is typically conducted using continuous systems due to their superior efficiency, scalability, and resource utilization. The choice between batch and continuous reactors involves trade-offs, and each offers specific advantages and limitations depending on the operational context and process requirements.

From an occupational safety standpoint, all scenarios involving sonication must account for potential noise hazards and chemical exposure, particularly where reactive species or cleaning solvents (e.g., ethanol) are used. Designing systems with shielding, automation, and safe handling protocols is therefore essential to support social sustainability.

While these aspects were not quantitatively assessed, the comparative insights

across scenarios suggest that simpler, reusable materials and accessible operating conditions may support better integration with social equity and deployment objectives. Future work could consider incorporating qualitative or semi-quantitative social indicators—such as ease of fabrication, labour intensity, and occupational risks—into the scenario optimization framework.

4.4 Discussion and outlook

This study presented a process-level environmental sustainability analysis of different sonochemical degradation scenarios for tetracycline removal, with a focus on energy demand, CO_2 emissions, and system optimization. Beyond the technical efficacy shown in Chapter 3, this chapter highlights how environmental metrics and trade-offs should also be considered alongside operational performance metrics. Several key insights emerged from this evaluation.

Firstly, it was evident that energy demand—particularly the electricity consumption, plays a dominant role in the environmental profile of sono-based AOP systems, especially using the current grid electricity with moderate carbon intensity. In this context, electricity use translates directly into significant carbon emissions. While TFN-based systems demonstrated high degradation rates and lower energy usage (3.27 vs 5.25 kWh/L), their embodied emissions from catalyst synthesis could offset the operational gains when green electricity becomes widely available. This relationship between energy consumption (kWh) and its associated carbon emissions (kg CO_2-eq)

becomes crucial: as cleaner electricity reduces the emissions impact of reactor operation, upstream synthesis emissions increasingly dominate. The effect of this change on the dominant emission source illustrates the dynamic nature of environmental hotspots, which evolve in parallel to the broader energy systems' decarbonization. Thus, the sustainability of a process is not static, but context-dependent, and should be evaluated accordingly.

The continuous-flow reactor configuration using Zn-based metal foams represents an important step toward practical system integration. Although the operational performance was somewhat lower when compared to the TNF-nanoshells, the system achieved a more favourable environmental balance due to its minimal material footprint and simplified catalyst preparation. This case underscores a broader paradigm shift: from maximizing operational performance toward optimizing system durability, simplicity, and life-cycle performance. It also demonstrates that materials with modest activity, but low synthesis burdens and high stability, may offer the most practical solutions in a decarbonizing world.

The behaviour in the mixed solution (e.g., tetracycline and ciprofloxacin) highlights a key consideration for real-world applications, as wastewater contains complex pollutant mixtures. The degradation rate of individual components may differ in a competitive environment compared to single-solute systems due to factors such as scavenging of reactive species or competition for active sites. Future design strategies could focus on enhancing catalyst selectivity to better target specific pollutants within complex matrices. This finding underscores the importance of moving beyond single-

pollutant models to evaluate the technology's potential under more realistic conditions.

Moreover, these findings support the idea that more intricate nanostructured catalysts, while academically appealing, may not always be justified when considering real-world trade-offs in environmental and operational reliability. In contrast, common metal structures such as foams or meshes, though less “sophisticated,” tend to offer higher durability and ease of handling, making them attractive for scaling up.

Despite these valuable insights, several limitations must be acknowledged. First, while the degradation efficiency of tetracycline was assessed, this study did not explicitly evaluate the fate of the degradation by-products. Incomplete mineralization or formation of potentially toxic intermediates could introduce environmental risks that are not captured in this CO_2 and energy-focused analysis. Although identifying all degradation products is analytically complex, future studies incorporating this dimension would offer a more holistic environmental risk profile.

Second, in the continuous-flow scenario, the environmental burden of the metal foam was conservatively estimated using data for scrap metal. In practice, manufacturing metal foam may require additional energy or chemical processing steps, which could marginally increase its actual carbon footprint. While this does not invalidate the main conclusions, it introduces some uncertainty that warrants further refinement when more specific data becomes available. The analysis suggests that both the reactor configuration and catalyst type are significant factors in the observed performance. The superior reaction kinetics in the continuous-flow reactor, compared

to the batch system, are attributed to enhanced cavitation from the possibly existing turbulent flow and the continuous generation of cavitation nuclei. Concerning the catalysts, the enhanced activity of the Ternary Functional Nanoparticles (TFNs) over the metal foam can be reasonably ascribed to their nanoscale size, which offers a higher density of cavitation nucleation sites and potentially greater synergy with sonoluminescence. It is crucial to note, however, that this performance gain is counterbalanced by a life-cycle assessment indicating the TFN catalyst has an environmental impact more than two orders of magnitude larger than the metal foam. Ultimately, the present data does not allow for a definitive decoupling of the individual effects of reactor configuration and catalyst morphology. Future studies should systematically isolate these variables to quantify their specific contributions to the performance differential.

Moreover, conducting a life cycle assessment based on lab-scale data introduces inherent uncertainties when extrapolating to industrial relevance. Key challenges include scaling effects on energy and material efficiency, the exclusion of ancillary industrial equipment (piping, control systems, infrastructure), and the difficulty of accurately forecasting the performance and lifetime of materials at a larger scale. While this study provides a valuable comparative assessment of processes, the absolute environmental impacts should be interpreted as preliminary, highlighting the most promising pathways rather than predicting exact commercial footprints.

Lastly, this analysis focused solely on the global warming potential and cumulative energy demand. Other impact categories, such as human toxicity, ecotoxicity, or water

use, were not assessed in this chapter. These could be particularly relevant for AOP systems involving chemical additives or complex materials. Expanding future assessments to include these dimensions would provide a more complete sustainability picture.

Social sustainability considerations suggest that while advanced nanomaterials and high-intensity sono-reactors may offer improved operational performance, they can introduce notable occupational and public health risks, particularly related to nanoparticle exposure and solvent handling. Simpler alternatives such as metal foam catalysts and batch-mode operation may offer more socially robust solutions by enhancing safety, accessibility, and ease of use, especially important for decentralized or small-scale water treatment scenarios.

Overall, this chapter serves not only as a comparative life cycle assessment study of sonochemical tetracycline degradation, but also as a methodological bridge between lab-scale innovation and system-level environmental assessment. The results offer practical guidance for environmentally sustainable design and lay the groundwork for the broader cross-technology benchmarking presented in the next chapter. Building on the findings of this case study, Chapter 5 will extend the analysis to a comparative life cycle and techno-economic evaluation across multiple AOP technologies. The benchmarking framework developed here serves as a conceptual foundation for that analysis, where the focus will shift from single-process sustainability optimization to system-level sustainability comparison across different treatment methods.

4.5 Conclusion

This chapter has demonstrated that environmental impact must be integrated as a core sustainability metric in evaluating and optimizing advanced oxidation processes, and in particular for sonochemical degradation processes. Among the tested sonochemical scenarios, TFNs-enabled systems delivered high degradation efficiency and low energy demand but carried significant embodied carbon and material emissions from material synthesis (0.37 kg-CO_2e/L). Sensitivity analysis confirmed that the environmental performance of each approach is highly dependent on contextual factors—particularly the carbon intensity of electricity generation (up to 71% CO_2 reduction) and the environmental impact of the reuse times of catalysts (up to 54% CO_2 reduction). While reusability of the metal foams was not experimentally assessed in this study, their simple and robust structure suggests potential for greater durability and reuse compared to more complex nanomaterials. The robust, monolithic structure of the metal foams allows them to be easily retrieved from the reaction mixture through simple physical means, such as sieving, for direct reuse. At the end-of-life, the metal foams can be fully recycled via standard smelting processes, aligning with circular economy principles.

To address the emission issue associated with catalyst fabrication, a continuous-flow reactor using simple metal foam was introduced. While this alternative system required more energy due to a slower degradation rate, it eliminated most synthesis-

related emissions and ultimately reduced the overall CO_2 footprint (~29% CO_2 reduction). This finding supports a shift in focus from purely reaction-based performance metrics toward broader environmental efficiency. Moreover, the distinction between batch and continuous processing also influences emissions. It is well established that, beyond a certain capacity, continuous systems are inherently more efficient—producing more output with less material, time, and energy, which typically leads to lower overall emissions.

In summary, this case study illustrates the need for a balanced, system-level perspective when designing and selecting AOP technologies. It provides both a methodology and rationale for environmentally optimized process configurations, forming a bridge between experimental innovation (Chapter 3) and cross-technology sustainability benchmarking (Chapter 5).

Chapter 5: Standardized Benchmarking of Advanced Oxidation Processes for Tetracycline Degradation Using Life Cycle Assessment and Techno-Economic Analysis

Published as: **Zong, Zhiyuan**, Yihao Huang, James Kwan, and Nicholas P. Hankins. "Standardized benchmarking of advanced oxidation processes for tetracycline degradation with life cycle assessment and economic evaluation." *Chemical Engineering Journal* (2025): 170664. [175]

All the work that reported in this chapter have been done by Zhiyuan Zong

Abstract

This chapter presents a comparative life cycle and techno-economic analysis of five AOPs—sonolysis (the method in chapter 3), photolysis, sonophotolysis, Fenton-like oxidation, and electrochemical treatment—for tetracycline degradation in water. All processes were evaluated under a harmonized functional unit (1 L of wastewater with single-component tetracycline treated to 90% removal) and combined with monetized environmental value (USD 2023) and operating cost metrics. The previous results showed that the sono-based system (the sonochemical method in chapter 3) achieved the fastest degradation rate but also the highest environmental burden under the current electricity grid. In contrast, Fenton oxidation exhibited a lower degradation

rate but the lowest CO_2 footprint and the most favourable economic profile (section 5.3.4, Figure 5.10). Platinum-based electrochemical treatment had the highest life cycle impact, with electrode-related emissions exceeding 80% of total burden. Sensitivity analysis indicated that increasing catalyst reusability could cut CO_2 emissions by 70%, and that electricity carbon intensity strongly influenced AOP sustainability rankings. Monetization of environmental damage revealed that indirect costs comprised up to 55% of total process costs. The findings highlight the critical need for life cycle-informed assessment frameworks to guide AOP technology development, ensuring sustainability is evaluated beyond reaction operational performance alone.

5.1. Introduction

While AOPs have been widely studied for their pollutant removal efficiency, there remains a critical lack of systematic, standardized comparison between technologies in terms of their life cycle environmental and economic performance [176]. Many studies report high degradation rates or rapid reaction kinetics but often overlook or inconsistently account for the embodied energy, materials, and chemical inputs required to achieve those outcomes [176–178]

For instance, a photolysis system may demonstrate strong antibiotic degradation under intense UV irradiation, but with high electricity use and frequent lamp replacement [102]. Similarly, a catalyst showing high activity in a sono-photo-Fenton process might involve the use of rare metals or toxic dopants with high embodied environmental costs [57]. Conversely, processes that appear slower or less efficient may be more sustainable overall if they rely on milder operational conditions, reusable catalysts, or lower energy inputs [165,179]. These complexities highlight the need for holistic assessment frameworks that go beyond isolated performance metrics.

Building on the case study presented in Chapter 4, which evaluated multiple scenarios within a single sono-based AOP system, this chapter expands the scope to include cross-technology benchmarking. The methodology developed previously—integrating experimental insights with life cycle-based environmental analysis—now serves as a foundation for comparing fundamentally different AOP strategies under standardized conditions. One of the core challenges in comparative AOP studies is the

variability in experimental conditions, system scales, and reporting metrics across the literature. This chapter addresses that challenge by applying a harmonized functional unit and impact categories, allowing for more meaningful cross-study comparison despite inherent uncertainties.

To address this need, this chapter presents a comparative TEA/LCA study of five representative AOP technologies for the treatment of tetracycline-contaminated wastewater: Sonolysis, Photolysis, Fenton-like oxidation, Sono-photo hybrid, and Thermal-assisted oxidation. Each technology is analysed under a harmonized functional unit: the treatment of 1 Litre of wastewater containing tetracycline at 40 mg/L, with a target removal efficiency of 90%. This single-component setup represents an idealized scenario with a clearly defined functional unit for the LCA. It was chosen to isolate the performance of each technology without the confounding effects of complex real wastewater matrices, which often contain variable and interacting pollutants that are difficult to model consistently. This enables a direct, apple-to-apple comparison of each system's performance in terms of:

- Environmental indicators: carbon footprint (t-CO_2 eq), energy demand (MJ), human/ecological toxicity, resource depletion [117,118,128].
- Economic indicators: direct operational costs (e.g., electricity, reagents, catalyst use) and monetized environmental impact (e.g., environmental damage and remediation costs, climate-related costs) [126,127,180].

A cradle-to-gate system boundary is adopted (Figure B.1), capturing all upstream

inputs—from raw material extraction and catalyst synthesis to process operation—while recognizing that end-of-life impacts (e.g., catalyst disposal, reactor retirement) are outside the scope of the current study but important for future work. This boundary choice reflects the current maturity of AOP-based technologies, which are primarily studied at the reaction and degradation stage. Downstream processes such as reactor decommissioning, catalyst disposal, and broader system integration are either insufficiently characterized or not yet demonstrated in practice, making their inclusion in LCA highly uncertain [21–23]. As such, a cradle-to-gate approach allows for a more reliable and focused assessment based on available experimental data, with the understanding that a cradle-to-grave analysis will be essential in future, more complete evaluations.

Representative case studies are selected for each technology based on the availability of detailed data on energy input, chemical usage, catalyst preparation, and degradation kinetics. For each, a LCI is constructed, forming the basis for LCA. TEA is then conducted using consistent cost parameters, including energy tariffs, reagent pricing, and environmental damage costs.

This integrated framework serves three key purposes:

1. Benchmarking: It identifies which AOPs are not only effective in removing tetracycline, but also environmentally and economically sustainable.
2. Trade-off analysis: It allows for quantification of environmental vs. economic trade-offs, supporting more informed decision-making.

3. Framework validation: It demonstrates a modular, scalable methodology that can be extended to other pollutants, treatment scales, or system configurations.

Ultimately, this chapter seeks to shift the conversation from narrow performance evaluations toward life cycle-informed technology development, ensuring that AOPs chosen for future deployment are both technically sound and aligned with broader sustainability goals. The findings aim to inform both researchers and practitioners seeking to implement AOPs in real-world antibiotics treatment settings, where sustainability trade-offs are often overlooked in favour of performance under idealized lab conditions.

5.2 Method

5.2.1 Technology selection criteria

To ensure a robust and meaningful comparison of AOPs for tetracycline degradation, five representative technologies were selected from recent peer-reviewed literature. These cases were chosen to reflect the diversity of AOP mechanisms and to align with the core research scope established in Chapters 3 and 4. All selected studies target the degradation of tetracycline in aqueous solutions, allowing consistency with the pollutant of interest across the analysis.

The technologies included in this study span five major AOP categories:

- Sonolysis-based (Sono [17])
- Photolysis-based (Photo [181])

- Sono-photolysis hybrid (Sonophoto [153])
- Fenton-based (Fenton [182])
- Electrochemical oxidation (Electro [183])

The selection process was governed by several key criteria:

1. Relevance and reliability: All selected studies were published in reputable, peer-reviewed journals within recent years, ensuring both scientific credibility and contemporary relevance.
2. Consistent degradation kinetics: Only studies reporting first-order reaction kinetics were included, with the rate constant falling within a comparable range (i.e., no more than one order of magnitude apart). This prevents the distortion of comparative metrics due to extreme performance outliers and enables a fair assessment of trade-offs between performance and sustainability.
3. Comparable initial conditions: The initial tetracycline concentrations reported in the studies were generally cantered around 40 mg/L, with slight variations above or below. No cases with significantly higher or lower concentrations (i.e., outside one order of magnitude) were included to preserve consistency in functional unit definition and ensure meaningful comparisons.
4. Diverse dependency profiles: The selected cases represent a range of operational dependencies. Some rely more heavily on chemical inputs (e.g., reagents or oxidants), others emphasize catalyst synthesis, while some are dominated by energy-intensive operating conditions such as heating or ultrasound. This diversity enables cross-technology trade-off analysis between

environmental and economic burdens across different input types.

5. Explicit reporting of energy inputs: A key inclusion criterion was the availability of clearly reported energy consumption data for the treatment setup. Only studies that documented power input or energy use during the reaction stage were considered, as this information is critical for calculating environmental impacts and performing LCA. To ensure comparability, a consistent electricity mix (e.g., average UK grid mix and projected 2050 grid) were applied across all cases; distinctions between fossil and renewable energy sources were standardized in the LCA modelling stage.
6. Catalyst synthesis transparency: All selected cases provide sufficiently detailed descriptions of the catalyst preparation steps. Although not every specific precursor may be present in the life cycle inventory database, suitable proxy materials with similar environmental profiles are available and were used to approximate the emissions associated with synthesis.

These carefully defined criteria ensure that the selected technologies are not only representative of the AOP field, but also sufficiently aligned in scope and granularity to allow for harmonized environmental and economic assessment. The resulting dataset forms the basis for the LCI and TEA presented in the subsequent sections. The related kinetics and lifecycle inventory data are presented in the Appendix Tables C.2 to C.6.

The key assumptions regarding reusability in our model were: (1) Constant Performance: We assumed no loss in catalytic activity or degradation efficiency over the number of reuse cycles. (2) No Material Loss: We assumed the catalyst could be

recovered and reused with 100% mass yield, neglecting physical losses during recovery (e.g., during filtration, washing, and handling). (3) Simple Regeneration: We assumed that a simple washing step (e.g., with water or solvent) would be sufficient to fully restore catalytic activity, neglecting the potential energy or chemical cost of a more intensive regeneration process. (4) Arbitrary Lifetime: The number of reuse cycles (e.g., 10, 50, 100 cycles) was selected based on a plausible range for sensitivity analysis rather than on experimental data from long-term testing.

5.2.2 Life cycle assessment

The LCA approach adopted in this study follows the ISO 14040 and ISO 14044 standards, encompassing four core stages: goal and scope definition, inventory analysis, impact assessment, and interpretation. This methodology is applied to evaluate and compare the environmental performance of five AOP technologies used for tetracycline degradation, expanding the framework introduced in Chapter 4 to a broader, cross-technology assessment.

1. Goal and Scope Definition

The primary objective of this comparative LCA is to assess the environmental trade-offs and sustainability implications of different AOPs for antibiotics degradation. The focus is placed on tetracycline removal from aqueous media, maintaining consistency with the experimental and case-study focus of previous chapters.

The system boundary (Figure B.1), scope and the unit functions are described in

the previous section 5.1.

2. LCI and Data Sources

a. Material acquisition and synthesis

The inventory includes inputs related to catalyst synthesis, reagent use, and preparation steps. Material and energy flows were extracted primarily from the Ecoinvent 3.9 database using the SimaPro v9.5 platform. In cases where exact materials were unavailable, proxy compounds with similar production pathways and environmental profiles were selected. All processes were scaled and normalized to the functional unit, ensuring methodological consistency.

b. Energy consumption during reaction

Electricity and thermal energy used during each AOP treatment process were calculated based on reported power ratings and reaction durations needed to reach the 90% degradation benchmark. First-order kinetic assumptions enabled a uniform basis for determining reaction time across technologies. All energy data are evaluated under a consistent electricity grid profile (UK grid-mixed), with a sensitivity analysis provided later in the chapter.

c. Assumptions and harmonization strategy

To ensure comparability and minimize bias, only studies meeting the following criteria are describe in section 5.2.1. This harmonized approach allows for a meaningful "apples-to-apples" comparison of environmental impacts despite differences in process mechanisms and experimental conditions.

3. Impact Assessment: ReCiPe 2016 Midpoint and Endpoint Methods

Environmental impacts were evaluated using the ReCiPe 2016 method [117], which provides both midpoint and endpoint indicators. The midpoint assessment covers a broad range of 18 environmental categories, including climate change i.e., GWP, freshwater and marine ecotoxicity, human toxicity, ozone depletion, resource depletion, and more. This enables a detailed evaluation of specific environmental stressors.

Table 5.1. The 18-midpoint environmental impact category indicators

Nomenclature	Midpoint impact category	Indicators
GW	Global warming	kg CO_2eq
SOD	Stratospheric ozone depletion	kg CFC11eq
IR	Ionizing radiation	kBq Co-60 eq
OFH	Ozone formation, Human health	kg NOx eq
FPM	Fine particulate matter formation	kg PM2.5 eq
OFT	Ozone formation, Terrestrial ecosystems	kg NOx eq
TA	Terrestrial acidification	kg SO_2 eq
FE	Freshwater eutrophication	kg P eq
ME	Marine eutrophication	kg N eq
TEt	Terrestrial ecotoxicity	kg 1,4-DCB
FEt	Freshwater ecotoxicity	kg 1,4-DCB

MEt	Marine ecotoxicity	kg 1,4-DCB
HCT	Human carcinogenic toxicity	kg 1,4-DCB
HNCT	Human non-carcinogenic toxicity	kg 1,4-DCB
LU	Land use	m^2a crop eq
MRS	Mineral resource scarcity	kg Cu eq
FRS	Fossil resource scarcity	kg oil eq
WC	Water consumption	m^3

Meanwhile, the ReCiPe 2016 Endpoint method is also used to quantify the different environmental impacts into three major categories, in terms of resources, human health, and ecosystem. Table C.1 in Appendix C shows the 22-endpoint environmental impacts that are associated with the three major categories. The endpoint (damage-oriented) analysis aggregates midpoint impacts into three overarching damage categories:

- Human Health (e.g., DALYs due to toxicity or air pollution)
- Ecosystems (e.g., species loss from land use, ecotoxicity, and climate change)
- Resources (e.g., economic value loss due to fossil or mineral depletion)

These three damage categories provide a higher-level, decision-relevant view of the environmental burden. In addition, this endpoint framework supports monetization, enabling the conversion of environmental damage into implicit economic costs via damage-to-cost factors—discussed in the subsequent section.

All impact assessments were conducted using characterization factors and

weighting models built into ReCiPe 2016 within the SimaPro software environment. Results are presented in both absolute and relative terms, allowing for direct comparison across technologies and highlighting key environmental trade-offs.

5.2.3 Economic evaluation

Economic performance is a crucial factor in the broader assessment of wastewater treatment technologies, particularly when considering potential scale-up and real-world implementation. In this study, the economic evaluation focuses on operating costs for antibiotic degradation processes. This approach reflects the early-stage, low-TRL (Technology Readiness Level) status of the selected AOP technologies, for which reliable CAPEX data is either unavailable or highly uncertain.

While standard TEAs at industrial or pilot scale typically include both CAPEX and OPEX—often using methods like Internal Rate of Return (IRR) or Net Present Value (NPV)—such frameworks rely on mature system designs where equipment costs and scaling factors can be quantified. For novel, lab-scale processes, CAPEX estimation is speculative due to the variability in lab setups, custom configurations, and lack of standardization. Therefore, this study focuses on operating costs, which are more consistently reported and comparable across technologies.

It is also worth noting that operating costs often dominate total expenditure at larger scales, as amortized capital costs decrease with scale (e.g., per the 6/10 scaling rule), while unit consumption of utilities and chemicals typically remains constant. Thus, while this TEA is based on lab-scale data, the emphasis on OPEX maintains relevance

for future scale-up scenarios.

1. Direct Operating Costs

The direct operating cost includes [184]:

- Utility costs, primarily electricity prices, are taken from the recent LCA/TEA studies [185,186].
- Material costs, encompassing chemicals and reagents used in the reaction (e.g., H_2O_2 ($1/kg [187]), anode (Pt-$33/g) and cathode (carbon-$0.15/kg [188]) materials).

These values are drawn from standardized market prices or reputable databases, and assumptions regarding chemical consumption and process repetition are harmonized across technologies.

2. Indirect (Monetized Environmental) Costs

In addition to direct operational expenses, this analysis incorporates indirect costs through the monetization of environmental damage, derived from the ReCiPe 2016 endpoint method [117]. As outlined in the previous section, ReCiPe translates multiple environmental impacts into three damage categories: Human health, Ecosystem quality, Resource depletion. Each of these categories can be monetized using established conversion factors, often used in sustainability and policy analysis. These conversion factors, expressed in $/DALY, $/species.year, and $/USD resource loss, enable the estimation of a monetized environmental burden that reflects the impact not captured in direct market prices. The environmental impact monetization is calculated by multiplying each endpoint damage assessment by its corresponding index, resulting in

values expressed in 2019 USD [126,189]. CEPCI stands for the Chemical Engineering Plant Cost Index. It is a widely used index for inflating capital costs of chemical plants from a past year to a current dollar value. Considering the rise of CEPCI, the monetary value is scaled to the 2023 value [190,191]. The methodology for applying monetization coefficients is detailed in Table 5.2.

Table 5.2. Monetization factors of the three-endpoint damage assessment value.

Endpoint indicator	Unit	Monetization factor (USD 2023)
Human health	DALY	2×10^5
Ecosystem	Species.yr	5.33×10^7
Resources depletion	USD2013	1.44

This two-tiered approach—combining explicit (direct) operating costs and implicit (indirect) environmental costs—aims to offer a more holistic understanding of the true cost of each AOP technology. This framework supports the identification of trade-offs between degradation efficiency, operational expenditure, and environmental impact, ultimately guiding the selection of sustainable and economically viable treatment strategies.

3. Indirect (carbon tax) Costs

In addition to monetized environmental damage derived from ReCiPe endpoint indicators, this study also considers the economic implications of carbon taxation policies, which are increasingly being adopted across the globe. Carbon taxes place a

direct cost on GHG emissions—primarily CO_2—with the objective of internalizing the environmental impact associated with fossil energy consumption. Many studies have incorporated carbon tax into comprehensive economic analyses across various fields, including hydrogen production, methanol synthesis, syngas generation, and biopolymer manufacturing [185,186,192–194].

To reflect this policy-driven economic burden, the total CO_2-equivalent emissions associated with each AOP process (as calculated in the life cycle inventory) are multiplied by a representative carbon price. For this study, a moderate carbon tax of $100 per metric ton of CO_2 is applied, consistent with carbon pricing scenarios projected by institutions such as the IEA [195], and various national regulatory bodies targeting net-zero commitments.

This carbon cost represents an additional indirect operational burden that aligns with current and emerging environmental policies. Including this component allows for a more policy-relevant economic evaluation, offering insight into how each technology might perform under realistic regulatory conditions. Moreover, it complements the monetized ReCiPe-based approach by specifically isolating the economic impact of climate-related emissions, which are often a major contributor in high-energy AOP systems.

Together, the incorporation of direct operating costs, monetized environmental impact, and carbon taxation scenarios provides a comprehensive and forward-looking framework to evaluate the economic sustainability of AOP technologies under both current market conditions and future policy environments.

5.3 Results

5.3.1 Kinetic and degradation performance

Figure 5.1 compares the degradation kinetics of tetracycline across five representative AOPs, including sonolysis, photolysis, sonophotolysis, electrochemical oxidation, and Fenton-like oxidation. All treatment processes were fitted to a first-order kinetic model, and the corresponding rate constants were used to estimate the time required to achieve 90% degradation.

Among all systems, the sono-based process (TFNs + H_2O_2) demonstrated the fastest degradation kinetics, requiring approximately 28 minutes to reach the 90% removal target. This high performance is attributed to the synergistic effect of acoustic cavitation, cavitation-enhancing nanostructured TFNs, and in situ radical generation via H_2O_2 activation, as discussed in Chapters 3 and 4. The photolysis-based process and the electrochemical oxidation process showed similarly fast reaction rates, completing 90% degradation in less than 30 minutes. These technologies utilize high-energy light or electrochemical potential to continuously generate reactive species, but are typically associated with high electricity consumption and potential electrode or lamp degradation over time. The sonophotolysis case demonstrated slower kinetics than individual photolysis or sonolysis, possibly due to suboptimal synergy or higher energy distribution losses in hybrid operation. In contrast, the Fenton-like process exhibited the slowest kinetics, requiring more than 120 minutes to achieve comparable

degradation. Despite its slower rate, this method does not require direct electrical input and remains one of the most established and chemically straightforward AOPs, relying on iron-catalysed H_2O_2 decomposition to generate hydroxyl radicals.

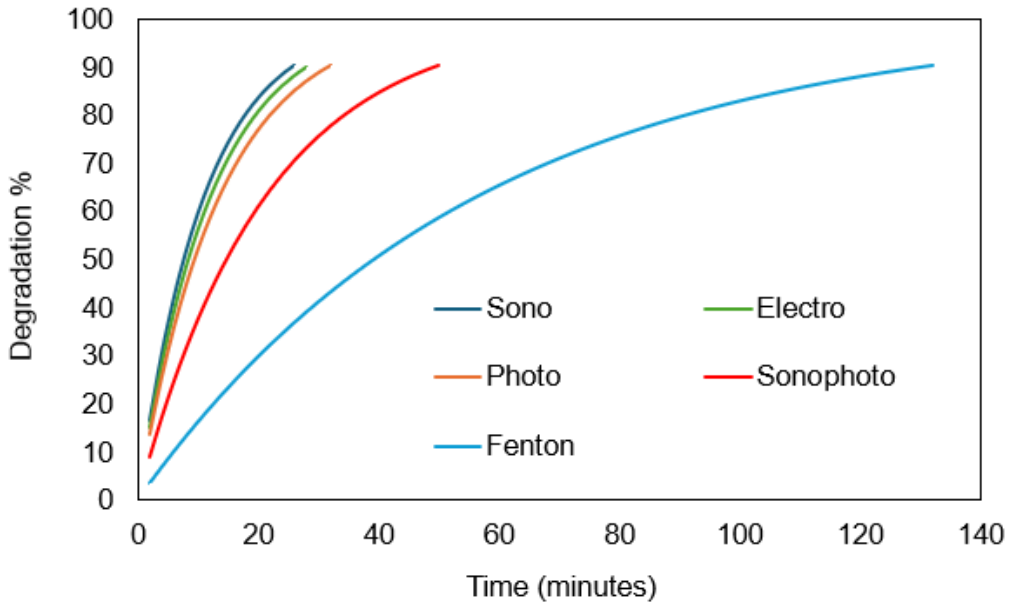

Figure 5.1. Time-dependent tetracycline degradation performance based on first-order reaction kinetics of five studied AOP processes

While degradation kinetics offer important insights into treatment performance, they do not reflect the complete sustainability profile of a given process. A fast-acting AOP may rely heavily on electricity, rare or toxic chemicals, or intensive catalyst synthesis steps, all of which contribute to environmental burdens that are not captured by kinetics alone. Conversely, a slower process may have a lower environmental footprint due to simpler inputs or less energy demand. Therefore, it is crucial to complement kinetic evaluation with a comprehensive environmental assessment that accounts for the full spectrum of process-related impacts—including electricity and chemical consumption during operation, as well as upstream emissions from catalyst

synthesis and material acquisition. This gap underscores the need for the life cycle-based comparison presented in the following section.

5.3.2 Environmental impact distribution of each process

This section aims to analyse midpoint environmental performance across 18 impact categories of five studied processes using the ReCiPe 2016 method. The following Figures 5.2-5.6 present the characterization results for the 18 midpoint impact categories and expressed in percentage terms to highlight the relative contribution of each component to the total environmental burden. For readers interested in the corresponding normalized values, detailed numerical data are provided in Tables C.7–C.11 in the Appendix C.

Figure 5.2 presents the detailed environmental impact distribution of the Sono-based process. Across nearly all categories, the electricity used during operation stands out as the dominant contributor, accounting for more than 80% of the impact in categories such as Stratospheric Ozone Depletion, Ionizing Radiation, and Marine eutrophication. This reflects the high energy input required for ultrasound-driven cavitation in the sonoreactor [196,197]. Despite using a relatively short treatment time compared to other AOPs (as shown in Section 5.3.1), the instantaneous power demand remains a critical driver of the environmental footprint.

The second-largest contributor is ethanol, which is used in multiple stages—catalyst synthesis, chemical preparation, and washing. Ethanol-related impacts are particularly notable in categories such as Fossil Resource Scarcity, Ozone formation

regarding human health and Terrestrial ecosystems, and Terrestrial Acidification. This is due to its solvent properties, volatility, and the upstream processes involved in ethanol production [198].

The titanium precursor (used for synthesizing TFNs) contributes moderately to categories linked to resource scarcity (e.g., Mineral Resource Scarcity), and Human Carcinogenic Toxicity, but its influence is far less significant than energy or ethanol inputs. Other materials such as styrene (used as a template agent in catalyst fabrication), potassium sulphate, and deionised water show minor contributions, generally below 5% in all categories. Their limited impact is due to the relatively small quantities used per unit of wastewater treated and the less energy-intensive nature of their production compared to solvents and electricity.

This analysis underscores that while the Sono process achieves superior degradation performance (as shown in Section 5.3.1), its environmental cost is heavily influenced by the operational electricity and ethanol usage. Optimizing the sonoreactor to improve energy efficiency and power it with renewable electricity would significantly enhance the environmental performance. It also reinforces the necessity of considering multi-dimensional environmental indicators when evaluating AOP technologies—since improvements in one category may come at the cost of another.

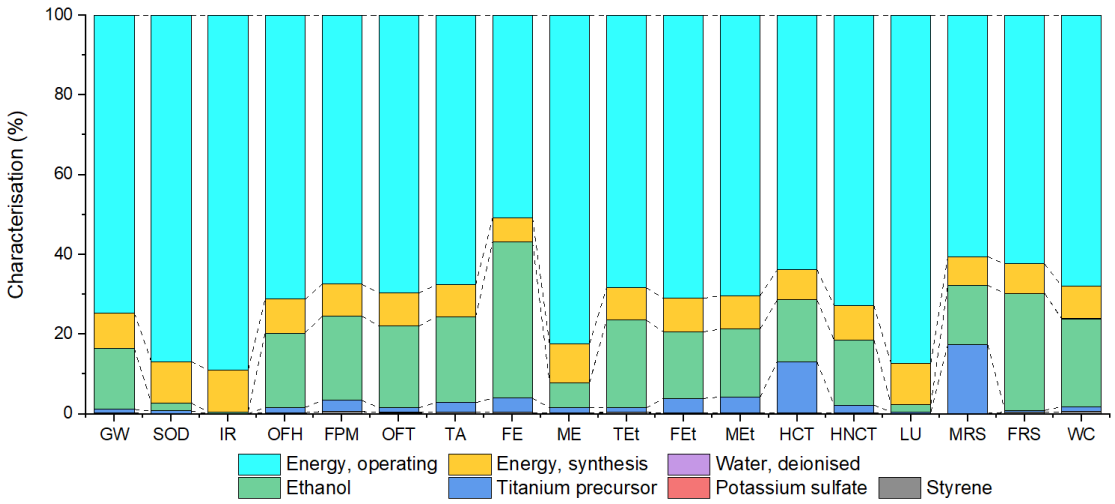

Figure 5.2. Detailed distribution of 18 midpoint environmental impacts in the Sono-based process

Figure 5.3 presents the midpoint environmental characterization of the photolysis-based process. The energy consumption during both catalyst synthesis and operation remains dominant, especially the energy consumption during the complicated catalyst synthesis steps, collectively contributing nearly two-thirds of the total impact across most environmental categories. This high burden stems from the lengthy and energy-intensive hydrothermal and drying procedures, including autoclave-based treatments, required to fabricate the catalyst.

Following energy contributions, sodium hydroxide emerges as the next major contributor, particularly in categories such as Terrestrial Acidification and Eutrophication due to its chemical intensity and common use in catalyst precipitation steps. The impact of TiO_2 nanoparticles is especially prominent in Human Carcinogenic Toxicity and Mineral Resource Scarcity [199]. This is because nanostructured TiO_2 materials, unlike Ti-salt or bulk TiO_2, require additional post-processing and finer control over morphology, increasing the embodied emissions during synthesis [200].

Glucose, while a relatively minor component overall, contributes noticeably to the ecotoxicity and land use indicator, reflecting the upstream agricultural and refinement burdens of biobased precursors.

In summary, although the photolysis process avoids reliance on exotic or rare materials, its broad material consumption and energy-intensive synthesis route led to a widespread environmental footprint. This highlights the importance of not only evaluating chemical efficiency but also optimizing process intensification and simplification when targeting sustainability improvements in catalyst-based photolytic systems.

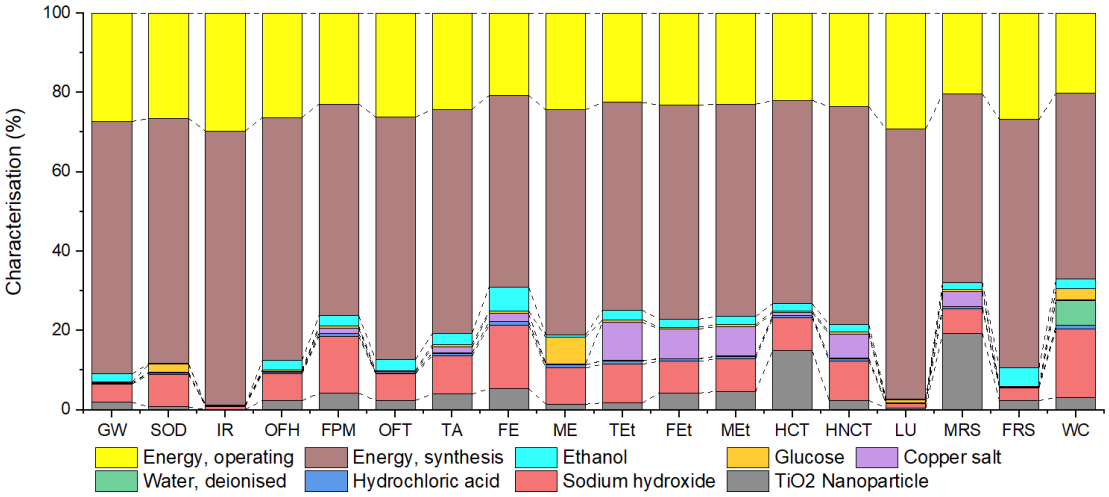

Figure 5.3. Detailed distribution of 18 midpoint environmental impacts in the Photo-based process

Figure 5.4 presents the midpoint-based environmental characterization for the sonophotolysis process, which combines ultrasonic and photonic energy inputs. A distinct feature of this process is the substantial contribution from tungsten precursors—used in the synthesis of the sonophoto catalyst—which dominate several

categories such as Marine Ecotoxicity, Human non-carcinogenic toxicity, Ecotoxicity-related indicators and Mineral Resource Scarcity [201,202]. This reflects the high environmental cost of mining and refining tungsten-based materials, and the intensive production and potential ecotoxicity of materials, especially when used in conjunction with carbon nanotube supports.

Energy for operating the combined sonophoto system contributes significantly across categories like Global Warming, Stratospheric Ozone Depletion, and Ionizing Radiation, due to the dual input of ultrasound and UV light. This elevates the power demand compared to single-mode AOPs, such as photo or sono alone. Catalyst synthesis energy—including high-temperature processing—further adds to the impact, particularly in Ionizing radiation. The use of ethanol and deionised water, while present across categories, has a relatively moderate contribution except in Water Consumption and certain toxicity indicators. Additionally, carbon nanotubes, though used in small quantities, made considerable contributions to impacts such as Water consumption, due to the use of liquid nitrogen and water during the CNT fabrication process [203,204].

Overall, this case illustrates the trade-off between improved operational performance and increased environmental burden, due to both high operating energy demand and the synthesis of complex, nanostructured materials. While the system performs well in terms of degradation, its sustainability is challenged by its material and energy footprint, emphasizing the importance of weighing performance gains against environmental costs.

For energy-intensive AOPs—such as sono, photo, and sonophoto methods—the

environmental impact is dominated by electricity consumption, both during operation and catalyst synthesis. Consequently, under current grid conditions with medium to high carbon intensity, these processes may be less environmentally favourable than conventional alternatives like Fenton oxidation. However, their performance is poised to improve significantly as electricity generation becomes more sustainable.

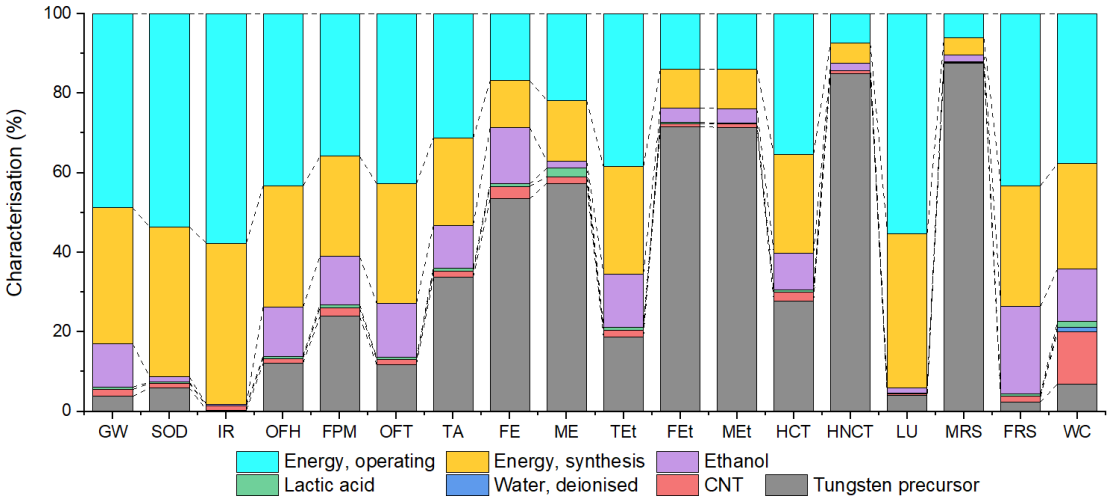

Figure 5.4. Detailed distribution of 18 midpoint environmental impacts in the Sonophoto-based process

Figure 5.5 displays the midpoint characterization of the Fenton-based process. Distinct from energy-intensive systems, this method demonstrates negligible environmental burden from operational energy consumption, as the core reaction is chemically driven and does not require significant external electricity or thermal input. This is reflected by the minimal contribution of operating energy across all 18 impact categories. However, the energy required for catalyst synthesis remains a significant contributor, particularly due to precursor processing steps. More critically, the environmental footprint of this process is dominated by chemical inputs, especially ethanol and ethylene glycol, which are widely used as solvents or stabilizers during

material preparation. These two inputs substantially affect categories such as acidification and eutrophication-related terms, Ozone formation-related terms, and Freshwater Resource Scarcity [205].

Hydrogen peroxide, a primary reagent for radical generation in the Fenton process, contributes modestly to the total impact—most notably in Water consumption—but does not dominate any specific category. Other reagents such as iron chloride, sodium hydroxide, and acetic acid show minimal impact contributions, highlighting the relatively low material intensity of the inorganic components involved.

In summary, while the Fenton process appears environmentally benign from an energy standpoint, its dependence on high-volume organic chemicals during catalyst synthesis introduces notable environmental burdens. Process improvements should thus prioritize solvent replacement or reduction, which could significantly enhance its sustainability profile without sacrificing performance.

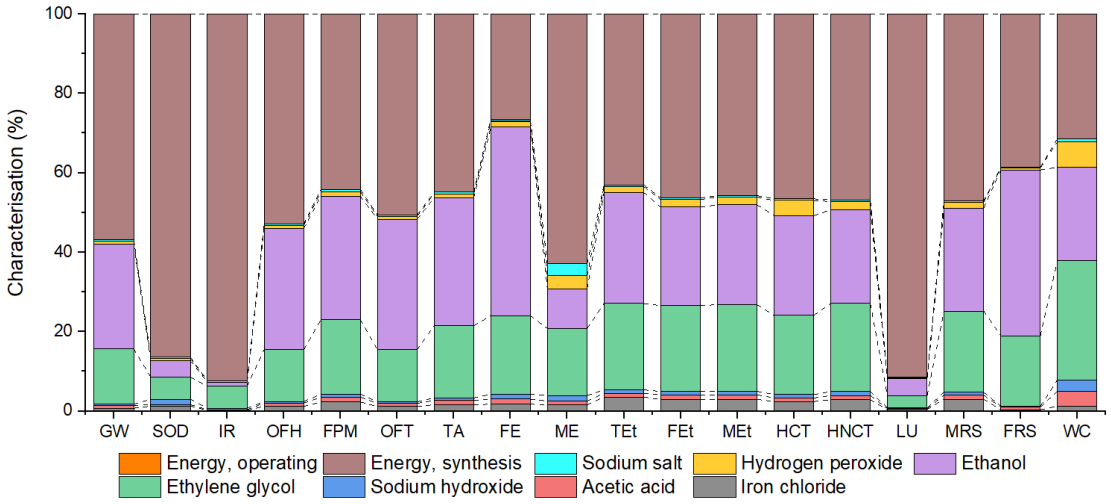

Figure 5.5. Detailed distribution of 18 midpoint environmental impacts in the Fenton-based process

Figure 5.6 presents the midpoint-level environmental impact breakdown of the electrochemical oxidation process. The most striking finding is the dominant contribution of platinum (assuming 10,000 hours lifetime, four times the conservative estimation [206]), which accounts for over 80% of the impact across nearly all categories. As the anode material in this system, platinum's extremely high embodied emissions—stemming from its mining, refinement, and scarcity—lead to significant burdens in Global Warming, Human and Ecotoxicity, Resource Scarcity, and Freshwater Eutrophication [160,161].

The second largest contributor is energy used during catalyst synthesis, followed by operating electricity, which together account for most of the remaining burden. This shows that while the system may rely less on frequent chemical inputs during operation, the upstream material intensity and synthesis-related energy demands are substantial. Although operating electricity is a relatively small contributor in this case compared to other AOPs, it still meaningfully affects categories. The overall energy consumption contributes significantly too, such as Ionizing Radiation, Terrestrial ecotoxicity, and Water Consumption, especially when non-renewable grids are considered.

Among the remaining factors, ethylenediaminetetraacetic acid (EDTA) appears prominently in the Marine Ecotoxicity category, likely due to its persistence and chelation behaviour in aquatic systems. Similarly, nickel nitrate has noticeable contributions in Terrestrial Ecotoxicity and Water Consumption, reflecting its toxicity profile and manufacturing intensity.

In summary, the electrochemical oxidation process is heavily influenced by the

environmental cost of platinum use, which dwarfs even energy-related impacts. This highlights a key trade-off: although such systems may offer high degradation efficiency and minimal reagent use, their overall sustainability is highly constrained by the choice of electrode material, reinforcing the need for alternative, lower-impact anode options in future designs.

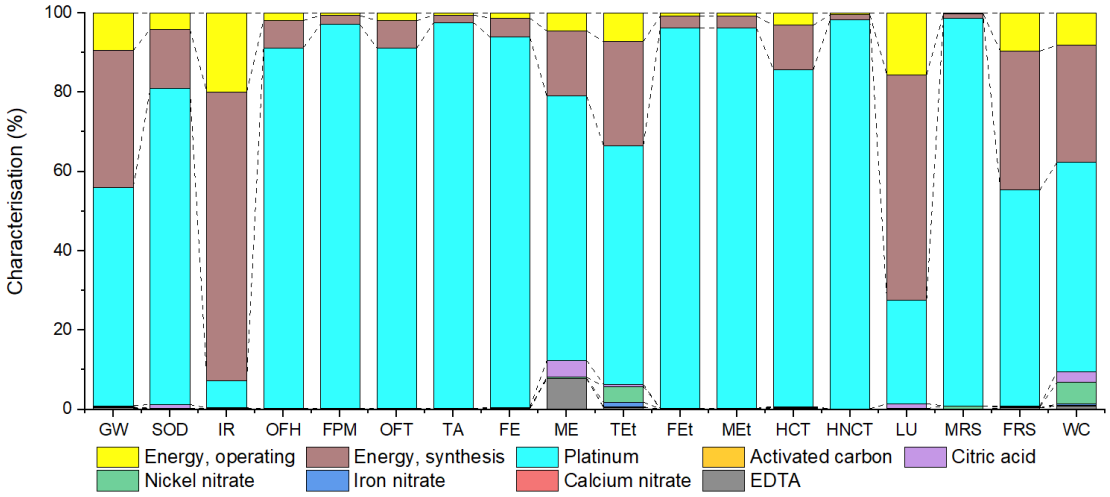

Figure 5.6. Detailed distribution of 18 midpoint environmental impacts in the Electro-based process

Across the analysed AOP technologies, a clear pattern emerges: energy consumption—both during operation and catalyst synthesis—is consistently one of the dominant contributors to environmental impact, especially in sonochemical and photo-driven processes. This reinforces the importance of considering total energy use rather than operational performance alone when evaluating sustainability. Additionally, while the direct impact from the metal content of catalysts is often perceived as minor, the associated chemical inputs, such as ethanol, play a disproportionately large role in several impact categories (e.g., human health and ecotoxicity). Ethanol, though commonly regarded as a benign solvent, can introduce significant burdens due to its

upstream production and usage volumes. Notably, the use of novel or high-impact metals such as tungsten and platinum—even in small quantities—can substantially elevate the environmental footprint, particularly in resource scarcity and toxicity categories. In contrast, catalysts based on conventional, low-impact metals (e.g., iron or copper) demonstrate more favourable environmental profiles. These findings suggest that material selection and process simplification are key levers for reducing the life cycle burden of AOP technologies.

5.3.3 Life cycle comparison across AOPs

Figure 5.7 presents a sensitivity analysis of GWP as a function of catalyst reusability for the five AOP technologies evaluated. Across all processes, increasing the number of reuse cycles significantly lowers CO_2 emissions per Lire of wastewater treated, particularly within the first 10–50 cycles, where the most substantial reductions are observed. This is due to the amortization of emissions associated with catalyst synthesis across more treated volume.

Among the five, the sono process initially shows the highest GWP at low reuse but converges closer to the electro process beyond ~5 cycles. In contrast, the Fenton process consistently achieves the lowest emissions as reuse increases, driven by its inherently low reliance on energy input and simplified chemical demands. Photo and sonophoto perform comparably well, especially as catalyst reusability improves, reflecting their moderate synthesis-related burdens and reasonable energy efficiency.

This analysis underscores that catalyst durability is a key driver of environmental sustainability and should be prioritized alongside performance metrics in AOP design. Processes with higher initial synthesis burdens (e.g., sono and electro) can still be viable if long-term reuse is ensured. Notably, when the number of reuse cycles reaches 100 or more, the CO_2 emissions from most AOPs can be reduced by over 60–80% compared to single-use scenarios. For example, the GWP of the sono-based process drops from approximately 0.37 kg CO_2/L at first use to below 0.12 kg CO_2/L after 100 reuses—representing a ~70% reduction. Similarly, photo and sonophoto processes show GWP reductions of over 65% at 100 reuses, while Fenton can achieve up to 90% CO_2 mitigation when reused extensively. These findings emphasize that catalyst reusability is not only economically beneficial but also a powerful strategy for minimizing climate-related impacts in AOP systems.

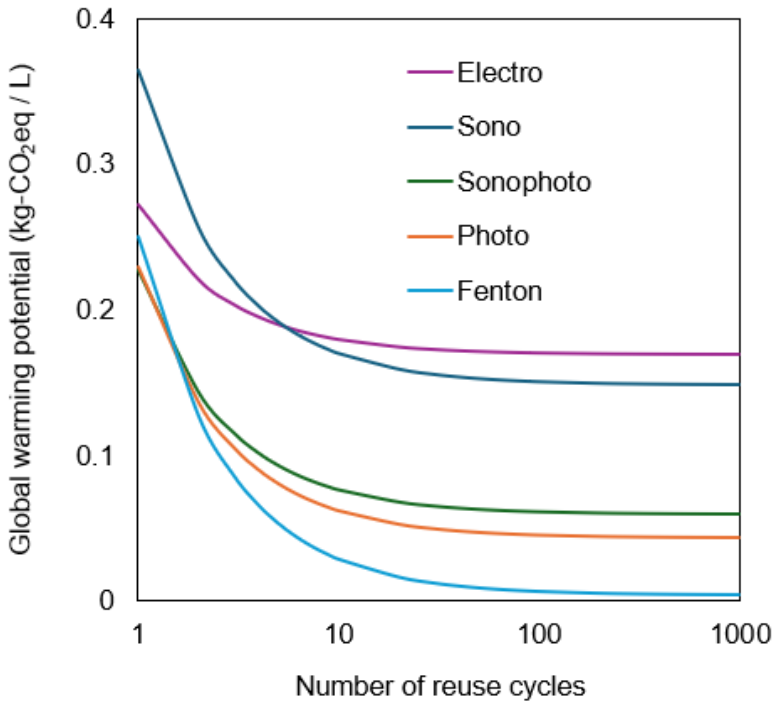

Figure 5.7. Sensitivity analysis of catalyst reusability on CO_2 emissions in tetracycline

degradation via selected AOP processes

The next sensitivity analysis (Figure 5.8) highlights the influence of electricity source carbon intensity on the overall CO_2 emissions (GWP) of different AOP technologies for tetracycline degradation. Among all five processes, sono exhibits the steepest slope, meaning its GWP is highly dependent on the carbon intensity of electricity. At very low CO_2 intensity (e.g., ~50 g-CO_2/kWh), the sono process can achieve emissions below 0.2 kg-CO_2/L. However, if powered by a carbon-intensive grid (~300 g-CO_2/kWh), emissions exceed 1.2 kg-CO_2/L—roughly a 6-fold increase. This suggests that while sono may be effective under clean energy grids, its sustainability deteriorates rapidly under fossil-dominant energy grids. The photo and sonophoto processes also show strong dependency on electricity emissions, with their GWP values more than tripling across the tested range. Sonophoto sits between sono and photo in sensitivity, reflecting its dual reliance on both light and ultrasound energy inputs.

In contrast, the electro process maintains nearly flat GWP performance regardless of electricity intensity. This is because its total emissions are dominated by the embodied emissions of materials—particularly platinum, used as the anode. The minimal slope here implies that even when ultra-low-carbon electricity is available, the benefit is limited due to the large, fixed emissions burden from materials. This observation aligns with the breakdown analysis in the previous section, where platinum alone contributed over 80% of the total impact. Fenton, while also relatively energy-lean during operation, shows a moderate slope. This is mainly due to its minimal electricity input combined with chemical reagents like H_2O_2 and Fe-based catalysts. As

electricity becomes cleaner, the Fenton process benefits incrementally, though the improvement is not as significant as for sono/photo processes.

Importantly, this analysis underscores that energy-efficient systems are not always environmentally superior unless the upstream electricity is decarbonized. In cleaner grid contexts (e.g., <100 g-CO_2/kWh), all five processes converge to relatively low GWP values, allowing room for performance-based selection. However, in current or fossil-dominant electricity grids, energy-intensive processes may inadvertently negate their treatment benefits by introducing high indirect emissions. Therefore, matching the AOP technology to regional electricity contexts is essential. In regions with fossil-dominant grids, lower-energy or material-efficient methods (e.g., Fenton or modified electro systems with less critical metals) may be preferable. In contrast, in areas with renewable-based electricity or when long-term decarbonization is assumed (e.g., under 2050 net-zero targets), high-performance, energy-intensive options like sono or sonophoto become more justifiable.

This insight supports the need for geo-contextual and time-evolving sustainability evaluations, rather than fixed conclusions based on laboratory-scale performance alone.

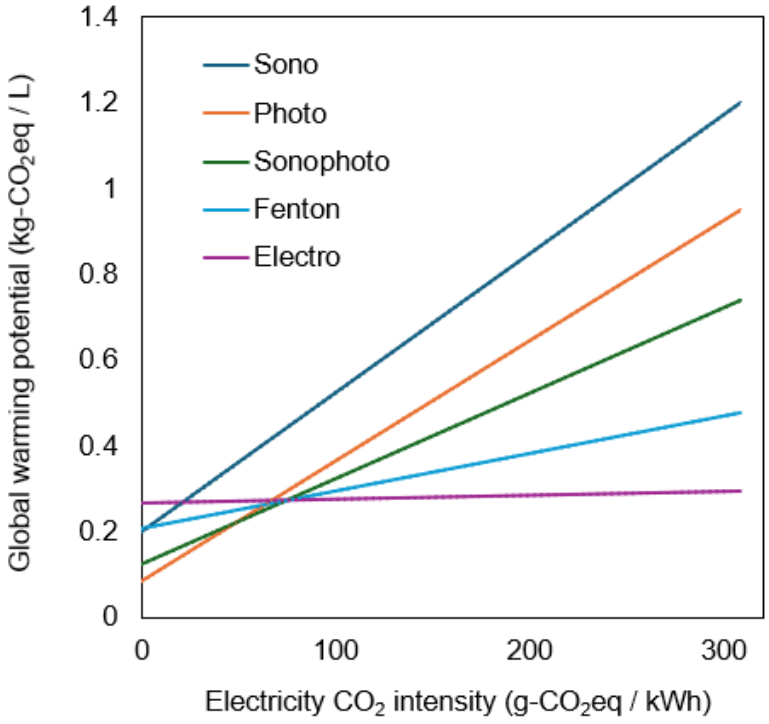

Figure 5.8. Sensitivity analysis on the effect of CO_2 intensity of electricity on CO_2 emissions in tetracycline degradation via selected AOP processes

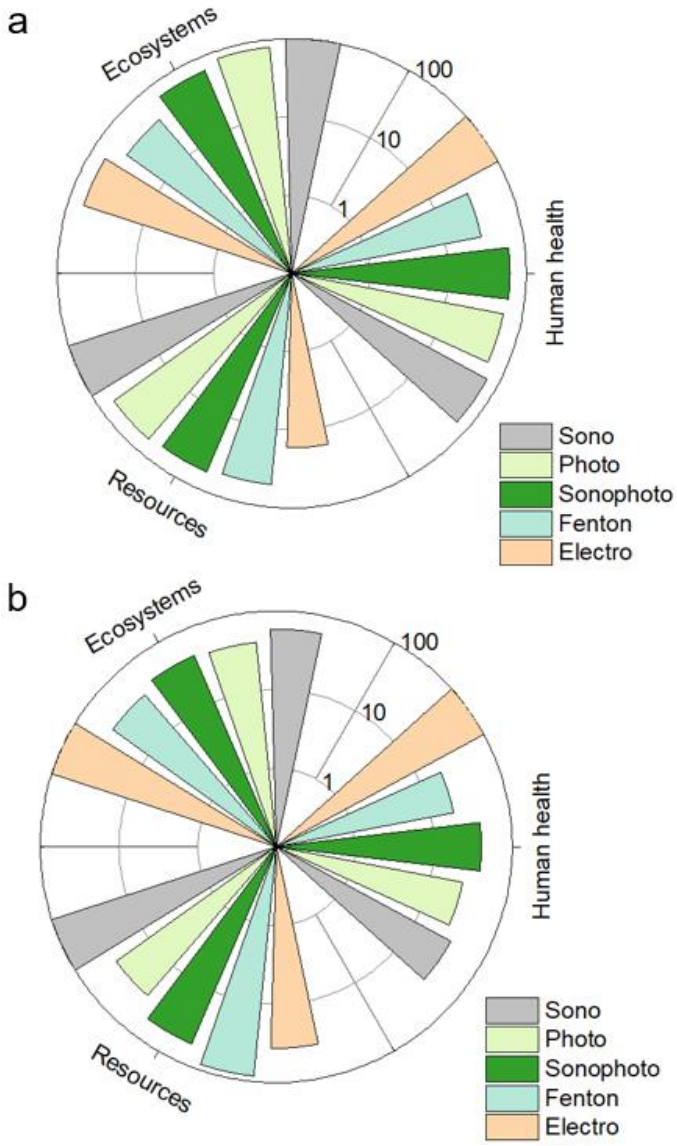

Figure 5.9. Environmental endpoint damage impact (ecosystem, human health, resources) of selected AOP processes using (a) current UK grid-mixed electricity (b) IEA projected electricity grid-mix in 2050

Figure 5.9 illustrates the endpoint environmental damage of five selected AOP technologies—sono, photo, sonophoto, Fenton, and electro—based on the ReCiPe 2016 method, categorized into impacts on ecosystems, human health, and resource availability. Panel (a) presents the assessment under the current UK grid-mixed electricity scenario, while panel (b) reflects the projected low-carbon electricity

scenario proposed by the IEA for 2050. The detailed characterized 22 endpoint environmental impacts of selected AOP processes are presented in the appendix C, Figures C.1 and C.2, and the normalized results are shown in Tables C.12 and C.13.

Under the current grid mix, the sono-based process demonstrates the highest environmental damage, particularly in the ecosystems and resource categories, due to the excessive electricity demand. The photo and sonophoto processes also show notable impacts across all three damage categories due to their elevated electricity demands and complex catalyst synthesis procedures, which often involve energy-intensive steps and organic solvents. Although the photo process performs slightly better than its hybrid or ultrasound-assisted counterparts, it still suffers from significant upstream emissions related to chemical usage and material fabrication. In contrast, the Fenton process shows the lowest damage potential across all three categories. Its relatively low reliance on external energy input and the use of more conventional reagents results in a notably smaller environmental footprint under current energy conditions.

When the electricity scenario shifts to the projected IEA 2050 grid-mix, which emphasizes a decarbonized energy supply, a substantial decrease in endpoint environmental damage is observed for the sono (52-65%), photo (55-79%), and sonophoto (36-61%) processes. This demonstrates the high sensitivity of these electricity-intensive technologies to the carbon intensity of the grid. Under this future scenario, the environmental gap between the Fenton process and the other AOPs begins to narrow. However, the electro process still remains among the least favourable options. This is largely attributed to its reliance on platinum as an anode material, which carries

an exceptionally high embodied environmental burden, indicating that material-related emissions are less affected by electricity source improvements. Overall, while grid decarbonization plays a critical role in improving the sustainability of AOP systems, this analysis highlights that material selection—especially the avoidance of rare or high-impact metals—is equally crucial for minimizing damage across human health, ecosystems, and resource depletion domains.

Each of the three endpoint categories captures a distinct aspect of environmental harm that extends beyond immediate emissions or resource consumption. Human health damage accounts for the potential burden of toxic emissions and pollutants that contribute to diseases, respiratory issues, or carcinogenic effects. In this context, processes involving solvents like ethanol, hazardous synthesis reagents, or high energy use (especially from fossil-dominant grids) tend to score poorly. For example, both sono and electro processes exhibit elevated human health impacts, due to either energy demands or high-impact materials like platinum. Ecosystem damage, on the other hand, reflects long-term risks to biodiversity, terrestrial and aquatic ecosystems, and land use disturbance. The use of ecotoxic or persistent chemicals—such as certain metal salts, acids, or nanomaterials—can drive this impact. Technologies relying on novel or poorly degradable materials (e.g., carbon nanotubes or advanced doped catalysts) are especially prone to higher ecosystem stress. Finally, the resource scarcity indicator reflects the depletion of non-renewable minerals and fossil resources. Electro and sonophoto processes score higher here due to their dependency on scarce metals like platinum or tungsten, which require energy-intensive extraction and processing, often

from geopolitically constrained sources.

These distinctions emphasize that no single process is optimal across all sustainability dimensions, and improvements in one domain (e.g., lower energy use) may inadvertently increase burdens elsewhere (e.g., rare metal use). Thus, integrated assessments that capture the broader environmental and societal consequences are essential to inform rational, context-sensitive decisions in advanced oxidation process (AOP) deployment.

5.3.4 Economic analysis

Figure 5.10 illustrates the hybrid operating costs of five selected AOP technologies, combining direct costs (electricity and chemical use) with monetized environmental damage (categorized under human health, ecosystems, and resource depletion) and policy-related carbon tax cost. This approach allows for a more holistic understanding of each process's actual cost by capturing not only market expenditure but also environmental impact which traditionally ignored in conventional economic analysis.

Among all processes, the electrochemical method exhibits the highest overall cost, reaching approximately $0.85/L. Strikingly, over 65% of this total comes from the monetized damage to human health, largely due to the use of platinum electrodes and associated upstream impacts. While its direct electricity and chemical costs appear modest, these hidden burdens significantly inflate its societal footprint.

The sono-based process follows with a total cost of around $0.57/L, of which electricity accounts for roughly 25.7%, and the combined environmental damages add

nearly $0.38/L. These high values highlight how electricity-intensive systems—despite strong degradation performance—may become unsustainable under carbon-intensive grids unless mitigation strategies are introduced.

On the other hand, the Fenton-based process, though slower kinetically, demonstrates the lowest hybrid cost, at just $0.29/L, with nearly 90% of that stemming from monetized costs from environmental and relatively minor direct operating cost due to minimal energy use and relatively benign reagents. The photo and sonophoto processes present balanced profiles at $0.31 and $0.40/L, respectively.

This hybrid cost analysis demonstrates that relying solely on traditional cost metrics (e.g., electricity and reagent prices) may lead to underestimation of a technology's full impact. By quantifying environmental damages in monetary terms, decision-makers can directly compare trade-offs and identify technologies that balance performance, affordability, and long-term sustainability. In this context, photolysis and Fenton processes emerge as promising options—not only for their economic affordability but also for their relatively low environmental impact when assessed comprehensively.

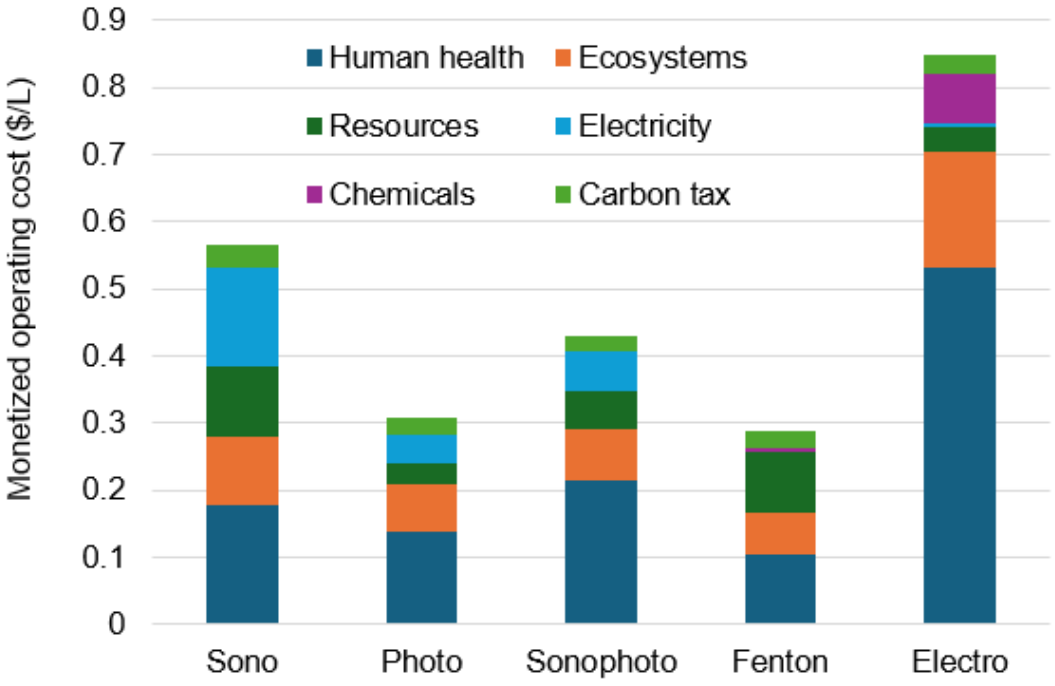

Figure 5.10. Operating costs of selected AOP processes, accounting for utilities, chemical use, and monetized environmental impacts

Additionally, carbon tax contributions, although relatively small compared to other categories, are non-negligible—particularly in the sono and electrochemical processes. For the electrochemical method, the carbon tax ($0.027/L) adds a measurable burden due to its upstream energy and material inputs, further compounding its already high societal cost. In the sono process, the carbon tax component ($0.037/L represents 6.4% of the total cost) reflects the significant electricity demand, underscoring the sensitivity of energy-intensive technologies to decarbonization policies. Conversely, the photolysis and Fenton processes exhibit minimal carbon tax penalties, aligning with their lower energy consumption and overall environmental impact. These findings reinforce the importance of integrating carbon pricing into economic evaluations, especially under scenarios aiming for climate-aligned transitions.

5.3.5 Social Considerations in Comparative AOP Evaluation

Beyond technical and environmental metrics, the sustainable deployment of advanced oxidation processes (AOPs) also hinges on their social viability. This includes factors such as occupational safety, public health implications, accessibility in low-resource settings, and alignment with principles of equity and fair labour. While these elements are often overlooked in early-stage technology assessment, they are pivotal for ensuring a just transition to sustainable water treatment systems.

The sono-based process, particularly when employing nanostructured catalysts such as TFNs (TiO_2-functionalized nanomaterials), introduces concerns in terms of occupational safety and long-term health impacts. Operators may be exposed to high-intensity ultrasound fields, which can lead to hearing damage without proper protection. Moreover, handling and synthesizing nanomaterials raises questions about nanoparticle release into air or water, posing inhalation or dermal exposure risks to workers. Although the process may be chemically efficient, these factors could limit its acceptability in settings without stringent health and safety protocols. Additionally, the synthesis of these nanomaterials often involves multi-step procedures using chemicals like ethanol and styrene, some of which are flammable or toxic. This elevates the need for trained personnel and increases fire and chemical hazard risks, particularly in non-industrial or decentralized facilities.

Photolysis relies heavily on long-duration hydrothermal synthesis and the use of nanostructured photocatalysts, which can complicate technology transfer to low-

resource settings. The process typically requires specialized equipment such as UV lamps or autoclaves, which demand stable electricity and technical training. The synthesis procedure often includes alkaline treatments (e.g., NaOH) and carbonaceous templates (e.g., glucose), raising waste handling and exposure concerns. In terms of social equity, photolysis systems may be more feasible in urban or centralized plants with the infrastructure to handle complex materials and operate under controlled conditions. However, their limited portability and maintenance complexity could pose challenges for deployment in rural or developing regions.

As a hybrid of the above, the sonophotolysis process inherits many safety and accessibility issues from both ultrasound and UV systems. The simultaneous use of multiple high-energy devices increases the need for electrical safety standards, equipment reliability, and operator training. While the technology might offer synergistic degradation performance, its complex operational requirements make it less suitable for informal sectors or low-skill environments. Furthermore, the need for continuous monitoring and precise control over reaction conditions (e.g., pH, light intensity, sonication power) demands higher operational sophistication, which may not be universally available or affordable.

The Fenton process, based on iron salts and hydrogen peroxide, offers several social advantages. It is low-cost, relatively easy to implement, and operates under mild conditions without requiring complex infrastructure. These attributes make it more accessible to decentralized or resource-limited communities. However, chemical handling still poses risks. Hydrogen peroxide, while common, is reactive and can cause

skin and eye irritation. Additionally, the iron sludge generated during the process must be handled properly to avoid secondary pollution or occupational exposure. Despite these concerns, the Fenton system remains one of the most socially inclusive options among the evaluated AOPs, especially when simple catalyst regeneration strategies are adopted.

Electrochemical oxidation processes (EAOPs) are often seen as scalable and effective, but their social sustainability is highly dependent on material choices. The use of platinum as an anode, as in the case assessed here, introduces ethical and social equity concerns tied to rare metal extraction, including labour exploitation, geopolitical conflicts, and ecosystem disruption in mining regions. Moreover, the high voltage requirements and potential gas evolution (e.g., oxygen, chlorine) demand strict safety procedures, including ventilation and electrical insulation, which may not be available in all operational contexts. The high cost of platinum also limits technology transfer to low-income areas unless alternative, earth-abundant materials are employed.

Across all technologies, the resilience of the workforce, fair labour conditions, and technology accessibility play central roles in long-term success. A process that is environmentally clean but requires rare chemicals or intensive labour under hazardous conditions may fail to gain community acceptance or regulatory approval. Incorporating life cycle social analysis (LCSA) in future studies would help quantify these dimensions more systematically.

5.4 Discussion and outlook

This chapter has demonstrated a comparative life cycle and economic evaluation of five representative AOPs for tetracycline degradation. While the results provide valuable insights into environmental trade-offs, it is important to reiterate that the primary objective of this study was not to declare a singular “best” AOP technology, but rather to explore how different processes perform from an environmental and economic perspective under standardized assessment criteria for a particular task, the degradation of the micropollutant tetracycline. Given the vast number of AOP configurations and catalyst formulations in literature, any attempt to rank them definitively would overlook the diversity of conditions, system scales, and research scopes. Instead, this work offers a framework for performance assessment that extends beyond operational performance, aiming to incorporate broader sustainability considerations often neglected in conventional evaluations.

The findings clearly indicate that while sonochemical processes tend to exhibit the fastest degradation rates, their environmental performance is heavily dependent on electricity input. In scenarios where carbon-intensive grids are in place, the sono-based process can result in the highest global warming potential (GWP) among the five technologies evaluated. In contrast, Fenton-like processes, although slower, demonstrated lower overall environmental footprints under current energy systems, due to minimal energy input and the use of simpler reagents.

One of the most impactful insights from this study is the recognition that environmental damage does not scale linearly with operational performance. For

instance, the marginal improvements in operational performance often pursued through the use of novel or complex catalyst systems may incur significant environmental burdens, particularly through energy-intensive synthesis routes or the use of scarce or toxic materials. Therefore, this work advocates a more balanced research focus: one that weighs performance gains against the life cycle impacts of catalyst production and operation. The use of ethanol—typically considered a benign solvent—was found to be a major contributor to environmental burdens, reinforcing the need to scrutinize even "commonplace" chemicals in sustainability evaluations.

Despite the contextual nature of process viability, several trends emerged that offer generalizable recommendations. Sonochemical and photochemical systems are more viable in low-carbon electricity scenarios, such as those anticipated in future grid projections. Conversely, under current grid mixes, Fenton-based systems may be more favourable due to their limited energy demands. The electrochemical process, while promising, hinges critically on the choice of electrode materials; using precious metals like platinum significantly elevates the embodied environmental and economic costs. Sustainable electrode alternatives must therefore be a priority in future development.

To improve the environmental profile of all catalyst-dependent processes, simplifying synthesis routes, minimizing unnecessary precursor use, and improving catalyst reusability are crucial. For sono-based systems in particular, enhancing cavitation efficiency—such as through reactor design optimization or intelligent deployment of cavitation agents—will be essential to reduce energy consumption per unit pollutant degraded.

While each AOP technology presents its own environmental and economic profile, their social sustainability varies widely. Simpler, low-energy systems like the Fenton process offer broader accessibility and lower operational risk, whereas advanced systems relying on nanomaterials or rare metals may raise concerns related to occupational safety, equity, and ethical sourcing. A comprehensive sustainability assessment must therefore extend beyond metrics of degradation and cost to include social implications such as safety, material justice, and deployment fairness.

Nevertheless, this study is not without limitations. The end-of-life treatment of catalysts was not included in the LCA boundaries, due to the lack of consistent data and the variability in disposal practices. Although its exclusion may lead to some underestimation of environmental impacts, its influence is expected to be smaller than those from operating inputs in many cases. Relying on data from a single or limited number of studies introduces uncertainty and potential bias into the LCA/TEA results. This limitation may affect the representativeness of the inventory data (e.g., energy consumption, material use, catalyst lifetime) and consequently influence the accuracy and generalizability of the environmental and economic impacts reported. To mitigate this, sensitivity analyses were conducted where possible to assess the influence of key assumptions and data variability on the final outcomes. Future work should prioritize integrating broader datasets, especially for industrial-scale processes, to enhance the robustness of the analysis. Furthermore, several novel or complex chemical inputs used in catalyst synthesis were not available in the Ecoinvent database. Where possible, similar substitutes were used, or the contributions were excluded via a cut-off approach

if their quantities were deemed negligible. However, these choices may introduce minor uncertainty into the analysis. Lastly, while sensitivity analysis was performed on catalyst reusability, the true reusability in practical settings remains uncertain, especially for systems with high degradation potential but low long-term stability. This remains a challenge not just for this study but for the broader LCA community in assessing lab-scale technologies with limited durability data.

Going forward, expanding LCA databases to include emerging materials, integrating end-of-life modelling, and establishing standardized experimental reporting for sustainability metrics will be essential to close the gap between environmental modelling and experimental development. More importantly, it is hoped that the framework demonstrated here can guide researchers and policymakers toward AOP strategies that are not only technically effective but also environmentally responsible and economically realistic.

5.3 Conclusion

This chapter conducted a standardized life cycle and economic comparison of five AOP technologies—sonolysis, photolysis, sonophotolysis, Fenton-like oxidation, and electrochemical oxidation—for tetracycline degradation, using a unified 90% removal target per 1 L of wastewater at 40 mg/L.

Despite offering the highest degradation rate, the sono-based process incurred the highest CO_2 emissions when operated under the current UK grid, and its electricity

consumption contributed over 2/3 of the impact of many environmental categories. Conversely, the Fenton process, with the slowest kinetics, had nevertheless the lowest carbon footprint, due to negligible electricity requirements and reliance on simpler reagents. The electrochemical process showed the highest total environmental burden, with platinum anodes contributing over 80% of emissions in multiple midpoint categories, including resource scarcity and toxicity. In contrast, environmental burdens in photolysis and sonophotolysis were primarily driven by electricity and catalyst synthesis, with ethanol use contributing up to 30–40% of toxicity-related categories.

The sensitivity analysis highlighted several critical drivers: catalyst reusability significantly affects life cycle emissions; green electricity greatly enhances the sustainability of energy-dependent AOPs; and the choice of synthesis route and input chemicals can outweigh the impact of the active metal itself. Incorporating environmental endpoint monetization alongside direct utility and chemical costs enabled a more comprehensive understanding of each process's true economic impact. The inclusion of carbon tax further highlights the vulnerability of energy-intensive processes to climate-related policies, reinforcing the comparative advantage of low-emission AOPs in future sustainable applications.

Ultimately, this study demonstrates that operational performance alone is an insufficient measure of sustainability. Instead, the life cycle, environmental and economic trade-offs must be considered to inform responsible technology development and deployment of AOPs.

Chapter 6: Conclusions and perspectives

6.1 Summary of the PhD study and key contributions

6.1.1 Summary of main work accomplished

This DPhil research systematically explored the development and environmental assessment of AOPs for the degradation of tetracycline, with a primary focus on sono-based technologies and broader cross-comparative sustainability evaluations. The work can be divided into three major phases, corresponding to the core chapters of the thesis.

In the first phase (Chapter 3), a novel sono-based AOP system was designed, developed, and experimentally validated. The system featured a bespoke pulsed sonoreactor in conjunction with a specially synthesized TFNs catalyst. Detailed experimental investigations were conducted to evaluate the effects of catalyst dosage, acoustic parameters, radical generation, solution chemistry, and operational configurations. The process achieved rapid tetracycline degradation, with up to 90% removal in just 6 minutes under optimized conditions, and demonstrated improved energy efficiency compared to conventional sonocatalytic setups. The study also showed synergistic effects with co-treatments such as hydrogen peroxide and visible light.

The second phase (Chapter 4) extended this investigation through a system-level environmental assessment using LCA. Following ISO 14040/44 standards, the environmental performance of different reaction scenarios—such as blank cavitation, H_2O_2-assisted cavitation, and TFNs-assisted cavitation—was quantitatively compared.

Critical environmental hotspots were identified, particularly emissions associated with electricity use and catalyst synthesis. A continuous-flow sonoreactor using metal foam as a cavitation-enhancing structure was subsequently introduced and evaluated as a low-impact alternative. Although this configuration exhibited slower reaction kinetics, it reduced total CO_2 emissions by 29% by eliminating the need for complex catalyst synthesis, highlighting the importance of holistic environmental optimization beyond operational performance alone.

The third phase (Chapter 5) expanded the scope of analysis to include a cross-technology benchmarking study of five AOP technologies: sonolysis, photolysis, sonophotolysis, Fenton-like oxidation, and electrochemical oxidation. These technologies were assessed under harmonized conditions using a unified functional unit (treatment of 1 L of wastewater to 90% tetracycline removal). Environmental impact was quantified using the ReCiPe 2016 method at both midpoint and endpoint levels, capturing 18 detailed impact categories and aggregated damage across human health, ecosystems, and resource scarcity. The analysis revealed that the fastest process (sono-based) had the highest environmental burden under current grid electricity (1.2 kg-CO_2/L), while the Fenton process, though slower, had the lowest CO_2 emissions (0.478 kg-CO_2/L) due to its minimal energy demand. The electrochemical process was heavily penalized by the environmental cost of platinum anodes, which contributed over 80% of total impact in several categories.

To complement the LCA, a detailed economic evaluation was also conducted, focusing on operating costs. A hybrid costing approach was adopted by monetizing

environmental damage indicators from the endpoint LCA results. This allowed for a more comprehensive assessment of true operating costs, beyond direct expenditure on chemicals and utilities. Notably, monetized environmental costs comprised up to 55% of total process cost in some cases, demonstrating the economic relevance of sustainability trade-offs.

Collectively, the work accomplished in this DPhil bridges the gap between laboratory-scale AOP development and real-world sustainability assessment. It contributes a modular framework that integrates experimental data, environmental modelling, and cost analysis—offering both methodological rigour and practical guidance for the development of next-generation water treatment technologies.

6.1.2 Key learnings and outcomes

This DPhil study provided several important learnings that extend beyond technical performance, offering insights into both experimental development and system-level sustainability assessment of AOPs. At the core, it underscored that reaction efficiency alone and operational performance in general is an insufficient metric for evaluating wastewater treatment technologies—particularly when the ultimate goal is practical, environmentally responsible, and economically viable implementation.

From the experimental perspective, a key takeaway was the realization that optimized reactor design—particularly the integration of cavitation-enhancing materials—can significantly influence degradation efficiency. The tailored sonoreactor

developed in this study demonstrated that cavitation intensity, agent geometry, and acoustic field parameters can be strategically manipulated to achieve high degradation rates with reduced energy input. A more effective reactor design could further enhance degradation rates, thereby lowering the energy consumption and associated with carbon emissions per unit of treated wastewater. Future reactor designs could focus on several key improvements to enhance degradation efficiency. Firstly, employing a multi-transducer configuration operating at dual frequencies could generate a more uniform and intense cavitation field. Secondly, immobilizing the catalyst onto fixed surfaces within the reactor would place it directly at the cavitation source, maximizing its activity while simplifying recovery and reuse. Finally, transitioning from a batch to a continuous-flow system with optimized internal geometry would improve mixing and mass transfer, significantly reducing the energy input and treatment time per unit volume of wastewater. Such improvements would likely reinforce the main conclusions of this study, particularly regarding the trade-offs between degradation efficiency, energy use, and material-related environmental impacts. The study also highlighted the performance potential of TFNs, not only in terms of catalytic activity but also reusability, although practical reuse remains a challenge.

A critical system-level learning emerged from the LCA. While sono-based processes yielded rapid tetracycline degradation, they often carried a higher environmental burden due to intensive electricity usage, particularly under conventional fossil-dominated grid conditions. This revealed a broader lesson: technologies with better operational performance may still underperform

environmentally, unless paired with green electricity or low-impact synthesis routes. Conversely, slower yet simpler methods—such as Fenton-based processes—demonstrated significantly lower emissions and environmental impacts, due to their reliance on basic, well-understood reagents and low energy demand.

Another major insight was the disproportionate contribution of catalyst synthesis—especially chemical solvents like ethanol and complex reagents—to overall environmental burden. In several cases, the environmental impact of the synthesis stage exceeded that of the active catalytic metal itself. This highlighted the need for designing synthesis routes with minimal material intensity, reduced heating requirements, and greater process efficiency.

The study also affirmed that reusability, scalability, and raw material selection play pivotal roles in determining the life cycle footprint of AOPs. Sensitivity analysis showed that improving catalyst reusability could reduce CO_2 emissions by over 70%, while substituting rare metals (e.g., Pt) with abundant alternatives significantly lessened the impacts of resource scarcity and toxicity.

Finally, the incorporation of economic monetization of endpoint environmental impacts enabled a more comprehensive understanding of true process costs. This integration bridged the often-separated domains of technical performance, environmental sustainability, and economic decision-making, providing a multi-dimensional framework for future research and industrial practice.

Overall, this research advocates for a paradigm shift—from optimizing AOPs

purely for efficient pollutant removal, toward designing systems that are energy-efficient, material-conscious, and environmentally justified throughout their life cycles. This holistic approach represents an important contribution to the sustainable development of water treatment technologies.

6.2 Limitations and future perspectives

6.2.1 Limitations

While this DPhil study provides a novel and systematic integration of experimental, environmental, and economic assessments for AOPs, several limitations must be recognized to properly contextualize its findings and encourage future improvements.

First, the LCA conducted in Chapters 4 and 5 excluded the end-of-life (EoL) treatment of catalysts and reactors. This omission was due to the lack of consistent and standardized data on catalyst disposal pathways, recycling rates, and system decommissioning practices. While this boundary truncation is common in lab-scale LCA studies and likely introduces only marginal errors compared to operational-phase emissions, its inclusion would yield a more complete environmental picture.

Second, several chemical inputs used in catalyst synthesis—particularly novel reagents or materials developed in the laboratory—were not available in the Ecoinvent database. In these cases, similar compounds were substituted, or cut-off criteria were applied when quantities were small. Although this approach aligns with standard practice in early-stage LCA, it introduces some uncertainty into impact calculations and

highlights the need for more comprehensive LCA databases that capture emerging materials.

Third, while sensitivity analyses were performed to evaluate catalyst reusability, the actual durability and reuse cycles of the catalysts are highly uncertain at this stage. Real-world operational longevity may vary widely based on system configuration, fouling, and catalyst deactivation mechanisms. As such, some assumptions were necessary for modelling reusability, which may not reflect performance under industrial or long-term operating conditions.

Additionally, although the cross-comparison of AOP technologies was conducted under harmonized functional units and degradation targets, inherent differences in experimental reporting (e.g., lab vs. pilot scale, reactor geometry, or local grid conditions) may still introduce inconsistencies. Moreover, some minor upstream impacts, such as land use for chemical production or indirect emissions from infrastructure, were not included.

Finally, while this work integrates environmental and economic metrics, broader sustainability dimensions—such as social acceptability, regulatory feasibility, or risk of toxic by-product formation—were outside the scope of this study but remain critical for real-world technology adoption. Despite these constraints, the methodological framework and insights developed here remain robust and transferable, offering a foundation for further investigation and refinement as data availability and technology maturity improve.

6.2.2 Future work

The findings and limitations of this DPhil study open several promising avenues for future research and development. These directions can support the evolution of AOPs from high-potential lab-scale systems into environmentally and economically viable solutions for large-scale water treatment.

1. Comprehensive Life Cycle Inventory Expansion:

As identified in this study, the limited availability of emerging materials in existing LCA databases introduces uncertainties. Future work should prioritize the development and integration of detailed LCI data for novel chemicals, nanomaterials, and synthesis methods commonly used in AOPs. Collaborative efforts between LCA researchers and material scientists can help close this data gap and improve impact accuracy.

2. Inclusion of End-of-Life and By-Product Analysis:

Future studies should include the end-of-life stage of catalyst and reactor systems. This includes potential regeneration, recycling, or safe disposal scenarios, along with their associated impacts. Furthermore, a detailed fate analysis of degradation by-products is needed to assess potential toxicity or secondary pollution—an important factor in ensuring that environmental burden is not simply shifted downstream.

3. Integration of Social and Regulatory Dimensions:

While this thesis emphasizes environmental and economic metrics, future work should include broader sustainability assessments encompassing social, health, and policy dimensions. Public acceptance, regulatory compatibility, and occupational safety of

different AOPs—especially those involving reactive intermediates or metal-based catalysts—should be studied using qualitative and quantitative tools (e.g., social LCA or multi-criteria decision analysis).

4. Technology Scale-Up and Real-World Application:

The performance of AOPs in real wastewater matrices can differ significantly from controlled lab experiments, due to matrix complexity, fouling, and dynamic flow conditions. Therefore, pilot-scale testing under realistic operational settings is essential. This will also allow for better estimation of reusability, maintenance cycles, and energy integration opportunities—crucial for scaling from lab concepts to commercial technologies. The life cycle and economic assessments in this work are based on lab-scale data, which introduces inherent uncertainties in scaling up processes where energy and mass transfer efficiencies may change. Furthermore, relying on data from a limited number of studies adds variability to inventory assumptions. These limitations emphasize that the results are most suitable for comparative analysis rather than absolute prediction, highlighting the need for pilot-scale validation and broader data integration in future studies.

5. Reactor and Process Optimization:

In sono-based systems, particular attention should be paid to optimizing reactor design to enhance cavitation efficiency, minimize energy consumption, and improve mass transfer. Design improvements such as continuous-flow configurations, modular reactor systems, and cavitation zone control can enhance both degradation performance and sustainability. Integration with low-carbon energy sources remains essential for

minimizing environmental impacts. To achieve this, future system designs should prioritize operational flexibility—scheduling high-energy processes during periods of high renewable availability—and optionally incorporate energy storage or hybrid renewable systems to address intermittency. While implementation poses infrastructural challenges, these strategies are critical for realizing the low-carbon benefits demonstrated in this study.

6. Effects of Complex Wastewater Matrices:

While this study focused on single contaminants, real wastewater contains mixtures of compounds that may compete for reactive species or active sites, potentially reducing the removal efficiency of target pollutants. This suggests that the performance observed under ideal conditions may represent a best-case scenario, and further research under complex, realistic conditions is essential for accurately evaluating the practical applicability of the proposed AOP systems.

7. Catalyst reusability:

To move from these necessary assumptions to more accurate data, future work should focus on: (1) Long-Term Stability Testing: Conducting extended reuse experiments to empirically determine the catalyst's lifespan, tracking the gradual deactivation rate and identifying the primary deactivation mechanisms (e.g., fouling, leaching, structural change). (2) Realistic Recovery Studies: Quantifying the actual mass loss of catalyst during a realistic recovery and regeneration process scaled from the lab.

8. Hybrid and Modular Treatment Systems:

Future research could explore hybrid combinations of AOPs with biological or physical treatment methods, aiming to create modular systems that can adapt to varying pollutant loads and regulatory requirements. Process integration with energy recovery or resource recovery units (e.g., nutrient reclamation) may further enhance sustainability and circularity.

9. Development of Decision-Making Tools:

Building on the TEA/LCA integration in this study, the creation of user-friendly decision-support tools can help stakeholders—from engineers to policymakers—evaluate the trade-offs between different AOP technologies in specific contexts. These tools could incorporate regional electricity mix, chemical availability, water quality, and sustainability goals.

Overall, future work should move toward a more holistic and scalable evaluation of AOP systems, combining robust environmental and economic modelling with practical engineering design and policy awareness. These directions will help ensure that AOPs contribute effectively and responsibly to global water pollution challenges.

Appendix A: Supplementary Information for Chapter 3

Figure A.1. TEM image of TiO_2 fractured nano-shell (to confirm the shape matches that in the previously reported paper [100])

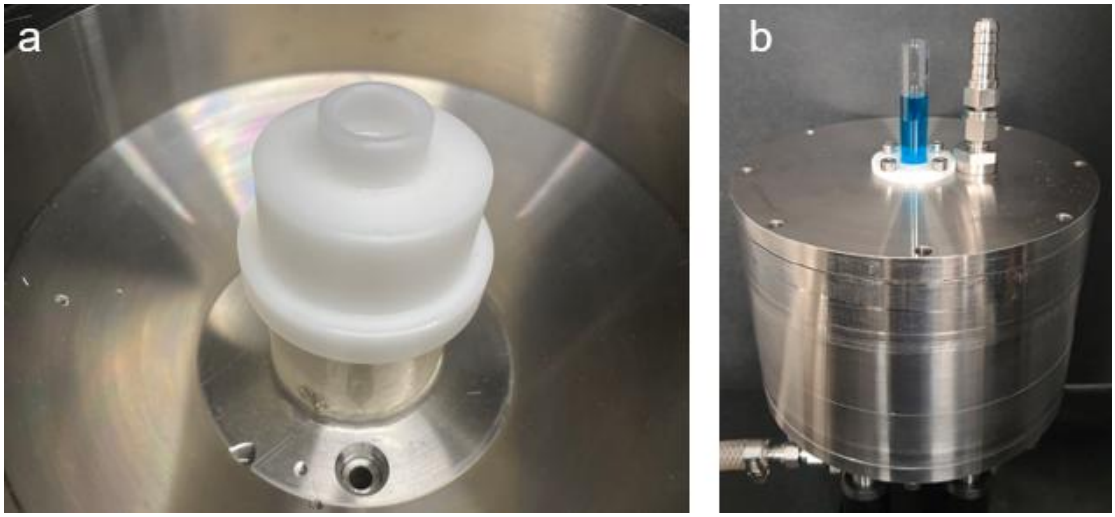

Figure A.2. The most recent photo of the sonoreactor (a) internal view of the transducer (b) external view (adapted from [85]). The cylindrical reactor has an internal height of 12 cm and a diameter of 16 cm, with a wall thickness of 1 cm. An ultrasonic transducer (4 cm in diameter, 3 cm in height) is mounted on the reactor. The transducer is cooled by a water jacket with a total volume of 800 mL.

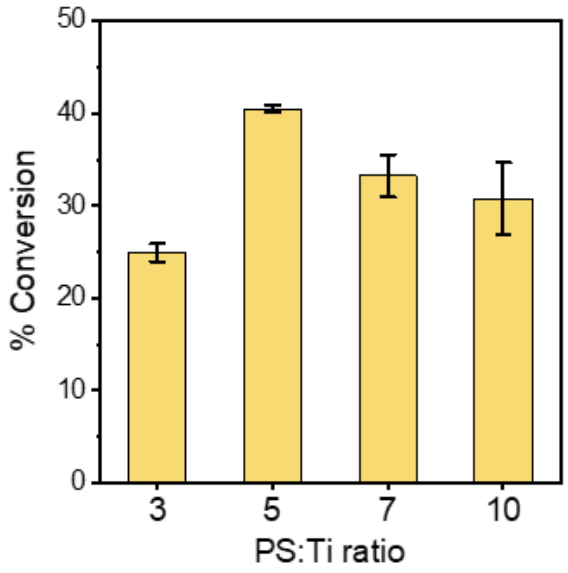

Figure A.3. The effect on sonocatalytic performance of the ratio of PS to titanium butoxide during catalyst preparation (Reaction conditions: Table 3.1)

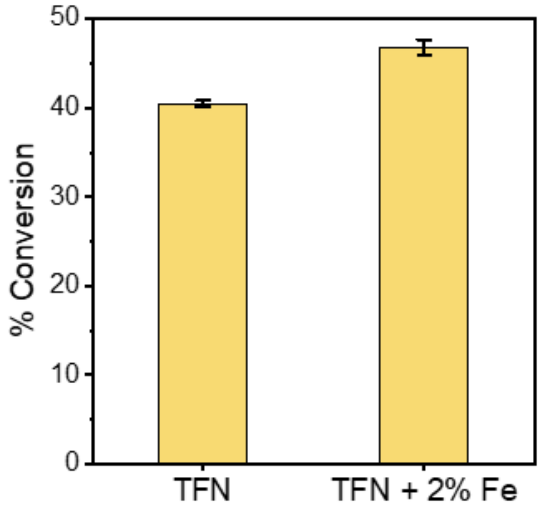

Figure A.4. Tetracycline degradation in six minutes with basic case TFNs and 2% Fe-doped TFNs (Reaction conditions: Table 3.1)

In this case, Titanium butoxide (Reagent grade, 97%, Sigma) and Iron (III) chloride hexahydrate (Sigma), which accounted for two mol% of Iron, were co-added dropwise (0.2:2 in ethanol v/v) to the prepared PS solution under stirring at 400 RPM.

Appendix B: Supplementary Information for Chapter 4

Table B.1. Benchmarking of energy consumption of equipment and chemicals used during catalyst synthesis and reuse. The power-based unit is required to multiply by the operational time indicated in each study.

	Hypothesis space used (%)	Energy	Unit
Furnace [207]	10	300	W/L at 1200 C
Heating oven [208]	10	1.4	kWh/kg
Vacuum Dryer [208]	10	5.8	kWh/kg
Stirrer [209]	30	10	W/L
US bath [210]	30	20	W/L
Centrifuge [211]	30	0.01	kWh/L
Wash	3 times for all cases		
Filtration [212]	3 times for all cases	0.001	kWh/L

Table B.2. Experimental parameters of continuous-flow sonoreactor

Residence time (min)	1
Volume (mL/min)	0.314
Metal sheet size (L*W*T in mm)	28, 4, 1.25
Number of cycles	100
Burst period (ms)	2.381
Frequency (kHz)	840
Duty cycle (%)	5
Input power (Watt)	197
Current (A)	4.7
Phase angle	20
Electric Power (W)	43

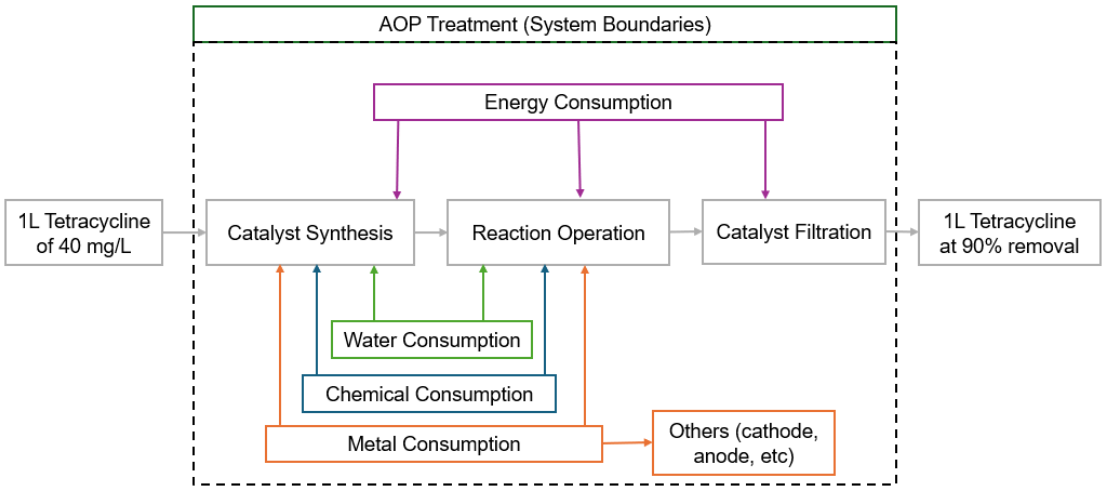

Figure B.1. System boundaries of Chapter 4 and Chapter 5.

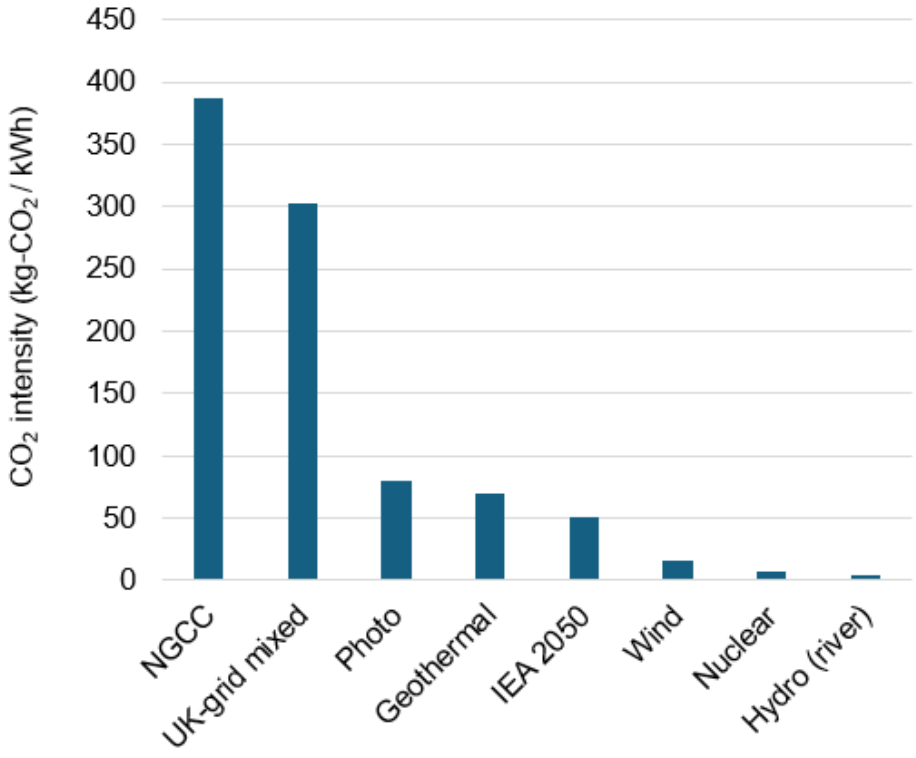

Figure B.2. CO_2 intensity (kg-CO_2/kWh) of various electricity generation sources [163].

Including natural gas combined cycle (NGCC), UK grid average, photovoltaic, geothermal, projected IEA 2050 mix, and renewable sources such as wind, nuclear, and hydroelectric (river). The figure illustrates the dramatic reduction in carbon intensity achievable through the transition to low-carbon and renewable electricity, highlighting the environmental benefits of green energy adoption in energy-intensive processes.

Table B.3. Life cycle inventory of reaction stage for Batch reactor

Batch processes	no cata	H2O2	cata
Volumn (ml)	3	3	3
Kinetic (min-1)	0.012	0.049	0.081
time (min)	191	47	28
Time (h) for 1L	1061.11	261.11	155.56
power (kW)	0.021	0.021	0.021
energy	22.28	5.48	3.27
H2O2 usage (g)	0.00	0.01	0.00
catalyst (g/L)	0.00	0.00	0.50

Table B.4. Life cycle inventory of reaction stage for continuous reactor

Continous processes	no cata	Ti	ZnO
Volumn (ml)	0.314	0.314	0.314
Kinetic (min-1)	0.0887	0.63	1
time (min)	26	3.6	2.3
Time (h) for 1L	1380.04	191.08	122.08
power (kW)	0.043	0.043	0.043
energy	59.34	8.22	5.25

Table B.5. Life cycle inventory of catalyst (TFNs) synthesis steps (Empty cells indicate that the information is not applicable or not material to the context)

Chemicals & experimental procedure	Volume (ml)	density (g/ml)	concentration (M)	molar mass	mass (g)	Time (h)	energy (kWh)
PS bead							
Styrene	5	0.9			4.5		
DI water	40	1			40		
stir						0.33	0.0005
potassium persulfate	5		0.16	270	0.216		
heat							0.62
Total	50						
TFNs							
ethanol	550				433.95		
Sonication						0.17	0.0067
Titanium butoxide mixture	110						
ethanol	100				78.9		
Titanium butoxide	10			340	10		
stir						2	0.044
ethanol washing	225				177.53		
centrifuge							0.033
dry			100				0.86
calcination						3	0.056
Filtration							0.003
Final TFNs Production					2.35		

Appendix C: Supplementary Information for Chapter 5

Table C.1. The 22-endpoint environmental impact category indicators

(Resources: Red; Human health: Blue; Ecosystems: Black) [117]

Nomenclature	Midpoint impact category	Indicators
FRS	Fossil resource scarcity	USD2013
MRS	Mineral resource scarcity	USD2013
WC	Water consumption, Human health	DALY
HNCT	Human non-carcinogenic toxicity	DALY
HCT	Human carcinogenic toxicity	DALY
FPM	Fine particulate matter formation	DALY
OFH	Ozone formation, Human health	DALY
IR	Ionizing radiation	DALY
SOD	Stratospheric ozone depletion	DALY
GW	Global warming, Human health	DALY
WCAE	Water consumption, Aquatic ecosystems	species.yr
WCTE	Water consumption, Terrestrial ecosystem	species.yr
LU	Land use	species.yr
MEt	Marine ecotoxicity	species.yr
FEt	Freshwater ecotoxicity	species.yr
TEt	Terrestrial ecotoxicity	species.yr
ME	Marine eutrophication	species.yr
FE	Freshwater eutrophication	species.yr
TA	Terrestrial acidification	species.yr
OFTE	Ozone formation, Terrestrial ecosystems	species.yr
GWFE	Global warming, Freshwater ecosystems	species.yr
GWTE	Global warming, Terrestrial ecosystems	species.yr

Table C.2. Comparison of Advanced Oxidation Processes: Kinetic Performance (first-order), Treatment Time, and Energy Consumption per Litre (Empty cells indicate that the information is not applicable or not material to the context)

Processes	Reaction volumn (mL)	Kinetic (min-1)	Time for 90% conversion (min)	Time required for 1L (h)	Power (W)	Energy (kWh/L)	Catalyst (g/L)
Sono	3	0.091	25	138.89	21	2.92	0.5
Photo	100	0.07404	32	5.33	155	0.83	1.5
sonophoto	300	0.0472	50	2.78	440	1.22	0.7
Fenton	30	0.01767	132	73.33	0		0.5
Electro	200	0.0828	28	2.33	38.2	0.09	0.06

Table C.3. Life cycle inventory of catalyst (photo) synthesis steps (Empty cells indicate that the information is not applicable or not material to the context)

Photo	Volume (ml)	density (g/ml)	concentration (M)	molar mass	mass (g)	Time (h)	Power	energy (kWh)
TiO2					1			
Sodium hydroxide	30		10	40	12			
stir						2		0.002
Autoclaved								0.42
HCl	200		0.1	36.5	0.73			
DI water					199.27			
Centrifuge								0.0077
Washing DI water	30	1			30			
Vaccum Dryer								0.29
Calcination						6		0.026
DI water	70	1			70			
Copper sulfate				160	0.192			
NaOH	2.4		1	40	0.096			
Glucose					2			
Stir						1		0.0023
thermal bath						12	78	1.24
wash DI water					22.88			
wash DI ethanol					22.88			
dry								0.13
Filtration								0.003
Catalyst synthesized					2.17			

Table C.4. Life cycle inventory of catalyst (sonophoto) synthesis steps (Empty cells indicate that the information is not applicable or not material to the context)

Sonophoto	Volume (ml)	density (g/ml)	concentration (M)	molar mass	mass (g)	Time (h)	Power	energy (kWh)
tungstate salt					1			
CNT					0.070			
DI water					60			
stir						0.42		0.0008
lactic acid	1	1.2		90	1.2			
stir						0.67		0.0013
autoclave								0.86
Ethanol					68.11			
centrigfuge								0.0043
autoclave								0.032
Catalyst synthesized					0.77			

Table C.5. Life cycle inventory of catalyst (fenton) synthesis steps (Empty cells indicate that the information is not applicable or not material to the context)

Fenton	Volume (ml)	density (g/ml)	concentration (M)	molar mass	mass (g)	Time (h)	Power	energy (kWh)
Iron chloride					0.43			
sodium citrate dihydrate					0.2			
Acetic acid					0.84			
Sodium hydroxide					0.48			
Ethylene glycol	20	1.11			22.2			
stir						1		0.0008
autoclave								0.34
Wash Ethanol					58.5			
Dry								0.11
Catalyst synthesized					0.25			

Table C.6. Life cycle inventory of catalyst (electro) synthesis steps (Empty cells indicate that the information is not applicable or not material to the context)

Electro	Volume (ml)	density (g/ml)	concentration (M)	molar mass	mass (g)	Time (h)	Power	energy (kWh)
calcium nitrate tetrahydrate					1.64			
iron(III) nitrate nonahydrate					9.12			
nickel(II) nitrate hexahydrate					1.98			
DI water	100				100			
EDTA					5.84			
citric acid					8.4			
Heating to 80								0.02
12h stir							12	0.05
12h heat loss							12	0.43
drying								7.32
Calcinate 700								0.03
Calcium salt					1.45			
sodium sulfate			0.05	142	7.1			
C 100 use					0.00			
Pt 100 use					0.00			
Catalyst synthesized					1.45			

Table C.7. Midpoint environmental impact of Sono-based process under current UK grid electricity scenario

Unit		Total	Styrene	Potassium sulfate	Titanium precursor	Ethanol	Water	Energy, synthesis	Energy, operating
kg CO2 eq	GW	1.20E+00	3.62E-03	5.04E-05	1.03E-02	1.84E-01	4.63E-06	1.07E-01	8.97E-01
kg CFC11 eq	SOD	5.70E-07	3.38E-10	1.74E-11	4.04E-09	1.14E-08	4.19E-12	5.88E-08	4.95E-07
kBq Co-60 eq	IR	6.55E-01	3.41E-05	1.90E-06	3.94E-04	2.87E-03	3.07E-07	6.92E-02	5.83E-01
kg NOx eq	OFH	2.17E-03	7.36E-06	1.88E-07	2.71E-05	4.06E-04	1.09E-08	1.83E-04	1.54E-03
kg PM2.5 eq	FPM	7.28E-04	4.37E-06	1.73E-07	2.02E-05	1.54E-04	1.20E-08	5.83E-05	4.91E-04
kg NOx eq	OFT	2.30E-03	8.01E-06	1.93E-07	2.77E-05	4.72E-04	1.13E-08	1.90E-04	1.60E-03
kg SO2 eq	TA	2.07E-03	1.06E-05	4.79E-07	4.76E-05	4.45E-04	3.00E-08	1.66E-04	1.40E-03
kg P eq	FE	1.80E-04	6.44E-07	2.66E-08	6.47E-06	7.09E-05	2.08E-09	1.09E-05	9.16E-05
kg N eq	ME	2.05E-05	4.95E-08	1.54E-09	2.71E-07	1.28E-06	1.61E-10	2.01E-06	1.69E-05
kg 1,4-DCB	TEt	2.25E+00	8.65E-03	1.25E-03	2.43E-02	4.95E-01	6.86E-05	1.82E-01	1.54E+00
kg 1,4-DCB	FEt	3.22E-02	6.12E-05	1.17E-05	1.18E-03	5.39E-03	6.75E-07	2.72E-03	2.29E-02
kg 1,4-DCB	MEt	4.13E-02	8.37E-05	1.53E-05	1.66E-03	7.05E-03	8.83E-07	3.45E-03	2.91E-02
kg 1,4-DCB	HCT	4.15E-02	1.09E-04	6.52E-06	5.32E-03	6.41E-03	5.17E-07	3.14E-03	2.65E-02
kg 1,4-DCB	HNCT	5.76E-01	1.51E-03	2.15E-04	1.10E-02	9.43E-02	1.34E-05	4.98E-02	4.19E-01
m2a crop eq	LU	1.06E-01	3.95E-05	2.99E-06	4.62E-04	2.07E-03	1.15E-07	1.10E-02	9.24E-02
kg Cu eq	MRS	2.89E-03	4.20E-06	8.67E-07	4.98E-04	4.28E-04	5.56E-08	2.08E-04	1.75E-03
kg oil eq	FRS	4.83E-01	2.07E-03	1.27E-05	2.28E-03	1.42E-01	1.09E-06	3.57E-02	3.01E-01
m3	WC	6.18E-03	3.47E-05	8.29E-07	7.63E-05	1.36E-03	9.23E-06	4.98E-04	4.20E-03

Table C.8. Midpoint environmental impact of Photo-based process under current UK grid electricity scenario

Unit		Total	TiO2 nanoparticle	NaOH	HCl	Water, deionised	Copper salt	Glucose	Ethanol	Energy, synthesis	Energy, operating
kg CO2 eq	GW	9.52E-01	1.83E-02	4.37E-02	1.75E-03	1.72E-04	5.32E-04	2.09E-03	1.95E-02	6.06E-01	2.60E-01
kg CFC11 eq	SOD	5.41E-07	4.19E-09	4.41E-08	2.40E-09	1.58E-10	5.06E-10	1.08E-08	1.12E-09	3.34E-07	1.43E-07
kBq Co-60 eq	IR	5.69E-01	5.03E-04	4.87E-03	5.09E-04	1.54E-05	4.22E-05	1.86E-04	2.99E-04	3.94E-01	1.69E-01
kg NOx eq	OFH	1.70E-03	3.98E-05	1.17E-04	3.93E-06	3.60E-07	4.13E-06	5.72E-06	4.15E-05	1.04E-03	4.47E-04
kg PM2.5 eq	FPM	6.22E-04	2.61E-05	8.94E-05	4.19E-06	4.85E-07	7.92E-06	3.50E-06	1.61E-05	3.32E-04	1.42E-04
kg NOx eq	OFT	1.77E-03	4.19E-05	1.19E-04	4.12E-06	3.73E-07	4.22E-06	5.95E-06	4.87E-05	1.08E-03	4.63E-04
kg SO2 eq	TA	1.67E-03	6.66E-05	1.61E-04	1.17E-05	1.30E-06	2.45E-05	1.10E-05	4.70E-05	9.46E-04	4.06E-04
kg P eq	FE	1.28E-04	6.83E-06	2.04E-05	1.14E-06	6.45E-08	2.58E-06	8.99E-07	7.65E-06	6.18E-05	2.65E-05
kg N eq	ME	2.01E-05	2.94E-07	1.83E-06	1.67E-07	6.13E-09	4.31E-08	1.35E-06	1.25E-07	1.14E-05	4.89E-06
kg 1,4-DCB	TEt	1.98E+00	3.49E-02	1.93E-01	1.64E-02	1.16E-03	1.92E-01	1.29E-02	4.67E-02	1.04E+00	4.45E-01
kg 1,4-DCB	FEt	2.86E-02	1.21E-03	2.29E-03	1.81E-04	1.14E-05	2.13E-03	1.42E-04	5.73E-04	1.55E-02	6.62E-03
kg 1,4-DCB	MEt	3.66E-02	1.70E-03	3.02E-03	2.37E-04	1.51E-05	2.73E-03	1.76E-04	7.46E-04	1.96E-02	8.41E-03
kg 1,4-DCB	HCT	3.49E-02	5.21E-03	2.87E-03	1.93E-04	1.83E-05	2.37E-04	1.45E-04	6.68E-04	1.79E-02	7.66E-03
kg 1,4-DCB	HNCT	5.15E-01	1.22E-02	5.10E-02	3.55E-03	2.46E-04	3.11E-02	2.59E-03	9.87E-03	2.83E-01	1.21E-01
m2a crop eq	LU	9.17E-02	4.70E-04	1.05E-03	6.39E-05	3.86E-06	6.70E-05	6.55E-04	2.01E-04	6.24E-02	2.68E-02
kg Cu eq	MRS	2.49E-03	4.80E-04	1.52E-04	1.31E-05	1.21E-06	9.50E-05	1.24E-05	4.51E-05	1.18E-03	5.07E-04
kg oil eq	FRS	3.25E-01	7.68E-03	1.06E-02	5.41E-04	4.08E-05	1.33E-04	4.87E-04	1.52E-02	2.03E-01	8.71E-02
m3	WC	6.04E-03	1.91E-04	1.04E-03	5.81E-05	3.69E-04	1.43E-05	1.69E-04	1.47E-04	2.83E-03	1.21E-03

Table C.9. Midpoint environmental impact of Sonophoto-based process under current UK grid electricity scenario

Unit		Total	Tungsten precursor	CNT	Water, deionised	Lactic acid	Ethanol	Energy, synthesis	Energy, operating
kg CO2 eq	GW	7.38E-01	2.81E-02	1.23E-02	2.45E-05	4.71E-03	7.99E-02	2.53E-01	3.60E-01
kg CFC11 eq	SOD	3.70E-07	2.20E-08	4.26E-09	2.25E-11	9.45E-10	4.96E-09	1.40E-07	1.99E-07
kBq Co-60 eq	IR	4.05E-01	1.23E-03	4.32E-03	2.19E-06	3.25E-04	1.25E-03	1.64E-01	2.34E-01
kg NOx eq	OFH	1.43E-03	1.73E-04	1.80E-05	5.14E-08	7.47E-06	1.76E-04	4.35E-04	6.19E-04
kg PM2.5 eq	FPM	5.50E-04	1.31E-04	1.15E-05	6.92E-08	4.58E-06	6.68E-05	1.39E-04	1.97E-04
kg NOx eq	OFT	1.50E-03	1.77E-04	1.90E-05	5.33E-08	8.01E-06	2.05E-04	4.52E-04	6.42E-04
kg SO2 eq	TA	1.80E-03	6.05E-04	2.88E-05	1.85E-07	1.29E-05	1.93E-04	3.95E-04	5.62E-04
kg P eq	FE	2.18E-04	1.17E-04	6.86E-06	9.20E-09	1.25E-06	3.08E-05	2.58E-05	3.67E-05
kg N eq	ME	3.11E-05	1.79E-05	5.08E-07	8.75E-10	6.70E-07	5.54E-07	4.77E-06	6.78E-06
kg 1,4-DCB	TEt	1.60E+00	3.01E-01	2.52E-02	1.66E-04	1.34E-02	2.15E-01	4.33E-01	6.16E-01
kg 1,4-DCB	FEt	6.58E-02	4.71E-02	5.08E-04	1.63E-06	1.63E-04	2.34E-03	6.45E-03	9.18E-03
kg 1,4-DCB	MEt	8.34E-02	5.95E-02	6.82E-04	2.16E-06	2.14E-04	3.06E-03	8.19E-03	1.17E-02
kg 1,4-DCB	HCT	3.01E-02	8.36E-03	6.46E-04	2.61E-06	2.08E-04	2.78E-03	7.46E-03	1.06E-02
kg 1,4-DCB	HNCT	2.29E+00	1.95E+00	1.52E-02	3.51E-05	3.16E-03	4.09E-02	1.18E-01	1.68E-01
m2a crop eq	LU	6.71E-02	2.70E-03	2.66E-04	5.50E-07	5.73E-05	8.96E-04	2.61E-02	3.71E-02
kg Cu eq	MRS	1.15E-02	1.00E-02	3.43E-05	1.73E-07	1.19E-05	1.86E-04	4.94E-04	7.02E-04
kg oil eq	FRS	2.79E-01	6.73E-03	3.75E-03	5.82E-06	1.82E-03	6.15E-02	8.49E-02	1.21E-01
m3	WC	4.47E-03	3.09E-04	5.89E-04	5.27E-05	6.44E-05	5.92E-04	1.18E-03	1.68E-03

Table C.10. Midpoint environmental impact of Fenton-based process under current UK grid electricity scenario

Unit		Total	Iron chloride	Acetic acid	NaOH	Ethylene glycol	Ethanol	H2O2	Sodium salt	Energy, synthesis	Energy, operating
kg CO2 eq	GW	4.78E-01	3.34E-03	3.31E-03	1.55E-03	6.63E-02	1.26E-01	4.02E-03	1.28E-03	2.71E-01	9.23E-04
kg CFC11 eq	SOD	1.74E-07	2.16E-09	6.26E-10	2.34E-09	9.61E-09	7.25E-09	9.84E-10	5.15E-10	1.50E-07	5.09E-10
kBq Co-60 eq	IR	1.91E-01	3.44E-04	3.14E-04	6.74E-04	1.07E-02	1.93E-03	5.62E-04	1.16E-04	1.76E-01	5.99E-04
kg NOx eq	OFH	8.84E-04	1.06E-05	7.22E-06	3.38E-06	1.16E-04	2.69E-04	6.57E-06	3.17E-06	4.67E-04	1.59E-06
kg PM2.5 eq	FPM	3.36E-04	7.68E-06	4.01E-06	2.55E-06	6.30E-05	1.05E-04	3.63E-06	1.92E-06	1.49E-04	5.05E-07
kg NOx eq	OFT	9.59E-04	1.08E-05	7.82E-06	3.49E-06	1.26E-04	3.15E-04	7.23E-06	3.28E-06	4.84E-04	1.65E-06
kg SO2 eq	TA	9.46E-04	1.53E-05	9.94E-06	6.14E-06	1.72E-04	3.04E-04	9.57E-06	4.28E-06	4.24E-04	1.44E-06
kg P eq	FE	1.04E-04	1.79E-06	1.36E-06	1.25E-06	2.06E-05	4.95E-05	1.51E-06	4.44E-07	2.77E-05	9.42E-08
kg N eq	ME	8.15E-06	1.26E-07	7.79E-08	1.12E-07	1.38E-06	8.12E-07	2.64E-07	2.52E-07	5.11E-06	1.74E-08
kg 1,4-DCB	TEt	1.08E+00	3.83E-02	1.03E-02	9.27E-03	2.35E-01	3.02E-01	1.59E-02	5.01E-03	4.65E-01	1.58E-03
kg 1,4-DCB	FEt	1.50E-02	4.35E-04	1.74E-04	1.29E-04	3.23E-03	3.71E-03	2.83E-04	5.57E-05	6.92E-03	2.35E-05
kg 1,4-DCB	MEt	1.93E-02	5.67E-04	2.21E-04	1.68E-04	4.20E-03	4.83E-03	3.73E-04	7.35E-05	8.79E-03	2.99E-05
kg 1,4-DCB	HCT	1.72E-02	4.14E-04	1.54E-04	1.46E-04	3.43E-03	4.32E-03	6.53E-04	6.85E-05	8.00E-03	2.72E-05
kg 1,4-DCB	HNCT	2.71E-01	7.67E-03	2.88E-03	2.76E-03	6.01E-02	6.39E-02	5.64E-03	1.18E-03	1.27E-01	4.31E-04
m2a crop eq	LU	3.07E-02	1.25E-04	6.40E-05	5.57E-05	9.57E-04	1.30E-03	7.55E-05	2.50E-05	2.80E-02	9.51E-05
kg Cu eq	MRS	1.13E-03	3.36E-05	1.13E-05	8.54E-06	2.30E-04	2.92E-04	1.60E-05	4.13E-06	5.29E-04	1.80E-06
kg oil eq	FRS	2.36E-01	8.24E-04	1.59E-03	4.03E-04	4.20E-02	9.85E-02	1.36E-03	3.36E-04	9.10E-02	3.10E-04
m3	WC	4.04E-03	4.96E-05	1.52E-04	1.15E-04	1.22E-03	9.50E-04	2.59E-04	2.98E-05	1.27E-03	4.32E-06

Table C.11. Midpoint environmental impact of Electro-based process under current UK grid electricity scenario

Unit		Total	EDTA	Calcium nitrate	Iron nitrate	Nickel nitrate	Citric acid	Activated carbon	Platinum	Energy, synthesis	Energy, operating
kg CO2 eq	GW	2.90E-01	1.06E-03	1.14E-04	1.38E-04	4.19E-04	9.82E-04	3.71E-06	1.60E-01	9.99E-02	2.74E-02
kg CFC11 eq	SOD	3.68E-07	2.99E-10	4.03E-10	6.13E-11	3.63E-10	3.48E-09	6.94E-13	2.93E-07	5.51E-08	1.51E-08
kBq Co-60 eq	IR	8.91E-02	7.77E-05	3.55E-06	1.03E-05	1.31E-04	1.30E-04	2.05E-07	6.06E-03	6.49E-02	1.78E-02
kg NOx eq	OFH	2.49E-03	1.72E-06	1.60E-07	7.57E-07	1.18E-06	2.03E-06	9.37E-09	2.26E-03	1.72E-04	4.71E-05
kg PM2.5 eq	FPM	2.41E-03	1.04E-06	1.16E-07	1.02E-06	2.27E-06	1.65E-06	6.42E-09	2.34E-03	5.47E-05	1.50E-05
kg NOx eq	OFT	2.55E-03	1.84E-06	1.71E-07	7.76E-07	1.24E-06	2.12E-06	9.52E-09	2.32E-03	1.78E-04	4.88E-05
kg SO2 eq	TA	8.33E-03	2.74E-06	4.68E-07	2.98E-06	7.09E-06	5.92E-06	1.91E-08	8.11E-03	1.56E-04	4.27E-05
kg P eq	FE	2.13E-04	3.05E-07	2.21E-08	1.18E-07	2.44E-07	3.90E-07	2.16E-09	1.99E-04	1.02E-05	2.79E-06
kg N eq	ME	1.15E-05	8.88E-07	1.31E-09	5.42E-09	3.97E-08	4.85E-07	1.37E-10	7.63E-06	1.88E-06	5.16E-07
kg 1,4-DCB	TEt	6.52E-01	3.34E-03	8.93E-04	7.70E-03	2.61E-02	3.55E-03	2.39E-06	3.93E-01	1.71E-01	4.69E-02
kg 1,4-DCB	FEt	8.52E-02	4.05E-05	9.61E-06	6.95E-05	1.05E-04	3.97E-05	7.92E-08	8.17E-02	2.55E-03	6.98E-04
kg 1,4-DCB	MEt	1.08E-01	5.24E-05	1.25E-05	9.08E-05	1.42E-04	5.02E-05	1.09E-07	1.04E-01	3.24E-03	8.86E-04
kg 1,4-DCB	HCT	2.61E-02	6.06E-05	8.39E-06	2.50E-05	4.51E-05	5.24E-05	1.65E-07	2.22E-02	2.95E-03	8.07E-04
kg 1,4-DCB	HNCT	3.44E+00	7.57E-04	1.53E-04	1.30E-03	2.75E-03	8.76E-04	4.09E-06	3.37E+00	4.67E-02	1.28E-02
m2a crop eq	LU	1.81E-02	1.35E-05	2.25E-06	7.95E-06	1.44E-05	2.23E-04	4.19E-08	4.74E-03	1.03E-02	2.82E-03
kg Cu eq	MRS	2.01E-02	3.05E-06	8.20E-07	1.25E-05	1.66E-04	3.40E-06	1.82E-09	1.96E-02	1.95E-04	5.34E-05
kg oil eq	FRS	9.56E-02	3.83E-04	2.59E-05	3.63E-05	1.40E-04	2.38E-04	1.08E-06	5.21E-02	3.35E-02	9.18E-03
m3	WC	1.58E-03	1.42E-05	1.68E-06	5.04E-06	8.62E-05	4.22E-05	8.35E-09	8.36E-04	4.67E-04	1.28E-04

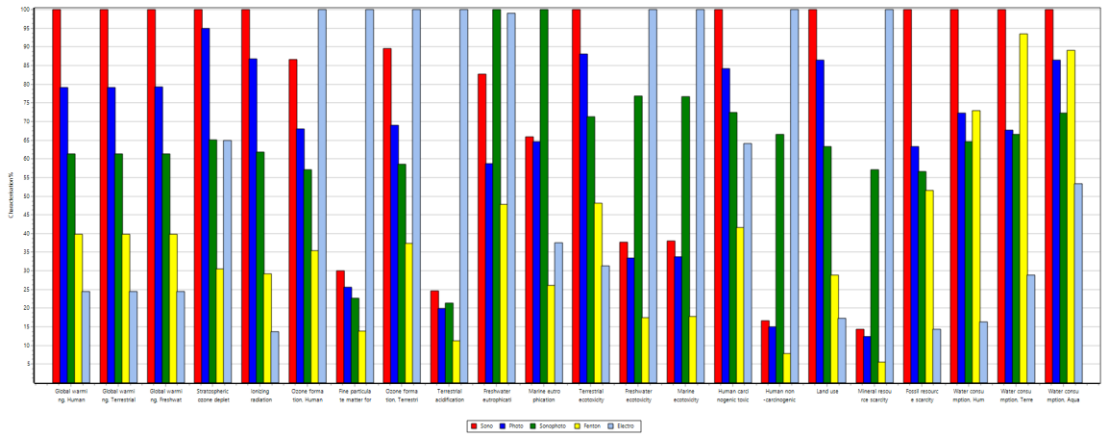

Figure C.1. Characterized 22 endpoint environmental impacts of selected AOP processes using current UK grid-mixed electricity

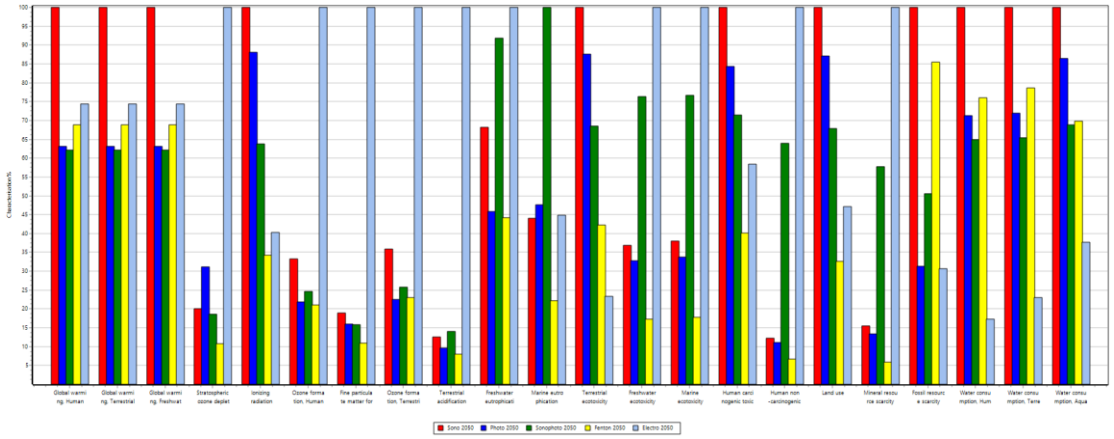

Figure C.2. Characterized 22 endpoint environmental impacts of selected AOP processes using IEA projected electricity

Table C.12. Characterized 22 endpoint environmental impacts of selected AOP processes using current UK grid-mixed electricity

Unit	Sono	Photo	Sonophoto	Fenton	Electro
USD2013	1.72E-01	1.09E-01	9.74E-02	8.86E-02	2.48E-02
USD2013	6.68E-04	5.75E-04	2.65E-03	2.60E-04	4.65E-03
species.yr	2.88E-15	2.50E-15	2.08E-15	2.57E-15	1.54E-15
species.yr	5.68E-11	3.85E-11	3.78E-11	5.31E-11	1.64E-11
species.yr	9.40E-10	8.13E-10	5.95E-10	2.72E-10	1.62E-10
species.yr	4.34E-12	3.85E-12	8.76E-12	2.02E-12	1.14E-11
species.yr	2.23E-11	1.98E-11	4.55E-11	1.04E-11	5.93E-11
species.yr	2.57E-11	2.26E-11	1.83E-11	1.24E-11	8.05E-12
species.yr	3.49E-14	3.42E-14	5.29E-14	1.39E-14	1.99E-14
species.yr	1.21E-10	8.57E-11	1.46E-10	6.98E-11	1.45E-10
species.yr	4.39E-10	3.55E-10	3.81E-10	2.01E-10	1.78E-09
species.yr	2.97E-10	2.28E-10	1.94E-10	1.24E-10	3.31E-10
species.yr	9.19E-14	7.28E-14	5.64E-14	3.66E-14	2.25E-14
species.yr	3.37E-09	2.67E-09	2.07E-09	1.34E-09	8.25E-10
DALY	1.39E-08	1.00E-08	8.98E-09	1.01E-08	2.27E-09
DALY	1.31E-07	1.17E-07	5.23E-07	6.19E-08	7.85E-07
DALY	1.38E-07	1.16E-07	9.98E-08	5.72E-08	8.82E-08
DALY	4.58E-07	3.91E-07	3.46E-07	2.11E-07	1.53E-06
DALY	1.97E-09	1.55E-09	1.30E-09	8.05E-10	2.28E-09
DALY	5.56E-09	4.82E-09	3.44E-09	1.62E-09	7.63E-10
DALY	3.02E-10	2.87E-10	1.97E-10	9.22E-11	1.96E-10
DALY	1.12E-06	8.83E-07	6.85E-07	4.44E-07	2.74E-07

Table C.13. Characterized 22 endpoint environmental impacts of selected AOP processes using current UK grid-mixed electricity

	Unit	Sono	Photo	Sonophoto	Fenton	Electro
FRS	USD2013	7.20E-02	2.25E-02	3.64E-02	6.15E-02	2.21E-02
MRS	USD2013	7.21E-04	6.21E-04	2.69E-03	2.75E-04	4.65E-03
WCAE	species.yr	4.19E-15	3.62E-15	2.88E-15	2.92E-15	1.58E-15
WCTE	species.yr	7.32E-11	5.26E-11	4.79E-11	5.76E-11	1.69E-11
LU	species.yr	3.08E-10	2.68E-10	2.09E-10	1.00E-10	1.45E-10
MEt	species.yr	4.35E-12	3.86E-12	8.77E-12	2.03E-12	1.14E-11
FEt	species.yr	2.18E-11	1.94E-11	4.52E-11	1.02E-11	5.93E-11
TEt	species.yr	3.57E-11	3.13E-11	2.45E-11	1.51E-11	8.32E-12
ME	species.yr	1.91E-14	2.06E-14	4.33E-14	9.58E-15	1.94E-14
FE	species.yr	9.81E-11	6.60E-11	1.32E-10	6.36E-11	1.44E-10
TA	species.yr	2.24E-10	1.69E-10	2.50E-10	1.42E-10	1.77E-09
OFTE	species.yr	1.17E-10	7.35E-11	8.42E-11	7.51E-11	3.26E-10
GWFE	species.yr	2.79E-14	1.76E-14	1.74E-14	1.92E-14	2.08E-14
GWTE	species.yr	1.02E-09	6.45E-10	6.36E-10	7.04E-10	7.61E-10
WC	DALY	1.30E-08	9.26E-09	8.44E-09	9.89E-09	2.25E-09
HNCT	DALY	9.61E-08	8.71E-08	5.01E-07	5.23E-08	7.84E-07
HCT	DALY	1.52E-07	1.28E-07	1.08E-07	6.10E-08	8.86E-08
FPM	DALY	2.87E-07	2.44E-07	2.41E-07	1.65E-07	1.52E-06
OFH	DALY	7.46E-10	4.91E-10	5.52E-10	4.72E-10	2.24E-09
IR	DALY	1.63E-09	1.43E-09	1.04E-09	5.58E-10	6.55E-10
SOD	DALY	3.78E-11	5.89E-11	3.50E-11	2.04E-11	1.89E-10
GW	DALY	3.39E-07	2.14E-07	2.11E-07	2.33E-07	2.52E-07

References:

[1] R.P. Schwarzenbach, B.I. Escher, K. Fenner, T.B. Hofstetter, C.A. Johnson, U. von Gunten, B. Wehrli, The challenge of micropollutants in aquatic systems, Science (1979) 313 (2006) 1072–1077.

[2] S.D. Richardson, Water Analysis: Emerging Contaminants and Current Issues, Analytical Chemistry (Washington) 79 (n.d.) 4295–4324. https://doi.org/10.1021/ac070719q.

[3] K.E. Murray, S.M. Thomas, A.A. Bodour, Prioritizing research for trace pollutants and emerging contaminants in the freshwater environment, Environmental Pollution (1987) 158 (2010) 3462–3471. https://doi.org/10.1016/j.envpol.2010.08.009.

[4] J.S. Cedeño-Muñoz, S.A. Aransiola, K.V. Reddy, P. Ranjit, M.O. Victor-Ekwebelem, O.J. Oyedele, I.B. Pérez-Almeida, N.R. Maddela, J.M. Rodríguez-Díaz, Antibiotic resistant bacteria and antibiotic resistance genes as contaminants of emerging concern: Occurrences, impacts, mitigations and future guidelines, Science of The Total Environment 952 (2024) 175906. https://doi.org/10.1016/J.SCITOTENV.2024.175906.

[5] Y. Deng, R. Zhao, Advanced oxidation processes (AOPs) in wastewater treatment, Curr Pollut Rep 1 (2015) 167–176.

[6] M.A. Oturan, J.-J. Aaron, Advanced oxidation processes in water/wastewater treatment: principles and applications. A review, Crit Rev Environ Sci Technol 44 (2014) 2577–2641.

[7] B.C. Hodges, E.L. Cates, J.-H. Kim, Challenges and prospects of advanced oxidation water treatment processes using catalytic nanomaterials, Nat Nanotechnol 13 (2018) 642–650.

[8] Q. Khan, M. Sayed, J.A. Khan, F. Rehman, S. Noreen, S. Sohni, I. Gul, Advanced oxidation/reduction processes (AO/RPs) for wastewater treatment, current challenges, and future perspectives: a review, Environmental Science and Pollution Research 31 (2024) 1863–1889.

[9] Y. Mao, W. Zuo, C. Wu, W. Ma, Y. Tian, J. Zhang, L. Li, W. Zhan, J. Qiu, Advances and challenges in the application of confined catalysts in heterogeneous advanced oxidation processes: A review, J Clean Prod 491 (2025) 144762. https://doi.org/10.1016/J.JCLEPRO.2025.144762.

[10] J. Wang, R. Zhuan, Degradation of antibiotics by advanced oxidation processes: An overview, Science of The Total Environment 701 (2020) 135023. https://doi.org/10.1016/J.SCITOTENV.2019.135023.

[11] M. Pirsaheb, N. Moradi, H. Hossini, Sonochemical processes for antibiotics removal from water and wastewater: A systematic review, Chemical Engineering

Research and Design 189 (2023) 401–439. https://doi.org/10.1016/J.CHERD.2022.11.019.

[12] C. Vom Eyser, A. Börgers, J. Richard, E. Dopp, N. Janzen, K. Bester, J. Tuerk, Chemical and toxicological evaluation of transformation products during advanced oxidation processes, Water Science and Technology 68 (2013) 1976–1983.

[13] B.P. Chaplin, Critical review of electrochemical advanced oxidation processes for water treatment applications, Environ Sci Process Impacts 16 (2014) 1182–1203.

[14] J. Fernandes, P.J. Ramísio, S.W.H.V. Hulle, H. Puga, Ultrasound-assisted advanced oxidation removal of contaminants of emerging concern: A review on present status and an outlook to future possibilities, J Hazard Mater 496 (2025) 139164. https://doi.org/10.1016/J.JHAZMAT.2025.139164.

[15] A. Hassani, M. Malhotra, A. V. Karim, S. Krishnan, P. V. Nidheesh, Recent progress on ultrasound-assisted electrochemical processes: A review on mechanism, reactor strategies, and applications for wastewater treatment, Environ Res 205 (2022) 112463. https://doi.org/10.1016/J.ENVRES.2021.112463.

[16] N.N. Mahamuni, Y.G. Adewuyi, Advanced oxidation processes (AOPs) involving ultrasound for waste water treatment: A review with emphasis on cost estimation, Ultrason Sonochem 17 (2010) 990–1003. https://doi.org/10.1016/J.ULTSONCH.2009.09.005.

[17] Z. Zong, E. Gilbert, C.C.Y. Wong, L. Usadi, Y. Qin, Y. Huang, J. Raymond, N. Hankins, J. Kwan, Efficient sonochemical catalytic degradation of tetracycline using TiO2 fractured nanoshells, Ultrason Sonochem 101 (2023) 106669. https://doi.org/10.1016/J.ULTSONCH.2023.106669.

[18] Z. Zong, N. Hankins, F. Parveen, The Application of Nanofiltration for Water Reuse in the Hybrid Nanofiltration-Forward Osmosis Process, in: Nanofiltration for Sustainability, CRC Press, 2023: pp. 153–170.

[19] Z. Zong, O. Daoud, N.P. Hankins, Q. She, C.D. Peters, Valorising desalination brine for green cement production: toward mitigating global CO2 emissions, Water Res 284 (2025) 123930. https://doi.org/10.1016/J.WATRES.2025.123930.

[20] T. Rantissi, V. Gitis, Z. Zong, N. Hankins, Transforming the Water-Energy Nexus in Gaza: A Systems Approach, Global Challenges (2024) 2300304.

[21] G. Maniakova, M.I. Polo López, I. Oller, S. Malato, L. Rizzo, Ozonation Vs sequential solar driven processes as simultaneous tertiary and quaternary treatments of urban wastewater: A life cycle assessment comparison, J Clean Prod 413 (2023) 137507. https://doi.org/10.1016/J.JCLEPRO.2023.137507.

[22] S. Guerra-Rodríguez, S. Cuesta, J. Pérez, E. Rodríguez, J. Rodríguez-Chueca,

Life Cycle Assessment of sulfate radical based-AOPs for wastewater disinfection, Chemical Engineering Journal 474 (2023) 145427. https://doi.org/10.1016/J.CEJ.2023.145427.

[23] R.W. Holloway, L. Miller-Robbie, M. Patel, J.R. Stokes, J. Munakata-Marr, J. Dadakis, T.Y. Cath, Life-cycle assessment of two potable water reuse technologies: MF/RO/UV–AOP treatment and hybrid osmotic membrane bioreactors, J Memb Sci 507 (2016) 165–178. https://doi.org/10.1016/J.MEMSCI.2016.01.045.

[24] E. Chatzisymeon, S. Foteinis, D. Mantzavinos, T. Tsoutsos, Life cycle assessment of advanced oxidation processes for olive mill wastewater treatment, J Clean Prod 54 (2013) 229–234. https://doi.org/10.1016/J.JCLEPRO.2013.05.013.

[25] G.L. Stephens, J.M. Slingo, E. Rignot, J.T. Reager, M.Z. Hakuba, P.J. Durack, J. Worden, R. Rocca, Earth's water reservoirs in a changing climate, Proceedings of the Royal Society A: Mathematical, Physical and Engineering Sciences 476 (2020) 20190458. https://doi.org/10.1098/rspa.2019.0458.

[26] W.W.A.P. (United Nations), Water for People, Water for Life: The United Nations World Water Development Report: Executive Summary, Unesco Pub., 2003.

[27] C. Silva, C.M.M. Almeida, J.A. Rodrigues, S. Silva, M. do Rosário Coelho, A. Martins, R. Lourinho, E. Cardoso, V.V. Cardoso, M.J. Benoliel, E. Mesquita, R. Ribeiro, M.J. Rosa, Improving the control of pharmaceutical compounds in activated sludge wastewater treatment plants: Key operating conditions and monitoring parameters, Journal of Water Process Engineering 54 (2023) 103985. https://doi.org/10.1016/J.JWPE.2023.103985.

[28] M. Kedzierski, B. Lechat, O. Sire, G. le Maguer, V. le Tilly, S. Bruzaud, Microplastic contamination of packaged meat: Occurrence and associated risks, Food Packag Shelf Life 24 (2020) 100489. https://doi.org/10.1016/J.FPSL.2020.100489.

[29] V.C. Shruti, F. Pérez-Guevara, I. Elizalde-Martínez, G. Kutralam-Muniasamy, Toward a unified framework for investigating micro(nano)plastics in packaged beverages intended for human consumption, Environmental Pollution 268 (2021) 115811. https://doi.org/10.1016/J.ENVPOL.2020.115811.

[30] F. Du, H. Cai, Q. Zhang, Q. Chen, H. Shi, Microplastics in take-out food containers, J Hazard Mater 399 (2020) 122969. https://doi.org/10.1016/J.JHAZMAT.2020.122969.

[31] K. Fenner, M. Scheringer, M. Macleod, M. Matthies, T. McKone, M. Stroebe, A. Beyer, M. Bonnell, A.C. le Gall, J. Klasmeier, Comparing estimates of persistence and long-range transport potential among multimedia models, (2005).

[32] R.W. Macdonald, L.A. Barrie, T.F. Bidleman, M.L. Diamond, D.J. Gregor, R.G. Semkin, W.M.J. Strachan, Y.F. Li, F. Wania, M. Alaee, Contaminants in the Canadian Arctic: 5 years of progress in understanding sources, occurrence and pathways, Science of the Total Environment 254 (2000) 93–234.

[33] A.B.A. Boxall, C.J. Sinclair, K. Fenner, D. Kolpin, S.J. Maund, Peer reviewed: when synthetic chemicals degrade in the environment, Environ Sci Technol 38 (2004) 368A-375A.

[34] M.H.A. Kester, S. Bulduk, D. Tibboel, W. Meinl, H. Glatt, C.N. Falany, M.W.H. Coughtrie, A.K.E. Bergman, S.H. Safe, G.G.J.M. Kuiper, Potent inhibition of estrogen sulfotransferase by hydroxylated PCB metabolites: a novel pathway explaining the estrogenic activity of PCBs, Endocrinology 141 (2000) 1897–1900.

[35] S.I. Polianciuc, A.E. Gurzău, B. Kiss, M.G. Ştefan, F. Loghin, Antibiotics in the environment: causes and consequences, Med Pharm Rep 93 (2020) 231.

[36] J. Lyu, Y. Chen, L. Zhang, Antibiotics in Drinking Water and Health Risks—China, 2017, China CDC Wkly 2 (2020) 413.

[37] M.-C. Danner, A. Robertson, V. Behrends, J. Reiss, Antibiotic pollution in surface fresh waters: occurrence and effects, Science of the Total Environment 664 (2019) 793–804.

[38] S.C. Roberts, T.R. Zembower, Global increases in antibiotic consumption: a concerning trend for WHO targets, Lancet Infect Dis 21 (2021) 10–11. https://doi.org/10.1016/S1473-3099(20)30456-4.

[39] I.T. Carvalho, L. Santos, Antibiotics in the aquatic environments: A review of the European scenario, Environ Int 94 (n.d.) 736–757. https://doi.org/10.1016/j.envint.2016.06.025.

[40] J. Margot, L. Rossi, D.A. Barry, C. Holliger, A review of the fate of micropollutants in wastewater treatment plants, Wiley Interdisciplinary Reviews: Water 2 (2015) 457–487.

[41] L. Serwecińska, Antimicrobials and antibiotic-resistant bacteria: a risk to the environment and to public health, Water (Basel) 12 (2020) 3313.

[42] S.F. Zhong, B. Yang, H.J. Lei, Q. Xiong, Q.Q. Zhang, F. Liu, G.G. Ying, Transformation products of tetracyclines in three typical municipal wastewater treatment plants, Science of The Total Environment 830 (2022) 154647. https://doi.org/10.1016/J.SCITOTENV.2022.154647.

[43] C. Wang, J.-J. Jian, Degradation and detoxicity of tetracycline by an enhanced sonolysis, J Water Environ Technol 13 (2015) 325–334.

[44] S. Ren, S. Wang, Y. Liu, Y. Wang, F. Gao, Y. Dai, A review on current pollution and removal methods of tetracycline in soil, Sep Sci Technol 58 (2023) 2578–

2602.

[45] F. Ahmad, D. Zhu, J. Sun, Environmental fate of tetracycline antibiotics: degradation pathway mechanisms, challenges, and perspectives, Environ Sci Eur 33 (2021) 64.

[46] J. Antos, M. Piosik, D. Ginter-Kramarczyk, J. Zembrzuska, I. Kruszelnicka, Tetracyclines contamination in European aquatic environments: A comprehensive review of occurrence, fate, and removal techniques, Chemosphere 353 (2024) 141519. https://doi.org/10.1016/J.CHEMOSPHERE.2024.141519.

[47] H. Salah, N. Shehata, N. Khedr, K.N.M. Elsayed, Management of a ciprofloxacin as a contaminant of emerging concern in water using microalgaebioremediation: mechanism, modeling, and kinetic studies, Microb Cell Fact 23 (2024) 329.

[48] N. Nandy, A. Pasupathi, Y. Subramaniam, S. Nachimuthu, Eliminating ciprofloxacin antibiotic contamination from water with a novel submerged thermal plasma technology, Chemosphere 326 (2023) 138470. https://doi.org/10.1016/J.CHEMOSPHERE.2023.138470.

[49] L. Qalyoubi, A. Al-Othman, S. Al-Asheh, Removal of ciprofloxacin antibiotic pollutants from wastewater using nano-composite adsorptive membranes, Environ Res 215 (2022) 114182. https://doi.org/10.1016/J.ENVRES.2022.114182.

[50] K.D. Burch, B. Han, J. Pichtel, T. Zubkov, Removal efficiency of commonly prescribed antibiotics via tertiary wastewater treatment, Environmental Science and Pollution Research 26 (2019) 6301–6310. https://doi.org/10.1007/s11356-019-04170-w.

[51] A. Gholizadeh, M. Khiadani, M. Foroughi, H. Alizade Siuki, H. Mehrfar, Wastewater treatment plants: The missing link in global One-Health surveillance and management of antibiotic resistance, J Infect Public Health 16 (2023) 217–224. https://doi.org/10.1016/J.JIPH.2023.09.017.

[52] S. Adhikari, H.H. Lee, D.-H. Kim, 'Primary' antibiotics in wastewater treatment plants, IScience 27 (2024) 110789. https://doi.org/10.1016/J.ISCI.2024.110789.

[53] M. Pei, B. Zhang, Y. He, J. Su, K. Gin, O. Lev, G. Shen, S. Hu, State of the art of tertiary treatment technologies for controlling antibiotic resistance in wastewater treatment plants, Environ Int 131 (2019) 105026. https://doi.org/10.1016/J.ENVINT.2019.105026.

[54] B. Liu, Y. Zhan, R. Xie, H. Huang, K. Li, Y. Zeng, R.P. Shrestha, N.T.K. Oanh, E. Winijkul, Efficient photocatalytic oxidation of gaseous toluene in a bubbling reactor of water, Chemosphere 233 (2019) 754–761.

[55] H.J.H. Fenton, LXXIII.—Oxidation of tartaric acid in presence of iron, Journal of the Chemical Society, Transactions 65 (1894) 899–910.

[56] L. Chen, J. Ma, X. Li, J. Zhang, J. Fang, Y. Guan, P. Xie, Strong enhancement on Fenton oxidation by addition of hydroxylamine to accelerate the ferric and ferrous iron cycles, Environ Sci Technol 45 (2011) 3925–3930.

[57] N. Wang, T. Zheng, G. Zhang, P. Wang, A review on Fenton-like processes for organic wastewater treatment, J Environ Chem Eng 4 (2016) 762–787.

[58] L. Lunar, D. Sicilia, S. Rubio, D. Pérez-Bendito, U. Nickel, Degradation of photographic developers by Fenton's reagent: condition optimization and kinetics for metol oxidation, Water Res 34 (2000) 1791–1802.

[59] G. Pliego, J.A. Zazo, P. Garcia-Muñoz, M. Munoz, J.A. Casas, J.J. Rodriguez, Trends in the intensification of the Fenton process for wastewater treatment: an overview, Crit Rev Environ Sci Technol 45 (2015) 2611–2692.

[60] M.L. Rodriguez, V.I. Timokhin, S. Contreras, E. Chamarro, S. Esplugas, Rate equation for the degradation of nitrobenzene by 'Fenton-like'reagent, Advances in Environmental Research 7 (2003) 583–595.

[61] Y. Wang, H. Li, P. Yi, H. Zhang, Degradation of clofibric acid by UV, O3 and UV/O3 processes: performance comparison and degradation pathways, J Hazard Mater 379 (2019) 120771.

[62] L. Xu, N.P. Liu, H.L. An, W.T. Ju, B. Liu, X.F. Wang, X. Wang, Preparation of Ag3PO4/CoWO4 S-scheme heterojunction and study on sonocatalytic degradation of tetracycline, Ultrason Sonochem 89 (2022) 106147. https://doi.org/10.1016/J.ULTSONCH.2022.106147.

[63] J. Qiao, H. Zhang, G. Li, S. Li, Z. Qu, M. Zhang, J. Wang, Y. Song, Fabrication of a novel Z-scheme SrTiO3/Ag2S/CoWO4 composite and its application in sonocatalytic degradation of tetracyclines, Sep Purif Technol 211 (2019) 843–856. https://doi.org/10.1016/J.SEPPUR.2018.10.058.

[64] L.L. He, J.Y. Bai, X.Y. Li, S. Qi, S. Li, X. Wang, BiOBr/MgFe2O4 composite as a novel catalyst for the sonocatalytic removal of tetracycline in aqueous environment, Surfaces and Interfaces 33 (2022) 102177. https://doi.org/10.1016/J.SURFIN.2022.102177.

[65] R.D.C. Soltani, M. Mashayekhi, M. Naderi, G. Boczkaj, S. Jorfi, M. Safari, Sonocatalytic degradation of tetracycline antibiotic using zinc oxide nanostructures loaded on nano-cellulose from waste straw as nanosonocatalyst, Ultrason Sonochem 55 (2019) 117–124. https://doi.org/10.1016/J.ULTSONCH.2019.03.009.

[66] A. Reheman, K. Kadeer, K. Okitsu, M. Halidan, Y. Tursun, T. Dilinuer, A. Abulikemu, Facile photo-ultrasonic assisted reduction for preparation of rGO/Ag2CO3 nanocomposites with enhanced photocatalytic oxidation activity for tetracycline, Ultrason Sonochem 51 (2019) 166–177. https://doi.org/10.1016/J.ULTSONCH.2018.10.030.

[67] W. Shi, F. Guo, H. Wang, M. Han, H. Li, S. Yuan, H. Huang, Y. Liu, Z. Kang, Carbon dots decorated the exposing high-reactive (111) facets CoO octahedrons with enhanced photocatalytic activity and stability for tetracycline degradation under visible light irradiation, Appl Catal B 219 (2017) 36–44. https://doi.org/10.1016/J.APCATB.2017.07.019.

[68] H. Shen, J. Wang, J. Jiang, B. Luo, B. Mao, W. Shi, All-solid-state Z-scheme system of RGO-Cu2O/Bi2O3 for tetracycline degradation under visible-light irradiation, Chemical Engineering Journal 313 (2017) 508–517. https://doi.org/10.1016/J.CEJ.2016.11.161.

[69] Y. Tang, X. Liu, C. Ma, M. Zhou, P. Huo, L. Yu, J. Pan, W. Shi, Y. Yan, Enhanced photocatalytic degradation of tetracycline antibiotics by reduced graphene oxide–CdS/ZnS heterostructure photocatalysts, New Journal of Chemistry 39 (2015) 5150–5160. https://doi.org/10.1039/C5NJ00681C.

[70] S. Heidari, M. Haghighi, M. Shabani, Ultrasound assisted dispersion of Bi2Sn2O7-C3N4 nanophotocatalyst over various amount of zeolite Y for enhanced solar-light photocatalytic degradation of tetracycline in aqueous solution, Ultrason Sonochem 43 (2018) 61–72. https://doi.org/10.1016/j.ultsonch.2018.01.001.

[71] V. Vinesh, A.R.M. Shaheer, B. Neppolian, Reduced graphene oxide (rGO) supported electron deficient B-doped TiO2 (Au/B-TiO2/rGO) nanocomposite: An efficient visible light sonophotocatalyst for the degradation of Tetracycline (TC), Ultrason Sonochem 50 (2019) 302–310. https://doi.org/10.1016/J.ULTSONCH.2018.09.030.

[72] A.A. Isari, M. Mehregan, S. Mehregan, F. Hayati, R. Rezaei Kalantary, B. Kakavandi, Sono-photocatalytic degradation of tetracycline and pharmaceutical wastewater using WO3/CNT heterojunction nanocomposite under US and visible light irradiations: A novel hybrid system, J Hazard Mater 390 (2020) 122050. https://doi.org/10.1016/J.JHAZMAT.2020.122050.

[73] A. Bembibre, M. Benamara, M. Hjiri, E. Gómez, H.R. Alamri, R. Dhahri, A. Serrà, Visible-light driven sonophotocatalytic removal of tetracycline using Ca-doped ZnO nanoparticles, Chem Eng J 427 (2022) 132006. https://doi.org/10.1016/j.cej.2021.132006.

[74] X. Li, X. Zhang, S. Wang, P. Yu, Y. Xu, Y. Sun, Highly enhanced heterogeneous photo-Fenton process for tetracycline degradation by Fe/SCN Fenton-like catalyst, J Environ Manage 312 (2022) 114856. https://doi.org/10.1016/J.JENVMAN.2022.114856.

[75] X. Shi, L. Wang, A.A. Zuh, Y. Jia, F. Ding, H. Cheng, Q. Wang, Photo-Fenton reaction for the degradation of tetracycline hydrochloride using a FeWO4/BiOCl nanocomposite, J Alloys Compd 903 (2022) 163889. https://doi.org/10.1016/J.JALLCOM.2022.163889.

[76] F. Mahmoudi, C.M. Park, J.J. Shim, Ultrasound-assisted heterogeneous Fenton-like process for efficient degradation of tetracycline over SmFeO3/Ti3C2Tx catalyst, Journal of Water Process Engineering 50 (2022) 103235. https://doi.org/10.1016/J.JWPE.2022.103235.

[77] G. Gopalakrishnan, R.B. Jeyakumar, A. Somanathan, Challenges and emerging trends in advanced oxidation technologies and integration of advanced oxidation processes with biological processes for wastewater treatment, Sustainability 15 (2023) 4235.

[78] M. Priyadarshini, I. Das, M.M. Ghangrekar, L. Blaney, Advanced oxidation processes: Performance, advantages, and scale-up of emerging technologies, J Environ Manage 316 (2022) 115295. https://doi.org/10.1016/J.JENVMAN.2022.115295.

[79] Y. Son, Advanced oxidation processes using ultrasound technology for water and wastewater treatment, Handbook of Ultrasonics and Sonochemistry (2016) 711–732.

[80] M.H. Dehghani, R.R. Karri, J.R. Koduru, S. Manickam, I. Tyagi, N.M. Mubarak, Suhas, Recent trends in the applications of sonochemical reactors as an advanced oxidation process for the remediation of microbial hazards associated with water and wastewater: A critical review, Ultrason Sonochem 94 (2023) 106302. https://doi.org/10.1016/J.ULTSONCH.2023.106302.

[81] Y. Yang, M. Shan, X. Kan, Y. Shangguan, Q. Han, Thermodynamic of collapsing cavitation bubble investigated by pseudopotential and thermal MRT-LBM, Ultrason Sonochem 62 (n.d.) 104873–104873. https://doi.org/10.1016/j.ultsonch.2019.104873.

[82] B. Kakavandi, N. Bahari, R. Rezaei Kalantary, E. Dehghani Fard, Enhanced sono-photocatalysis of tetracycline antibiotic using TiO2 decorated on magnetic activated carbon (MAC@T) coupled with US and UV: A new hybrid system, Ultrason Sonochem 55 (2019) 75–85. https://doi.org/10.1016/J.ULTSONCH.2019.02.026.

[83] R. Yang, Z. Wu, Y. Yang, Y. Li, L. Zhang, B. Yu, Understanding the origin of synergistic catalytic activities for ZnO based sonophotocatalytic degradation of methyl orange, J Taiwan Inst Chem Eng 119 (2021) 128–135. https://doi.org/10.1016/J.JTICE.2021.01.028.

[84] P. Gholami, A. Khataee, R.D.C. Soltani, A. Bhatnagar, A review on carbon-based materials for heterogeneous sonocatalysis: Fundamentals, properties and applications, Ultrason Sonochem 58 (2019) 104681. https://doi.org/10.1016/J.ULTSONCH.2019.104681.

[85] C.C.Y. Wong, J.L. Raymond, L.N. Usadi, Z. Zong, S.C. Walton, A.C. Sedgwick, J. Kwan, Enhancement of sonochemical production of hydroxyl radicals from pulsed cylindrically converging ultrasound waves, Ultrason Sonochem (2023)

106559. https://doi.org/10.1016/J.ULTSONCH.2023.106559.

[86] S.E. Ahmed, A.M. Martins, G.A. Husseini, The use of ultrasound to release chemotherapeutic drugs from micelles and liposomes, J Drug Target 23 (n.d.) 16–42. https://doi.org/10.3109/1061186X.2014.954119.

[87] J.R. Blake, Cavitation and Bubble Dynamics. By C. E. BRENNEN. Oxford University Press, 1995. 282 pp. ISBN 0 19 509409. £60, J Fluid Mech 316 (n.d.) 376–377. https://doi.org/10.1017/S0022112096230599.

[88] M. Ashokkumar, The characterization of acoustic cavitation bubbles – An overview, Ultrason Sonochem 18 (2011) 864–872. https://doi.org/10.1016/j.ultsonch.2010.11.016.

[89] M. Wang, Y. Zhou, Numerical investigation of the inertial cavitation threshold by dual-frequency excitation in the fluid and tissue, Ultrason Sonochem 42 (n.d.) 327–338. https://doi.org/10.1016/j.ultsonch.2017.11.045.

[90] P. Qiu, B. Park, J. Choi, B. Thokchom, A.B. Pandit, J. Khim, A review on heterogeneous sonocatalyst for treatment of organic pollutants in aqueous phase based on catalytic mechanism, Ultrason Sonochem 45 (n.d.) 29–49. https://doi.org/10.1016/j.ultsonch.2018.03.003.

[91] E.C. Ilinoiu, R. Pode, F. Manea, L.A. Colar, A. Jakab, C. Orha, C. Ratiu, C. Lazau, P. Sfarloaga, Photocatalytic activity of a nitrogen-doped TiO2 modified zeolite in the degradation of Reactive Yellow 125 azo dye, J Taiwan Inst Chem Eng 44 (2013) 270–278. https://doi.org/10.1016/J.JTICE.2012.09.006.

[92] R. Ahmad, Z. Ahmad, A.U. Khan, N.R. Mastoi, M. Aslam, J. Kim, Photocatalytic systems as an advanced environmental remediation: Recent developments, limitations and new avenues for applications, J Environ Chem Eng 4 (2016) 4143–4164. https://doi.org/10.1016/J.JECE.2016.09.009.

[93] R. Pflieger, S.I. Nikitenko, C. Cairós, R. Mettin, Sonoluminescence, in: Characterization of Cavitation Bubbles and Sonoluminescence, Springer, 2019: pp. 39–60.

[94] L. v. Bora, R.K. Mewada, Visible/solar light active photocatalysts for organic effluent treatment: Fundamentals, mechanisms and parametric review, Renewable and Sustainable Energy Reviews 76 (2017) 1393–1421. https://doi.org/10.1016/J.RSER.2017.01.130.

[95] A. Ren, C. Liu, Y. Hong, W. Shi, S. Lin, P. Li, Enhanced visible-light-driven photocatalytic activity for antibiotic degradation using magnetic NiFe2O4/Bi2O3 heterostructures, Chemical Engineering Journal 258 (2014) 301–308. https://doi.org/10.1016/J.CEJ.2014.07.071.

[96] M. Chen, J. Yao, Y. Huang, H. Gong, W. Chu, Enhanced photocatalytic degradation of ciprofloxacin over Bi2O3/(BiO)2CO3 heterojunctions: Efficiency, kinetics, pathways, mechanisms and toxicity evaluation, Chemical

Engineering Journal 334 (2018) 453–461. https://doi.org/10.1016/J.CEJ.2017.10.064.

[97] J. Gao, Y. Gao, Z. Sui, Z. Dong, S. Wang, D. Zou, Hydrothermal synthesis of BiOBr/FeWO4 composite photocatalysts and their photocatalytic degradation of doxycycline, J Alloys Compd 732 (2018) 43–51. https://doi.org/10.1016/J.JALLCOM.2017.10.092.

[98] X.-J. Wen, C.-G. Niu, L. Zhang, C. Liang, G.-M. Zeng, A novel Ag2O/CeO2 heterojunction photocatalysts for photocatalytic degradation of enrofloxacin: possible degradation pathways, mineralization activity and an in depth mechanism insight, Appl Catal B 221 (2018) 701–714.

[99] S. Gautam, H. Agrawal, M. Thakur, A. Akbari, H. Sharda, R. Kaur, M. Amini, Metal oxides and metal organic frameworks for the photocatalytic degradation: A review, J Environ Chem Eng 8 (2020) 103726. https://doi.org/10.1016/J.JECE.2020.103726.

[100] U.S. Jonnalagadda, X. Su, J.J. Kwan, Nanostructured TiO2 cavitation agents for dual-modal sonophotocatalysis with pulsed ultrasound, Ultrason Sonochem 73 (2021) 105530. https://doi.org/10.1016/J.ULTSONCH.2021.105530.

[101] C.G. Joseph, G. Li Puma, A. Bono, D. Krishnaiah, Sonophotocatalysis in advanced oxidation process: A short review, Ultrason Sonochem 16 (2009) 583–589. https://doi.org/10.1016/J.ULTSONCH.2009.02.002.

[102] C. Wong, J.L. Raymond, L.N. Usadi, Z. Zong, S. Walton, A. Sedgwick, J. Kwan, Improving sonochemical efficiency by pulsing cylindrically converging acoustic waves, J Acoust Soc Am 153 (2023) A73–A73.

[103] M. Hoseini, G.H. Safari, H. Kamani, J. Jaafari, M. Ghanbarain, A.H. Mahvi, Sonocatalytic degradation of tetracycline antibiotic in aqueous solution by sonocatalysis, Toxicol Environ Chem 95 (2013) 1680–1689.

[104] H. Deng, Y. Jin, B. Yan, Y. Jiang, S. Yang, T. Song, Degradation of tetracycline by heat/peroxymonosulfate and ultrasound/peroxymonosulfate systems: performance and kinetics, Water Science & Technology 89 (2024) 421–433.

[105] L. Xu, X.Q. Wu, C.Y. Li, N.P. Liu, H.L. An, W.T. Ju, W. Lu, B. Liu, X.F. Wang, Y. Wang, X. Wang, Sonocatalytic degradation of tetracycline by BiOBr/FeWO4 nanomaterials and enhancement of sonocatalytic effect, J Clean Prod 394 (2023) 136275. https://doi.org/10.1016/J.JCLEPRO.2023.136275.

[106] P. Kumari, A. Kumar, ADVANCED OXIDATION PROCESS: A remediation technique for organic and non-biodegradable pollutant, Results in Surfaces and Interfaces 11 (2023) 100122. https://doi.org/10.1016/J.RSURFI.2023.100122.

[107] M. Zhao, Y. Liu, M. Feng, X. Yu, L. Wang, Degradation mechanisms of antibiotics in UV222/H2O2 and UV222/persulfate systems: Dual roles of inorganic anions, Chemical Engineering Journal 489 (2024) 151371.

https://doi.org/10.1016/J.CEJ.2024.151371.

[108] J. Yang, S. Wang, X. Luo, Z. Yu, Y. Zhou, Fenton-like process in antibiotic-containing wastewater treatment: applications and toxicity evaluation, Chinese Chemical Letters (2025) 110996. https://doi.org/10.1016/J.CCLET.2025.110996.

[109] P. Liu, Z. Wu, A. V. Abramova, G. Cravotto, Sonochemical processes for the degradation of antibiotics in aqueous solutions: A review, Ultrason Sonochem 74 (2021) 105566. https://doi.org/10.1016/J.ULTSONCH.2021.105566.

[110] Y. Ahmed, A.A.S. Maya, P. Akhtar, H. AlMohamadi, A.W. Mohammad, S.M. Ashekuzzaman, A.I. Olbert, M.G. Uddin, Advancements and challenges in Fenton-based advanced oxidation processes for antibiotic removal in wastewater: From the laboratory to practical applications, J Environ Chem Eng 13 (2025) 115068. https://doi.org/10.1016/J.JECE.2024.115068.

[111] Z. Honarmandrad, X. Sun, Z. Wang, M. Naushad, G. Boczkaj, Activated persulfate and peroxymonosulfate based advanced oxidation processes (AOPs) for antibiotics degradation – A review, Water Resour Ind 29 (2023) 100194. https://doi.org/10.1016/J.WRI.2022.100194.

[112] G. Lu, X. Li, W. Li, Y. Liu, N. Wang, Z. Pan, G. Zhang, Y. Zhang, B. Lai, Thermo-activated periodate oxidation process for tetracycline degradation: Kinetics and byproducts transformation pathways, J Hazard Mater 461 (2024) 132696. https://doi.org/10.1016/J.JHAZMAT.2023.132696.

[113] R. López-Timoner, L. Santos-Juanes, A.M. Amat, F. Arfelli, D. Cespi, F. Passarini, M.I. Polo, E. Zuriaga, A. Arques, Life cycle assessment of UVC-based advanced oxidation processes as quaternary treatments: Clostridium spp. inactivation and comparison with CECs removal, Science of The Total Environment 972 (2025) 179029. https://doi.org/10.1016/J.SCITOTENV.2025.179029.

[114] Y. Chai, X. Chen, Y. Wang, X. Guo, R. Zhang, H. Wei, H. Jin, Z. Li, L. Ma, Environmental and economic assessment of advanced oxidation for the treatment of unsymmetrical dimethylhydrazine wastewater from a life cycle perspective, Science of The Total Environment 873 (2023) 162264. https://doi.org/10.1016/J.SCITOTENV.2023.162264.

[115] S. Arzate, S. Pfister, C. Oberschelp, J.A. Sánchez-Pérez, Environmental impacts of an advanced oxidation process as tertiary treatment in a wastewater treatment plant, Science of The Total Environment 694 (2019) 133572. https://doi.org/10.1016/J.SCITOTENV.2019.07.378.

[116] I. ISO, ISO 14040. Environmental management–Life cycle assessment–Principles and framework (ISO 14040: 2006), (2006).

[117] M.A.J. Huijbregts, Z.J.N. Steinmann, P.M.F. Elshout, G. Stam, F. Verones, M. Vieira, M. Zijp, A. Hollander, R. Van Zelm, ReCiPe2016: a harmonised life cycle

impact assessment method at midpoint and endpoint level, Int J Life Cycle Assess 22 (2017) 138–147.

[118] A. Bjørn, A. Moltesen, A. Laurent, M. Owsianiak, A. Corona, M. Birkved, M.Z. Hauschild, Life cycle inventory analysis, Life Cycle Assessment: Theory and Practice (2018) 117–165.

[119] L. Pourzahedi, M.J. Eckelman, Comparative life cycle assessment of silver nanoparticle synthesis routes, Environ Sci Nano 2 (2015) 361–369.

[120] B. Salieri, D.A. Turner, B. Nowack, R. Hischier, Life cycle assessment of manufactured nanomaterials: Where are we?, NanoImpact 10 (2018) 108–120. https://doi.org/10.1016/J.IMPACT.2017.12.003.

[121] N.U.M. Nizam, M.M. Hanafiah, K.S. Woon, A content review of life cycle assessment of nanomaterials: current practices, challenges, and future prospects, Nanomaterials 11 (2021) 3324.

[122] J. Gimenez, B. Bayarri, O. Gonzalez, S. Malato, J. Peral, S. Esplugas, Advanced oxidation processes at laboratory scale: environmental and economic impacts, ACS Sustain Chem Eng 3 (2015) 3188–3196.

[123] R. Lima-Thompson, S.L. Gora, Techno-Economic Assessment of the Application of Advanced Oxidation Processes for the Removal of Seasonal and Year-Round Contaminants from Drinking Water, in: Advanced Oxidation Processes for Micropollutant Remediation, CRC Press, 2023: pp. 187–214.

[124] V. Innocenzi, G. Mazziotti di Celso, M. Prisciandaro, Techno-economic analysis of olive wastewater treatment with a closed water approach by integrated membrane processes and advanced oxidation processes, Water Reuse 11 (2021) 122–135.

[125] R. Stirling, W.S. Walker, P. Westerhoff, S. Garcia-Segura, Techno-economic analysis to identify key innovations required for electrochemical oxidation as point-of-use treatment systems, Electrochim Acta 338 (2020) 135874. https://doi.org/10.1016/J.ELECTACTA.2020.135874.

[126] A. Al-Qahtani, B. Parkinson, K. Hellgardt, N. Shah, G. Guillen-Gosalbez, Uncovering the true cost of hydrogen production routes using life cycle monetisation, Appl Energy 281 (2021) 115958. https://doi.org/10.1016/J.APENERGY.2020.115958.

[127] P.H. Kobos, T.E. Drennen, A. V Outkin, E.K. Webb, S.M. Paap, S. Wiryadinata, Techno-economic analysis: Best practices and assessment tools, Sandia National Lab.(SNL-CA), Livermore, CA (United States); Sandia National …, 2020.

[128] G. Rebitzer, T. Ekvall, R. Frischknecht, D. Hunkeler, G. Norris, T. Rydberg, W.-P. Schmidt, S. Suh, B.P. Weidema, D.W. Pennington, Life cycle assessment: Part 1: Framework, goal and scope definition, inventory analysis, and applications, Environ Int 30 (2004) 701–720.

[129] P. Asaithambi, M.B. Yesuf, R. Govindarajan, N.M. Hariharan, P. Thangavelu, E. Alemayehu, A review of hybrid process development based on electrochemical and advanced oxidation processes for the treatment of industrial wastewater, International Journal of Chemical Engineering 2022 (2022) 1105376.

[130] K.E. O'Shea, D.D. Dionysiou, Advanced Oxidation Processes for Water Treatment, J Phys Chem Lett 3 (2012) 2112–2113. https://doi.org/10.1021/jz300929x.

[131] D. Ma, H. Yi, C. Lai, X. Liu, X. Huo, Z. An, L. Li, Y. Fu, B. Li, M. Zhang, L. Qin, S. Liu, L. Yang, Critical review of advanced oxidation processes in organic wastewater treatment, Chemosphere 275 (2021) 130104. https://doi.org/10.1016/J.CHEMOSPHERE.2021.130104.

[132] P. Kokkinos, D. Venieri, D. Mantzavinos, Advanced Oxidation Processes for Water and Wastewater Viral Disinfection. A Systematic Review, Food Environ Virol 13 (2021) 283–302. https://doi.org/10.1007/s12560-021-09481-1.

[133] M.H. Abdurahman, A.Z. Abdullah, N.F. Shoparwe, A comprehensive review on sonocatalytic, photocatalytic, and sonophotocatalytic processes for the degradation of antibiotics in water: Synergistic mechanism and degradation pathway, Chemical Engineering Journal 413 (2021) 127412. https://doi.org/10.1016/J.CEJ.2020.127412.

[134] Q. Shao, L.-Y. Wang, X.-J. Wang, M.-C. Yang, S.-S. Ge, X.-K. Yang, J.-X. Wang, Hydrothermal synthesis and photocatalytic property of porous CuO hollow microspheres via PS latex as templates, Solid State Sci 20 (2013) 29–35.

[135] J. Wang, J. Yu, X. Zhu, X.Z. Kong, Preparation of hollow TiO2 nanoparticles through TiO2 deposition on polystyrene latex particles and characterizations of their structure and photocatalytic activity, Nanoscale Res Lett 7 (2012) 1–8.

[136] S. Carmen T, B. David S, Separations of Tetracycline Antibiotics by Reversed Phase HPLC, Using Discovery Columns, Merck (2023). https://www.sigmaaldrich.com/GB/en/technical-documents/protocol/analytical-chemistry/small-molecule-hplc/separations-of-tetracycline (accessed March 29, 2023).

[137] Our World in Data, Carbon intensity of electricity, 2021, (2022). https://ourworldindata.org/grapher/carbon-intensity-electricity (accessed October 4, 2022).

[138] The Greenhouse Gases, Regulated Emissions, and Energy Use in Technologies (GREET®) Model, (2021).

[139] N. Geng, W. Chen, H. Xu, M. Ding, T. Lin, Q. Wu, L. Zhang, Insights into the novel application of Fe-MOFs in ultrasound-assisted heterogeneous Fenton system: Efficiency, kinetics and mechanism, Ultrason Sonochem 72 (2021) 105411. https://doi.org/https://doi.org/10.1016/j.ultsonch.2020.105411.

[140] A. Manickavasagan, R. Ramachandran, S.M. Chen, M. Velluchamy, Ultrasonic assisted fabrication of silver tungstate encrusted polypyrrole nanocomposite for effective photocatalytic and electrocatalytic applications, Ultrason Sonochem 64 (2020) 104913. https://doi.org/10.1016/J.ULTSONCH.2019.104913.

[141] E.D. Revellame, D.L. Fortela, W. Sharp, R. Hernandez, M.E. Zappi, Adsorption kinetic modeling using pseudo-first order and pseudo-second order rate laws: A review, Clean Eng Technol 1 (2020) 100032. https://doi.org/10.1016/J.CLET.2020.100032.

[142] J.J. Kwan, G. Lajoinie, N. de Jong, E. Stride, M. Versluis, C.C. Coussios, Ultrahigh-speed dynamics of micrometer-scale inertial cavitation from nanoparticles, Phys Rev Appl 6 (2016) 044004.

[143] C.R. Stephens, K. Murai, K.J. Brunings, R.B. Woodward, Acidity constants of the tetracycline antibiotics, J Am Chem Soc 78 (1956) 4155–4158.

[144] M. Kosmulski, The significance of the difference in the point of zero charge between rutile and anatase, Adv Colloid Interface Sci 99 (2002) 255–264. https://doi.org/10.1016/S0001-8686(02)00080-5.

[145] J. Tu, T.J. Matula, A.A. Brayman, L.A. Crum, Inertial cavitation dose produced in ex vivo rabbit ear arteries with optison® by 1-mhz pulsed ultrasound, Ultrasound Med Biol 32 (2006) 281–288. https://doi.org/https://doi.org/10.1016/j.ultrasmedbio.2005.10.001.

[146] T.-B. Fan, J. Tu, L.-J. Luo, X.-S. Guo, P.-T. Huang, D. Zhang, The Relationship of Cavitation to the Negative Acoustic Pressure Amplitude in Ultrasonic Therapy*, Chinese Physics Letters 33 (2016) 084302. https://doi.org/10.1088/0256-307X/33/8/084302.

[147] J. Lee, M. Ashokkumar, S. Kentish, F. Grieser, Determination of the Size Distribution of Sonoluminescence Bubbles in a Pulsed Acoustic Field, J Am Chem Soc 127 (2005) 16810–16811. https://doi.org/10.1021/ja0566432.

[148] T. Tuziuti, K. Yasui, J. Lee, T. Kozuka, A. Towata, Y. Iida, Mechanism of enhancement of sonochemical-reaction efficiency by pulsed ultrasound, J Phys Chem A 112 (2008) 4875–4878.

[149] V. Etacheri, C. Di Valentin, J. Schneider, D. Bahnemann, S.C. Pillai, Visible-light activation of TiO2 photocatalysts: Advances in theory and experiments, Journal of Photochemistry and Photobiology C: Photochemistry Reviews 25 (2015) 1–29. https://doi.org/https://doi.org/10.1016/j.jphotochemrev.2015.08.003.

[150] T. Tan, D. Beydoun, R. Amal, Effects of organic hole scavengers on the photocatalytic reduction of selenium anions, J Photochem Photobiol A Chem 159 (2003) 273–280. https://doi.org/https://doi.org/10.1016/S1010-6030(03)00171-0.

[151] J. Bogdan, J. Pławińska-Czarnak, J. Zarzyńska, Nanoparticles of titanium and zinc oxides as novel agents in tumor treatment: a review, Nanoscale Res Lett 12 (2017) 1–15.

[152] Y.T. Didenko, K.S. Suslick, The energy efficiency of formation of photons, radicals and ions during single-bubble cavitation, Nature 418 (2002) 394–397.

[153] A.A. Isari, M. Mehregan, S. Mehregan, F. Hayati, R. Rezaei Kalantary, B. Kakavandi, Sono-photocatalytic degradation of tetracycline and pharmaceutical wastewater using WO3/CNT heterojunction nanocomposite under US and visible light irradiations: A novel hybrid system, J Hazard Mater 390 (2020) 122050. https://doi.org/10.1016/J.JHAZMAT.2020.122050.

[154] R.H. Crawford, Validation of a hybrid life-cycle inventory analysis method, J Environ Manage 88 (2008) 496–506. https://doi.org/10.1016/J.JENVMAN.2007.03.024.

[155] E. Marsh, S. Allen, L. Hattam, Tackling uncertainty in life cycle assessments for the built environment: A review, Build Environ 231 (2023) 109941. https://doi.org/10.1016/J.BUILDENV.2022.109941.

[156] S. Legg, IPCC, 2021: Climate change 2021-the physical science basis, Interaction 49 (2021) 44–45.

[157] IPCC (Intergovernmental Panel on Climate Change), Chapter 8: Anthropogenic and natural radiative forcing, Climate Change 2013: The Physical Science Basis. Contribution of Working Group I to the Fifth Assessment Rep. of the Intergovernmental Panel on Climate Change (2013).

[158] R. Frischknecht, F. Wyss, S. Büsser Knöpfel, T. Lützkendorf, M. Balouktsi, Cumulative energy demand in LCA: the energy harvested approach, Int J Life Cycle Assess 20 (2015) 957–969.

[159] IEA, World Energy Outlook 2023, Paris, 2023. https://iea.blob.core.windows.net/assets/86ede39e-4436-42d7-ba2a-edf61467e070/WorldEnergyOutlook2023.pdf (accessed June 18, 2024).

[160] V. Balaram, Environmental impact of platinum, palladium, and rhodium emissions from autocatalytic converters–a brief review of the latest developments, Handbook of Environmental Materials Management (2020) 1–37.

[161] I.K. Kalavrouziotis, P.H. Koukoulakis, The environmental impact of the platinum group elements (Pt, Pd, Rh) emitted by the automobile catalyst converters, Water Air Soil Pollut 196 (2009) 393–402.

[162] M.U. Luescher, F. Gallou, B.H. Lipshutz, The impact of earth-abundant metals as a replacement for Pd in cross coupling reactions, Chem Sci 15 (2024) 9016–9025.

[163] G. Wernet, C. Bauer, B. Steubing, J. Reinhard, E. Moreno-Ruiz, B. Weidema,

The ecoinvent database version 3 (part I): overview and methodology, Int J Life Cycle Assess 21 (2016) 1218–1230.

[164] V. Abramov, A. Abramova, V. Bayazitov, S. Kameneva, V. Veselova, D. Kozlov, M. Sozarukova, A. Baranchikov, I. Fedulov, R. Nikonov, G. Cravotto, Fast Degradation of Tetracycline and Ciprofloxacin in Municipal Water under Hydrodynamic Cavitation/Plasma with CeO2 Nanocatalyst, Processes 10 (2022). https://doi.org/10.3390/pr10102063.

[165] H. Xiao, Y. Wang, H. Peng, Y. Zhu, D. Fang, G. Wu, L. Li, Z. Zeng, Highly Efficient Degradation of Tetracycline Hydrochloride in Water by Oxygenation of Carboxymethyl Cellulose-Stabilized FeS Nanofluids, Int J Environ Res Public Health 19 (2022). https://doi.org/10.3390/ijerph191811447.

[166] S.P. Onkani, P.N. Diagboya, S.O. Akpotu, F. Mtunzi, High-Performance Photocatalytic Degradation of Tetracycline and Ciprofloxacin by Ag-ZnO-Decorated Graphene Oxide Sponge, Ind Eng Chem Res 64 (2025) 11815–11825. https://doi.org/10.1021/acs.iecr.5c01064.

[167] A.K. Jha, S. Chakraborty, Photocatalytic degradation of tetracycline and ciprofloxacin antibiotic residues in aqueous phase by biosynthesized nZVI using Sal (Shorea robusta) leaf extract, AQUA - Water Infrastructure, Ecosystems and Society 72 (2023) 230–245. https://doi.org/10.2166/aqua.2023.113.

[168] S.P. Onkani, S.O. Akpotu, P.N. Diagboya, F. Mtunzi, E. Osabohien, Enhanced Aqueous Photo-Degradation of Ciprofloxacin and Tetracycline Using Ag-Decorated ZnO Plasmonic Catalyst, ACS Sustainable Resource Management 1 (2024) 2294–2303. https://doi.org/10.1021/acssusresmgt.4c00318.

[169] G. Yi, X. Li, Y. Yuan, Y. Zhang, Redox active Zn/ZnO duo generating superoxide (˙ O 2−) and H 2 O 2 under all conditions for environmental sanitation, Environ Sci Nano 6 (2019) 68–74.

[170] X. Wu, Y. Chang, S. Lin, Titanium radical redox catalysis: Recent innovations in catalysts, reactions, and modes of activation, Chem 8 (2022) 1805–1821. https://doi.org/10.1016/J.CHEMPR.2022.06.005.

[171] S. Sun, Z. Wang, Q. Pu, X. Li, Y. Cui, H. Yang, Y. Li, Identification and mechanistic analysis of toxic degradation products in the advanced oxidation pathways of fluoroquinolone antibiotics, Toxics 12 (2024) 203.

[172] Y. Amangelsin, Y. Semenova, M. Dadar, M. Aljofan, G. Bjørklund, The impact of tetracycline pollution on the aquatic environment and removal strategies, Antibiotics 12 (2023) 440.

[173] Y. Niu, Q. Shi, T. Peng, X. Cao, Y. Lv, Research Progress on the Synthesis of Nanostructured Photocatalysts and Their Environmental Applications, Nanomaterials 15 (2025) 681.

[174] M. Shokouhimehr, Magnetically separable and sustainable nanostructured

catalysts for heterogeneous reduction of nitroaromatics. Catalysts 5 (2): 534–560, (2015).

[175] Z. Zong, Y. Huang, J. Kwan, N.P. Hankins, Standardized benchmarking of advanced oxidation processes for tetracycline degradation with life cycle assessment and economic evaluation, Chemical Engineering Journal 525 (2025) 170664. https://doi.org/10.1016/J.CEJ.2025.170664.

[176] Y. Sun, S. Bai, X. Wang, N. Ren, S. You, Prospective Life Cycle Assessment for the Electrochemical Oxidation Wastewater Treatment Process: From Laboratory to Industrial Scale, Environ Sci Technol 57 (2023) 1456–1466. https://doi.org/10.1021/acs.est.2c04185.

[177] S. Arzate, S. Pfister, C. Oberschelp, J.A. Sánchez-Pérez, Environmental impacts of an advanced oxidation process as tertiary treatment in a wastewater treatment plant, Science of The Total Environment 694 (2019) 133572. https://doi.org/10.1016/J.SCITOTENV.2019.07.378.

[178] R. López-Timoner, L. Santos-Juanes, A.M. Amat, F. Arfelli, D. Cespi, F. Passarini, M.I. Polo, E. Zuriaga, A. Arques, Life cycle assessment of UVC-based advanced oxidation processes as quaternary treatments: Clostridium spp. inactivation and comparison with CECs removal, Science of The Total Environment 972 (2025) 179029. https://doi.org/10.1016/J.SCITOTENV.2025.179029.

[179] B. Notarnicola, G. Tassielli, P.A. Renzulli, R. Di Capua, F. Astuto, G. Mascolo, S. Murgolo, C. De Ceglie, M.L. Curri, R. Comparelli, M. Dell'Edera, Life Cycle Assessment of UV-C based treatment systems for the removal of compounds of emerging concern from urban wastewater, Science of The Total Environment 857 (2023) 159309. https://doi.org/10.1016/J.SCITOTENV.2022.159309.

[180] G. Towler, R. Sinnott, Economic evaluation of projects, Chemical Engineering Design (2022) 305–337. https://doi.org/10.1016/B978-0-12-821179-3.00009-1.

[181] M. Sharma, M.K. Mandal, S. Pandey, R. Kumar, K.K. Dubey, Visible-light-driven photocatalytic degradation of tetracycline using heterostructured Cu2O–TiO2 nanotubes, kinetics, and toxicity evaluation of degraded products on cell lines, ACS Omega 7 (2022) 33572–33586.

[182] M. Nie, Y. Li, J. He, C. Xie, Z. Wu, B. Sun, K. Zhang, L. Kong, J. Liu, Degradation of tetracycline in water using Fe 3 O 4 nanospheres as Fenton-like catalysts: kinetics, mechanisms and pathways, New Journal of Chemistry 44 (2020) 2847–2857.

[183] Y. Liang, A. Feng, N.A. Al-Dhabi, J. Zhang, W. Xing, T. Chen, Y. Han, G. Zeng, L. Tang, W. Tang, Efficient antibiotic tetracycline degradation and toxicity abatement via the perovskite-type CaFexNi1-xO3 assisted heterogeneous electro-Fenton system, Water Res 279 (2025) 123432. https://doi.org/10.1016/J.WATRES.2025.123432.

[184] J.L. Sorrels, T.G. Walton, Chapter 2—Cost Estimation: Concepts and Methodology, EPA Air Pollution Control Cost Manual; US Environmental Protection Agency: Washington, DC, USA (2017) 35.

[185] Z. Zong, N. Koers, G. Cai, D.C. Upham, CO2-to-methanol: Economic and environmental comparison of emerging and established technologies with dry reforming and methane pyrolysis, Chemical Engineering Journal (2024) 150274. https://doi.org/10.1016/J.CEJ.2024.150274.

[186] B. Parkinson, M. Tabatabaei, D.C. Upham, B. Ballinger, C. Greig, S. Smart, E. McFarland, Hydrogen production using methane: Techno-economics of decarbonizing fuels and chemicals, Int J Hydrogen Energy 43 (2018) 2540–2555. https://doi.org/10.1016/j.ijhydene.2017.12.081.

[187] Y. Li, Y. Zhang, G. Xia, J. Zhan, G. Yu, Y. Wang, Evaluation of the technoeconomic feasibility of electrochemical hydrogen peroxide production for decentralized water treatment, Front Environ Sci Eng 15 (2021) 1–15.

[188] G.A. Von Wald, M.S. Masnadi, D.C. Upham, A.R. Brandt, Optimization-based technoeconomic analysis of molten-media methane pyrolysis for reducing industrial sector CO 2 emissions, Sustain Energy Fuels 4 (2020) 4598–4613.

[189] B.P. Weidema, Comparing three life cycle impact assessment methods from an endpoint perspective, J Ind Ecol 19 (2015) 20–26.

[190] S. Jenkins, 2023 CEPCI annual average value decreases from previous year, Chemical Engineering Magazine (2024).

[191] S. Jenkins, 2020 ANNUAL CEPCI AVERAGE VALUE, (2021). https://www.chemengonline.com/2020-annual-cepci-average-value/ (accessed August 11, 2021).

[192] Z. Zong, G. Cai, M. Tabbara, D. Chester Upham, CO2-negative fuel production using low-CO2 electricity: Syngas from a combination of methane pyrolysis and dry reforming with techno-economic analysis, Energy Convers Manag 277 (2023) 116624. https://doi.org/10.1016/J.ENCONMAN.2022.116624.

[193] B. Parkinson, P. Balcombe, J.F. Speirs, A.D. Hawkes, K. Hellgardt, Levelized cost of CO2 mitigation from hydrogen production routes, Energy Environ Sci 12 (2019) 19–40. https://doi.org/10.1039/C8EE02079E.

[194] Z. Zong, C. Rao, C. Du, R. Lu, D.C. Upham, Polyhydroxyalkanoates (PHA) production in a circular CO2 economy: it's role in mitigating global CO2 emissions, Resour Conserv Recycl 219 (2025) 108303. https://doi.org/10.1016/J.RESCONREC.2025.108303.

[195] IEA, Fossil Fuel Subsidies in Clean Energy Transitions: Time for a New Approach?, (2023). https://www.iea.org/reports/fossil-fuel-subsidies-in-clean-energy-transitions-time-for-a-new-approach (accessed May 22, 2025).

[196] S. Singh, A. Dhar, S. Powar, Perspectives on life cycle analysis of solar technologies with emphasis on production in India, J Environ Manage 366 (2024) 121755. https://doi.org/10.1016/J.JENVMAN.2024.121755.

[197] P. Ghisellini, R. Passaro, S. Ulgiati, Environmental assessment of multiple "cleaner electricity mix" scenarios within just energy and circular economy transitions, in Italy and Europe, J Clean Prod 388 (2023) 135891. https://doi.org/10.1016/J.JCLEPRO.2023.135891.

[198] N. Sharif, N. Munir, M. Hasnain, S. Naz, M. Arshad, Environmental impacts of ethanol production system, Sustainable Ethanol and Climate Change: Sustainability Assessment for Ethanol Distilleries (2021) 205–223.

[199] A.D. Racovita, Titanium dioxide: structure, impact, and toxicity, Int J Environ Res Public Health 19 (2022) 5681.

[200] F. Wu, Z. Zhou, A.L. Hicks, Life cycle impact of titanium dioxide nanoparticle synthesis through physical, chemical, and biological routes, Environ Sci Technol 53 (2019) 4078–4087.

[201] A.M. Bolt, Tungsten toxicity and carcinogenesis, Adv Pharmacol 96 (2023) 119–150. https://doi.org/10.1016/BS.APHA.2022.10.004.

[202] N. Strigul, Does speciation matter for tungsten ecotoxicology?, Ecotoxicol Environ Saf 73 (2010) 1099–1113. https://doi.org/10.1016/J.ECOENV.2010.05.005.

[203] H.Y. Teah, T. Sato, K. Namiki, M. Asaka, K. Feng, S. Noda, Life cycle greenhouse gas emissions of long and pure carbon nanotubes synthesized via on-substrate and fluidized-bed chemical vapor deposition, ACS Sustain Chem Eng 8 (2020) 1730–1740.

[204] O.G. Griffiths, J.P. O'Byrne, L. Torrente-Murciano, M.D. Jones, D. Mattia, M.C. McManus, Identifying the largest environmental life cycle impacts during carbon nanotube synthesis via chemical vapour deposition, J Clean Prod 42 (2013) 180–189. https://doi.org/10.1016/J.JCLEPRO.2012.10.040.

[205] S. Xu, Z. Li, Q. Yang, G. Chu, J. Zhang, D. Zhang, H. Zhou, M. Gao, Comparative life cycle assessment of energy consumption, pollutant emission, and cost analysis of coal/oil/biomass to ethylene glycol, ACS Sustain Chem Eng 9 (2021) 15849–15860.

[206] H. Itoh, Sintering Behavior and Performance of Anode Materials for SOFC, Proceedings - Electrochemical Society 1995–1 (1995) 639–648. https://doi.org/10.1149/199501.0639PV.

[207] Auxilab, muffle furnaces SERIES642, (n.d.). https://www.auxilab.es/controles/ObtenerPDF.ashx?f=%5c00%5c05%5cax%5ckn_F_JBP001_5_I.pdf (accessed May 22, 2025).

[208] A. Motevali, S. Minaei, A. Banakar, B. Ghobadian, M.H. Khoshtaghaza, Comparison of energy parameters in various dryers, Energy Convers Manag 87 (2014) 711–725. https://doi.org/10.1016/J.ENCONMAN.2014.07.012.

[209] P.M. Doran, Mixing, Bioprocess Engineering Principles (2013) 255–332. https://doi.org/10.1016/B978-0-12-220851-5.00008-3.

[210] Grant Instruments, XUB Digital Ultrasonic Bath Range, (n.d.). https://www.grantinstruments.com/products/xub-digital-ultrasonic-bath-range (accessed May 22, 2025).

[211] Y.S.H. Najjar, A. Abu-Shamleh, Harvesting of microalgae by centrifugation for biodiesel production: A review, Algal Res 51 (2020) 102046. https://doi.org/10.1016/J.ALGAL.2020.102046.

[212] E. Arkhangelsky, I. Levitsky, V. Gitis, Considering energy efficiency in filtration of engineering nanoparticles, Water Sci Technol Water Supply 17 (2017) 1212–1218.